



This is to certify that the

thesis entitled

YIELD OPTIMIZATION ANALYSIS OF COMPLEX CHEMICAL REACTIONS IN ISOTHERMAL CHEMICAL REACTORS UNDER FORCED PERIODIC OPERATION

presented by

Richard Dale Skeirik

has been accepted towards fulfillment of the requirements for

M.S. degree in Chemical Engineering

Major professor

Feb. 10, 1981

O-7639



OVERDUE FINES: 25¢ per day per item

RETURNING LIBRARY MATERIALS: Place in book return to remove charge from circulation records

YIELD OPTIMIZATION ANALYSIS OF COMPLEX CHEMICAL REACTIONS IN ISOTHERMAL CHEMICAL REACTORS UNDER FORCED PERIODIC OPERATION

Ву

Richard Dale Skeirik

A THESIS

Submitted to
Michigan State University
in partial fulfillment of the requirements
for the degree of

MASTER OF SCIENCE

Department of Chemical Engineering

ABSTRACT

YIELD OPTIMIZATION ANALYSIS OF COMPLEX CHEMICAL REACTIONS IN ISOTHERMAL CHEMICAL REACTORS UNDER FORCED PERIODIC OPERATION

By

Richard Dale Skeirik

Periodic forcing of feed concentration to isothermal CSTR's with Van de Vusse kinetics has been examined. Square wave and sinusoidal forcing to homogeneous reactors and square wave forcing to a CSTR with one dimensional diffusion inside the catalyst pellets have been considered. For the homogenous reactors, analytic or semi-analytic solutions have been developed for species concentrations as well as time averages. The heterogeneous reactor was treated numerically. All cases showed a decrease in yield of the intermediate and an increase in yield of the side product. The effects of periodic operation increase as the forcing frequency decreases, hence the maximum effect of forcing can be achieved by a smaller steady state reactor.

TABLE OF CONTENTS

Chantau	Page
Chapter I. PERIODIC SQUARE WAVE FEED CONCENTRATION TO A HOMOGENEOUS ISOTHERMAL CSTR WITH VAN DE VUSSE REACTION NETWORK	. 1
The Choice of the System The Method of Comparison The Periodic Scheme First Order Kinetics Van de Vusse Kinetics Calculative Results Conclusions	
II. PERIODIC SINUSOIDAL FEED CONCENTRATION TO A HOMOGENEOUS ISOTHERMAL CSTR WITH A VAN DE VUSSE REACTION NETWORK	. 40
The Method of Comparison Consecutive Parallel Reactions Van de Vusse Kinetics Numerical Results Conclusion	
III. PERIODIC SQUARE WAVE FEED CONCENTRATION TO AN ISOTHERMAL CSTR WITH A VAN DE VUSSE REACTION OCCURRING IN POROUS SLAB CATALYST PARTICLES	. 82
Numerical Results Conclusion	
LIST OF REFERENCES	. 104

LIST OF FIGURES

Chapter 1 Figure		P	age
1.(a-d)	Behavior of the Van de Vusse system for a case of intermediate cycling frequency. $K_1 = K_2 = K_3 = 1$, $\theta_0 = 1$	•	24
2.(a-d)	Behavior of the Van de Vusse system for a case of slow cycling frequency. $K_1 = K_2 = K_3 = 1$, $\theta_0 = 10$	•	29
3.(a-d)	Behavior of the Van de Vusse system for a case of rapid cycling frequency. $K_1 = K_2 = K_3 = 1$, $\theta_0 = .3$	•	34
Chapter 2			
Figure 1.(a-g)	Behavior of Van de Vusse system for $\tau k_1 = k_2/k_1 = \tau k_3 A_0 = \Lambda = 1$, $\epsilon = .1$	•	60
2.(a-g)	Behavior of Van de Vusse system for $\tau k_1 = k_2/k_1 = \tau k_3 A_0 = \Lambda = 1$, $\epsilon = 1$	•	6 3
3.(a-b)	Behavior of Van de Vusse system for $\tau k_1 = k_2/k_1 = \tau k_3 A_0 = \Lambda = 1$, $\epsilon = .75$	•	66
4.(a-b)	Behavior of Van de Vusse system for $\tau k_1 = k_2/k_1 = \tau k_3 A_0 = \Lambda = 1$, $\epsilon = .25$	•	66
5.(a-b)	Deviation of perturbation solution from numerical simulation for Van de Vusse system $\tau k_1 = k_2/k_1 = 1$ $\tau k_3 A_0 = 5$ $\Lambda = 1$ $\epsilon = .25$. % error = $(C_{pert} - C_{num})/C_{num}$	•	69
6.(a-b)	numerical simulation for Van de Vusse system $\tau k_1 = k_2/k_1 = 1$ $\tau k_3 A_0 = 5$		
	$\Lambda = 1 \epsilon = .75$. % error = $(\tilde{C}_{pert} - C_{num})/C_{num}$	•	69

7.(a-b)	Deviation of perturbation solution from numerical simulation for Van de Vusse system $\tau k_1 = k_2/k_1 = 5$ $\tau k_3 A_0 = 1$ $\Lambda = 1$ $\epsilon = .25$. % error = $(C_{pert} - C_{num})/C_{num} \cdot 100 \dots 70$
8.(a-b)	Deviation of perturbation solution from numerical simulation for Van de Vusse system $\tau k_1 = k_2/k_1 = 5$ $\tau k_3 A_0 = 1$ $\Lambda = 1$ $\epsilon = .75$. % error = $(C_{pert} - C_{num})/C_{num} \cdot 100 \dots 70$
9.(a-b)	Deviation of perturbation solution from numerical simulation for Van de Vusse system
10.(a-b)	Deviation of perturbation solution from numerical simulation for Van de Vusse system
11.(a-b)	Deviation of perturbation solution from numerical simulation for Van de Vusse system
12.(a-b)	Deviation of perturbation solution from numerical simulation for Van de Vusse system $\tau k_1 = k_2/k_1 = \tau k_3 A_0 = 1$ $\Lambda = 5$ $\epsilon = .75$. % error = $(C_{pert} - C_{num})/C_{num} \cdot 100 \dots 75$
13.(a-b)	Deviation of perturbation solution from numerical simulation for Van de Vusse system $\tau k_1 = k_2/k_1 = \tau k_3 A_0 = 1$ $\Lambda = .2$ $\epsilon = .25$. % error = $(C_{pert} - C_{num})/C_{num} \cdot 100$
14.(a-b)	
Chapter 3	
Figure 1.	Bulk phase reactant concentration vs. time for square wave cycling. $\phi=1$. $\nu=1$. $\beta=1$. $K_3=1$. $h=1$. $K_2=1$. $\Lambda=1$. $\psi=1$ 90

2.	Bulk phase intermediate concentration vs. time for square wave cycling. ϕ =1. ν =1. β =1. K_3 =1. h =1. K_2 =1. Λ =1. ψ =1	92
	Bulk phase plane behavior for square wave cycling. ϕ =1. ν =1. β =1. K_3 =1. h =1. K_2 =1. Λ =1. ψ =1	94
4.	Reactant concentration profile within the pellet at five selected points in the limit cycle. ϕ =1. ν =1. β =1. K_3 =1. k_2 =1. Λ =1. ν =1	96
5.	Intermediate concentration profile within the pellet at five selected pointed in the limit cycle. ϕ =1. ν =1. β =1. K_3 =1. h =1. K_2 =1. Λ =1. ψ =1	98

LIST OF TABLES

							Pag	e
Chapte	er l						•	
	Enhancement of time average periodic concentrations over steady state concentrations. Approximation to consecutive reactions when $K_3 \simeq 0$. Approximation to second order reaction when $K_1 \simeq 0$, $K_2 \simeq 0$.	•	•	•	•	•	. 2	:0
Chapte	er 2							
	Percent deviation of approximate time average concentrations [equations (24)] from numerically simulated time average concentrations; percent enhancement of approximate time average concentrations over steady state concentrations	 •	•	•	•	•	. 7	9
Chapte	er 3							
	Percent increase in time average of periodic bulk phase concentrations over steady state concentrations for square wave perturbation	 •	 •	•	•		. 10	0

NOTATIONS--CHAPTER 1

Α	Concentration of reactant species
Αo	Reference concentration
В	Concentration of intermediate species
b	B/A ₀
Б	Time average b for periodic limit cycle
С	Product species
c _i	Constants, defined by eqns. (14c),(20c-20h)(20o)(16e)
D	Concentration of product species
d	D/A ₀
ā	Time average d for periodic limit cycle
F(f)	Locus of zero slope in b-f or d-f phase plane
f	A/A _o
f ₁ (jθ ₀)	Initial condition at beginning of Region 1
$f_2(n\theta_0)$	Initial condition at beginning of Region 2
7	Time average f for periodic limit cycle
9 _i	Represents behavior of b(f) or d(f) in proof
Ki	Dimensionless rate constant eqns (4), (12)
k _i	Reaction rate constant
q	Volumetric flow rate
t	Time
t _o	Period of 1/2 of feed cycle
V	CSTR volume vii

Subscripts

f Feed condition

i Denotes interchangability of Regions 1 and 2

ss Steady state

1 Portion of feed cycle in which dimensionless feed concentration is 2.0

2 Portion of feed cycle in which dimensionless feed concentration is 0.0

Greek Symbols

œ

```
\theta_0, 3\theta_0, 5\theta_0,...
jθο
n<sub>0</sub>
            0, 2\theta_0, 4\theta_0, \dots
             Defined by eqn (14d)
α(nθ₀)
\alpha(n\theta_0)_{\infty}
            Defined by eqn (25f)
ā(jθ₀)
            Defined by eqn (14e)
\bar{\alpha}(j\theta_0)_{\infty}
             Defined by eqn (25g)
             Constant in eqns (18)
β
θ
             t/τ
            t_0/\tau
θο
            Defined by eqns (2)
ξ
             V/g
τ
             Constants, defined by eqns (20i)-(20n)
Φi
             Substitution parameter
\Psi_{\mathbf{i}}
```

Approaching infinity

NOTATIONS--CHAPTER 2

Α	Concentration of reactant species
a	Constant, defined by eqn (15n)
ā _{ij}	Constants, defined by eqn (15u)
a _i	Constants, defined by eqns (6)
В	Concentration of intermediate species
b	B/A _O
Б	Time average b
Б _і	Constants, defined by eqn (15v)
С	Concentration of product species
С	C/A _o
c	Time average c
c _i	Constants, defined by eqns (10), (17d)
ē;	Constants, defined by eqn (15w)
D	Concentration of product species
d	D/A _o
đ	Time average d
f	A/A _o
7	Time average f
1 _i	Integration constants
k _i	Reaction rate constant
q	Volumetric flow rate

```
P;
            Periodic functions
t
            Time
٧
            CSTR volume
Greek Symbols
            Defined by (15n)
α
            Constants, defined by eqn (15x)
\alpha_{\mathbf{i}}
            Constants, defined by eqn (15p)
\beta_{\mathbf{i}}
            Constants, defined by eqn (15q)
Υį
            Adjustable parameter controlling the amplitude of the input
ε
            disturbance--perturbation parameter for Van de Vusse kinetics
            Defined by eqns (19s)-(19w)
ζi
            Constants, defined by eqn (15r)
\eta_{\mathbf{i}}
θ
            t/τ
\lambda_{i,i}
            Defined by eqn (15n)
Λ
            ωτ
            Constant, defined by eqn (18e)
\mu_{\mathbf{i}}
μį
            Constant, defined by eqn (18f)
            Constants, defined by eqn (15s)
v_i
            Constants, defined by eqn (15t)
\sigma_{\mathbf{i}}
τ
            V/q
            Constants defined by eqns (23s)-(23w)
Xi
            Substitution parameter
\psi_{\mathbf{i}}
```

Frequency of input disturbance

Defined by eqn (18d)

ω

ω_{ℓ,i}

Subscripts

- f Feed condition
- o Reference concentration
- s Steady state

NOTATIONS--CHAPTER 3

А	Concentration of reactant species
x	Spatial distance within catalyst particle
$^{D}e_{A}$	Effective diffusivity of species A
$^{D}e_{B}$	Effective diffusivity of species B
t	Time
k _i	Effective rate constant based on concentration in bulk phase adjacent to surface
q	Volumetric flow rate
A	External surface of one catalyst pellet perpendicular to mass flux
n _p	Number of catalyst particles in CSTR
В	Concentration of intermediate species
Ĺ	1/2 thickness of catalyst slab
u	A/A _O , eqn (3a)
К ₃	k_3A_0/k_1 , eqn (3a)
b	B/A _O
K ₂	k_2/k_1
h	$^{\mathrm{D}}\mathbf{e}_{\mathrm{A}}^{\mathrm{D}}\mathbf{e}_{\mathrm{B}}^{\mathrm{D}}$

Greek Symbols

 ϵ Fraction of CSTR volume not occupied by catalyst

pellets

¢² Thiele modulus, eqn (3a)

ξ X/L

 $^{\theta}$ t $^{D}e_{A}^{\prime}L^{2}$

VE D_e/qL²

 ${}^{D}e_{A}^{n}p^{A/qL}$

 $^{\vee}$ $^{k}_{g}$ $^{L/D}e_{A}$

A Dimensionless frequency of input disturbance

Superscripts

^ bulk phase

Subscripts

o Reference concentration

f Feed

CHAPTER 1

PERIODIC SQUARE WAVE FEED CONCENTRATION TO A HOMOGENEOUS ISOTHERMAL CSTR WITH VAN DE VUSSE REACTION NETWORK

Chemical reactors under forced periodic operation often give a time average output which is different from the corresponding steady state. In general, this is true whenever some of the output variables depend in a non-linear way on the forcing input variable. For those selectivity reactions which exhibit an absolute maximum yield or selectivity under steady state operation, forced periodic operation is a promising method of improving on steady state performance.

A large segment of the work done in this area has centered on non-isothermal systems, which allows the exploitation of the exponential non-linearity of the Arrhenius rate expression. However, the complexity of the simultaneous heat and mass balances combined with at least one exponential non-linearity virtually eliminates the possibility of obtaining an analytic solution. Hence the treatments have been either approximate, usually through the use of some kind of perturbation technique, or numerical. While Douglas and coworkers [1] [2] [3] [4], Renken [5] [6], and Farhadpour and Gibalaro [14] have studied specific reacting systems under forced periodic operation, no one has yet obtained a fully analytic prediction of system behavior.

In contrast, this work treats complex kinetics occurring in an isothermal CSTR with a square wave feed concentration and provides fully analytic solutions for the reactant and product concentrations as well as their time averages.

THE CHOICE OF THE SYSTEM

In deciding on a complex kinetics system, the number of possible choices is infinite. Some important characteristics led to the choice

of the Van de Vusse system, A+B+C, 2A+D, for this work. As Van de Vusse proposed, the system cannot be easily classified by general reactor selection guidelines. The intermediate B exhibits an absolute maximum concentration under steady state operation [3], thus this is a system which explores the real potential of periodic operation. Probably most important from the perspective of enhancing reactor performance, under some reactor conditions, the intermediate B increases through a transient maximum, even though it is already above the steady state it is approaching. Hence periodic operation provides an inviting method to capitalize on this phenomenon. Any initial optimism about this aspect of the system must be tempered, however, by the fact that B also goes through a transient minimum even when below the eventual steady state [7].

THE METHOD OF COMPARISON

In order to draw any meaningful conclusions from the study of periodic operation of chemical reactors, comparison against a corresponding steady state is necessary. In addition, the comparison is subject to certain restrictions.

(1) Residence Time:

- (a) For those products for which steady state operation can be made more effective by simply using a longer residence time (for example, the reactant A in the Van de Vusse kinetics scheme), the comparison should be based on the same residence time for periodic and steady state operation.
- (b) For those species which exhibit an absolute maximum concentration with respect to residence time in steady state mode, the comparison should be between the optimum steady state concentration and the optimum periodic concentration, regardless of the periodic process residence time.

- (2) Equal time average molar flow rates of reactant species into the reactor should be used in both periodic and steady state mode.
- (3) Initial transients are ignored. For steady state (i.e., non-periodic) mode, only the steady state concentrations should be considered. For the periodic mode, time averages should be taken only after the effluent concentrations achieve a stable repetitive cycle (limit cycle).
- (4) For the feed concentration disturbance used here, volumetric flow rate in the periodic process should not vary with time.

THE PERIODIC SCHEME

The input disturbance used here consists of a symmetric square wave reactant feed concentration. The feed oscillates between dimensionless concentrations of 0.0 and 2.0. Each phase of the cycle lasts for a period t_0 , giving the inlet disturbance an overall period of $2t_0$. The steady state against which the periodic process is compared is simply the same process with an invariant dimensionless feed concentration of 1.0. To simplify the solution, the process is arbitrarily defined to begin operation at time t=0 with a feed concentration of 2.0 at the beginning of a feed cycle.

The square wave input disturbance has several important characteristics. First, the input concentration during either half of the feed cycle is constant. The transient mass balance for the reactant species during either portion of the feed cycle can therefore be represented by an autonomous ordinary differential equation. If some other disturbance, such as a sine wave, were introduced, the reactant mass balance would become nonautonomous, and an analytic solution would most likely be impossible.

Second, because of the different inlet molar flow rates, the reactant mass balances for the two portions of the feed cycle are different, and there does not appear to be any way to combine the two. The mathematical treatment of the problem thus becomes a series of initial value problems, in which the final value of the solution in one region becomes the initial value for the solution in the next region.

In order to do a rigorous analysis of the periodic process, the governing mass balances should be solvable, which for this kinetics virtually requires the system to be autonomous. However, the treatment of the system as a series of initial value problems presents some serious difficulties. The solution, although its value is always continuous, is not represented by a single function. During one portion of the feed cycle, the solution is given by one expression; during the other portion, by a different expression. It is not possible to conclude from inspection of the solution that the output will exhibit a stable periodicity as time becomes large. Hence, even after the solutions to the system concentrations as a function of time are known, a great deal of analysis remains to determine how the system will behave as time progresses. Once it is shown that the system goes to a stable, repetitive cycle, or limit cycle, the concentration functions can be integrated over one cycle to obtain the time average concentrations.

The original objective of this work was to examine Van de Vusse kinetics. However, because of the apparent difficulty of proving the limiting behavior of the system, we first examined simple first order kinetics, and then extended the techniques of that analysis to Van de Vusse kinetics.

In each case the approach to the problem was the same. First, full transient solutions for the species in question were obtained. Then, by

a qualitative examination of the governing differential equations, the limiting behavior of the system was established. This qualitative information about the system allowed calculation of the asymptotic limits of the output concentrations at the end of each region of the feed cycle. The transient solution for the output concentrations were then integrated over the time period of one feed cycle, using the limiting values as initial and final conditions, giving analytical expressions for the time averages of these quantities.

Definitions

The treatment of the periodic process necessitates the definition of some terminology. Since there will be separate solutions to the mass balances for each part of the feed cycle, the two are distinguished by subscripts. The subscript 1 is used to designate that half of the feed cycle in which the dimensionless feed concentration is 2.0; this is identified as Region 1. The subscript 2 designates the portion of the cycle with a feed concentration of 0.0; call this Region 2. Moreover, the solution takes the form of a series of functions, each of which depends on the value of the solution at the end of the previous region. Since each portion of the feed cycle lasts for a duration θ_0 (=t₀/ τ), and since we have defined the process to start at t=0 at the beginning of Region 1, then Region 1 will always end and Region 2 begin on an odd multiple of θ_0 . Similarly, Region 2 will end and Region 1 begin on even multiples of θ_0 . The symbols

$$n\theta_0 = 0, 2\theta_0, 4\theta_0, \dots$$
 (1a)

$$\mathbf{j}\theta_0 = \theta_0, 3\theta_0, 5\theta_0, \dots \tag{1b}$$

allow a general representation of the beginning of either region.

The "initial" condition for any concentration function in a region is expressed by the subscript representing the region and the nomenclature for the beginning of the region i.e., eqns (1). Thus the solution to $f(\theta)$ in Region 1, beginning at $n\theta_0$, has its initial condition represented by $f_1(n\theta_0)$. Similarly $f_2(\theta)$ would have the initial condition $f_2(j\theta_0)$.

Although the solutions depend on time, it is only the time elapsed since the beginning of the region which is important. The substitution

$$\xi = \theta - n\theta_0$$
; Region 1 (2a)

$$\xi = \theta - j\theta_0$$
; Region 2 (2b)

is defined.

FIRST ORDER KINETICS

Although a first order reaction

$$A \stackrel{k}{\rightarrow} B$$

taking place in an isothermal CSTR shows an increase in conversion under periodic operation, the methodology used for this case illustrates the methods used for Van de Vusse kinetics. The transient mass balance on the reactant species is given by

$$qA_f - qA - k_1VA = V \frac{dA}{dt}$$
 (3)

The problem is treated as two separate differential equations for the two regions of the feed cycle. Substituting the dimensionless variables

$$f = \frac{A}{A_0}$$
 $T = \frac{V}{Q}$ $\theta = \frac{t}{\tau}$ $K_1 = \tau k_1$ (4)

we obtain the following two differential equations

$$\frac{\mathrm{d}\mathsf{f}_1}{\mathrm{d}\theta} = 2 - (1+\mathsf{K}_1)\mathsf{f}_1 \tag{5a}$$

$$\frac{\mathrm{df_2}}{\mathrm{d\theta}} = -\left(1 + \mathrm{K_1}\right) \mathrm{f_1} \tag{5b}$$

The solutions to equations (5) are given by

$$f_1(\xi) = f_{SS_1} - [f_{SS_1} - f_1(n\theta_0)] \exp[-(1+K_1)\xi]$$
 (6a)

$$f_2(\xi) = f_2(j\theta_0) \exp[-(1+K_1)\xi]$$
 (6b)

The solution to equation (5a) with the time derivative set equal to zero is

$$f_{SS1} = \frac{2}{1+K_1} \tag{6c}$$

System Behavior

The behavior of the system for large θ can be established by a qualitative examination of the governing differential equations, (5). First, $\frac{df_2}{d\theta} < 0$, and f_2 approaches zero asymptotically. Also

$$\frac{df_1}{d\theta} \left\{ \begin{array}{l} < 0 , f_1 > f_{SS1} \\ = 0 , f_1 = f_{SS1} \\ > 0 , f_1 < f_{SS1} \end{array} \right\}$$

and f_1 approaches f_{SS^1} asymptotically.

If $f(\theta=0)>f_{SS1}$, both $\frac{df_1}{d\theta}$ and $\frac{df_2}{d\theta}$ are <0 at least for the first cycle. f_1 and f_2 will decrease with time until f_2 crosses f_{SS1} at some θ_C . Once this happens, we have $\frac{df_1}{d\theta} > 0$ and $\frac{df_2}{d\theta} < 0$. Moreover, since the functions approach their steady states asymptotically, the values of f_1 and f_2 are bounded by f_{SS1} and 0, which guarantees $\frac{df_1}{d\theta} > 0$ and $\frac{df_2}{d\theta} < 0$ for $\theta>\theta_C$. Hence we have an oscillation for f.

For the case $f(\theta=0) < f_{SS1}$, $\frac{df_1}{d\theta} > 0$ and $\frac{df_2}{d\theta} < 0$ for all θ and hence oscillation is immediately established. Here θ_C becomes immaterial.

At any time θ^* (at the start of some cycle or half a cycle) during the oscillation, one of three events could occur, viz. $f(\theta^*+2\theta_0) \leq f(\theta^*)$. By the property of uniqueness of ordinary differential equations, it becomes evident that $f(\theta^*) \leq f(\theta^*+2\theta_0) \leq f(\theta^*+4\theta_0)$, etc. Therefore, the system produces a characteristic of either increasing, decreasing, or unchanging sequence of initial conditions. Furthermore since $f_{\epsilon}(0,f_{SS^1})$, the sequence of initial conditions must approach an asymptotic limit. Hence, a limit cycle is established. The uniqueness of the limit cycle is discussed next.

Asymptotic Limits and Time Averages

Denoting the asymptotic limits at $n\theta_0$ and $j\theta_0$ by the symbols $f_1(n\theta_0)_{\infty}$ and $f_2(j\theta_0)_{\infty}$, we make use of the fact that if $f_2(j\theta_0)_{\infty}$ is the initial condition for $f_2(\xi)$, then its value after a time θ_0 must equal $f_1(n\theta_0)_{\infty}$. Similarly $f_1(n\theta_0)_{\infty}$ used as initial condition for Region 1 over an interval θ_0 must return the value $f_2(j\theta_0)_{\infty}$. This gives

$$f_1(n\theta_0)_{\infty} = f_2(j\theta_0)_{\infty} \exp \left[-(1+K_1)\theta_0\right]$$
 (7a)

$$f_2(j\theta_0)_{\infty} = f_{SS_1} - [f_{SS_1} - f_1(n\theta_0)_{\infty}] \exp[-(1+K_1)\theta_0]$$
 (7b)

The solution of this linear system is unique and is easily found to be

$$f_1(n\theta_0)_{\infty} = f_{SS_1} \left[\frac{1 - \exp[-(1+K_1)\theta_0]}{2 \sinh[(1+K_1)\theta_0]} \right]$$
 (8a)

$$f_2(j\theta_0)_{\infty} = f_{SS^1} \left[\frac{\exp[(1+K_1)\theta_0]-1}{2 \sinh[(1+K_1)\theta_0]} \right]$$
 (8b)

Once these limits are known, we can integrate over one full cycle using these values as initial conditions to determine the time average f. We define the time average, \bar{f} as

$$\bar{f} = \frac{\int_0^{\theta_0} f_1(\xi) d\xi + \int_0^{\theta_0} f_2(\xi) d\xi}{2\theta_0}$$
 (9a)

where,
$$f_1(\xi=0) = f_1(n\theta_0)_m$$
; $f_2(\xi=0) = f_2(j\theta_0)_m$ (9b)

Evaluation of the integrals gives

$$\bar{f} = \frac{1}{(1+K_1)} . \tag{10a}$$

The steady state against which comparison is made is identical except for its invariant dimensionless feed concentration of 1. The steady state solution to this system, f_{ss} , is simply

$$f_{SS} = \frac{1}{(1+K_1)} \tag{10b}$$

The time average for the periodic limit cycle is equal to the corresponding steady state f. Hence there is no enhancement of conversion for the first order case under periodic operation.

VAN de VUSSE KINETICS

Van de Vusse kinetics is a good example of a complex kinetics scheme which exhibits an absolute maximum steady state concentration of an intermediate species. The scheme,

$$A^{k_1}B^{k_2}C \cdot A + A \stackrel{k_3}{\rightarrow} D$$

also gives second order, $A + A \rightarrow D$, and consecutive, $A \rightarrow B \rightarrow C$, kinetics if, respectively, k_1 or k_3 is made sufficiently small. The transient mass balances for components A, B and D are

$$qA_f - qA - V(k_1A + k_3A^2) = V \frac{dA}{dt}$$
 (11a)

$$qB_f - qB - Vk_2B + Vk_1A = V \frac{dB}{dt}$$
 (11b)

$$qD_{f} - qD + Vk_{3}A^{2} = V \frac{dD}{dt}$$
 (11c)

We assume that no products are present in the feed, and using the dimensionless variables in (4) along with

$$b = B/A_0$$
 $d = D/A_0$ $K_2 = k_2/k_1$ $K_3 = \tau k_3 A_0$ (12)

we obtain

$$\frac{df_1}{d\theta} = 2 - (1+K_1)f_1 - K_3f_1^2 \tag{13a}$$

$$\frac{df_2}{d\hat{v}} = -(1+K_1)f_2 - K_3f_2^2 \tag{13b}$$

$$\frac{db_{i}}{d\hat{e}} = -(1+K_{2})b_{i} + K_{1}f_{i} , i = 1,2$$
 (13c)

$$\frac{dd_{i}}{d\theta} = -d_{i} + K_{3}f_{i}^{2} , i = 1,2$$
 (13d)

with initial conditions

$$\theta$$
=0: f=f(0); b = 0, d = 0. (13e)

where again the subscript 1 refers to the region of the feed cycle in which the dimensionless feed concentration is 2.0, while the subscript 2 denotes the region in the cycle for which the feed concentration is 0.0. The subscript i indicates the region where the differential equations for b and d apply.

Equations (13a) and (13b) can be solved in a straightforward manner. The solution to (13c) using a series expansion is given by DeVera and Varma [7]. Equation (13d) can be solved with techniques similar to those used for (13c). Making the minor variable substitution in (2), the solutions are

$$f_{1}(\xi) = f_{SS1} \left[\frac{1 + c_{3}\alpha(n\theta_{0})e^{-c_{2}\xi}}{1 - \alpha(n\theta_{0})e^{-c_{2}\xi}} \right]$$
(14a)

$$f_{2}(\xi) = \frac{-c_{1}\bar{\alpha}(j\theta_{0})e^{-c_{1}\xi}}{1 + K_{3}\bar{\alpha}(j\theta_{0})e^{-c_{1}\xi}}$$
(14b)

where

$$c_1 = (1+K_1); c_2 = \sqrt{(1+k_1)^2+8K_3}; c_3 = \frac{c_2+c_1}{c_2-c_1}$$
 (14c)

$$\alpha(n\theta_0) = \frac{2K_3f_1(n\theta_0) + c_1 - c_2}{2K_3f_1(n\theta_0) + c_1 + c_2}$$
(14d)

$$\bar{\alpha}(j\theta_0) = \frac{-f_2(j\theta_0)}{K_3f_2(j\theta_0) + c_1}$$
 (14e)

$$f_{SS^1} = \frac{c_2 - c_1}{2K_3} \tag{14f}$$

and

$$b_1(\xi) = b_1(n\theta_0)e^{-C_4\xi} + f_{SS_1}K_1\left\{\frac{1}{C_4}\sum_{j=0}^{\infty}\psi_1[\xi,j,\alpha(\theta_0)] + c_3\psi_2[\xi,\alpha(n\theta_0)]\right\}$$
(15a)

where

$$\psi_{1}[\xi,j,\alpha] = \begin{cases} \frac{\alpha^{j}}{c_{5}j+1} \left[e^{-c_{2}j\xi}-e^{-c_{4}\xi}\right]; & c_{5}j \neq -1 \\ \\ c_{4}\alpha^{j}\xi e^{-c_{4}\xi} & ; & c_{5}j = -1 \end{cases}$$
(15b)

$$\psi_{2}(\xi,\alpha) = \left\{ \begin{array}{l} \frac{\alpha}{C_{4}-C_{2}} \sum_{j=0}^{\infty} \psi_{3}(\xi,j,\alpha) ; c_{6} \text{ finite} \\ \frac{\alpha}{C_{2}} e^{-C_{4}\xi} \ln \left\{ \frac{[1-\alpha]e^{-C_{2}\xi}}{1-\alpha e^{-C_{2}\xi}} \right\} ; c_{6} = \infty \end{array} \right\}$$
(15c)

$$\psi_{3}(\xi,j,\alpha) = \begin{cases} \frac{\alpha^{j}}{c_{6}j+1} \left[e^{-c_{2}(j+1)\xi} - e^{-c_{4}\xi} \right]; c_{6}j \neq -1 \\ \\ \alpha^{j}(c_{4}-c_{2})\xi e^{-c_{4}\xi} \end{cases}; c_{6}j = -1 \end{cases}$$
(15d)

$$b_2(\xi) = b_2(j\theta_0)e^{-C_4\xi} - K_1c_1\bar{\alpha}(j\theta_0)\psi_4[\xi,\bar{\alpha}(j\theta_0)]$$
 (15e)

$$\psi_{4}(\xi,\bar{\alpha}) = \begin{cases} \frac{1}{K_{1}(K_{2}-1)} \sum_{\ell=0}^{\infty} \psi_{5}(\xi,\ell,\bar{\alpha}) ; K_{2} \neq 1 \\ \frac{e^{-C_{1}\xi}}{C_{1}} \ln \left\{ \frac{e^{C_{1}\xi}+K_{3}\bar{\alpha}}{1+K_{3}\bar{\alpha}} \right\}; K_{2} = 1 \end{cases}$$
(15f)

$$\psi_{5}(\xi,\ell,\bar{\alpha}) = \begin{cases} \frac{\left[-K_{3}\bar{\alpha}\right]^{\ell}}{c_{7}\ell+1} \left[e^{-(\ell+1)c_{1}\xi}-e^{-c_{4}\xi}\right] & ; c_{7}\ell \neq -1 \\ \left[-K_{3}\bar{\alpha}\right]^{\ell} K_{1}(K_{2}-1)\xi e^{-c_{4}\xi} & ; c_{7}\ell = -1 \end{cases}$$
(15g)

$$d_{1}(\xi) = d_{1}(n\theta_{0})e^{-\xi} - \frac{K_{3}f_{SS_{1}}^{2}}{c_{2}} \left\{ -c_{2}[1-e^{-\xi}] + 2(1+c_{3}) \sum_{\ell=1}^{\infty} \psi_{6}[\xi,\ell,\alpha(n\theta_{0})] + (1+c_{3})^{2} \sum_{\ell=2}^{\infty} (\hat{\lambda}-1) \psi_{6}[\xi,\ell,\alpha(n\theta_{0})] \right\}$$
(16a)

$$\psi_6(\xi, \ell, \alpha) = \frac{\alpha^{\ell} C_2}{C_2 \ell - 1} \left[e^{-C_2 \ell \xi} - e^{-\xi} \right]$$
 (16b)

$$d_{2}(\xi) = d_{2}(j\theta_{0})e^{-\xi} - \frac{c_{1}[-\bar{\alpha}(j\theta_{0})]^{1/c_{1}}}{[K_{3}]^{(c_{1}-1)/c_{1}}} \sum_{\ell=0}^{\infty} (\ell+1)\psi_{7}[\xi,\ell,\bar{\alpha}(j\theta_{0})]$$
 (16c)

$$\psi_{7}(\xi, \ell, \bar{\alpha}) = \frac{\left[-\bar{\alpha}K_{3}\right]^{\ell+2-1/c_{1}}}{\ell+2-1/c_{1}} \left[e^{-(\ell+2)c_{1}\xi} - e^{-\xi}\right]$$
(16d)

$$c_4 = 1 + K_2;$$
 $c_5 = \frac{-c_2}{c_4};$ $c_6 = \frac{c_2}{c_2 - c_4};$ $c_7 = \frac{c_1}{K_1(1 - K_2)}$ (16e)

System Behavior

The qualitative behavior of f is identical to the first order case, therefore the solution to f will oscillate regularly, and approach asymptotic limits either from above or below, except in the case where the asymptotic limit is established immediately.

The proof of the limit cycles for $b(\theta)$ and $d(\theta)$ rest on phase plane arguments. Since the form of equations (13c) and (13d) are similar, the phase plane behavior of b(f) and d(f) are also similar.

The differential equations governing the behavior in the phase plane of b(f) and d(f) are obtained by dividing equations (13c) and (13d) by either (13a) or (13b), depending on which region is being considered. Points in the phase plane where $\frac{db}{df}$ or $\frac{dd}{df}$ become zero are found by setting the numerators of these expressions to zero. This is equivalent to solving for the locus of steady state solutions to (13c) and (13d). The loci of zero slope in the phase plane (loci of steady state values) are given by

$$b_{s} = \frac{K_{1}f_{s}}{(1+K_{2})}; d_{s} = K_{3}f_{s}^{2}$$
 (17)

For the purpose of the proof that follows it is sufficient to note that both loci are monotone increasing and pass through the origin. Hence, the proofs for the two cases are similar.

The four differential equations in the phase plane can be represented by

$$\frac{dg_{i}}{df_{i}} = \frac{F(f_{i})-g_{i}}{\beta \frac{df_{i}}{d\theta}} \qquad ; i = 1,2$$
(18)

where g represents either b or d, F(f) is given by equations (17), and β is a positive constant. The numerators of equations (18) will be positive for g < F(f) and negative for g > F(f). Since we know the signs of $\frac{df}{d\theta}$ after oscillation of f has begun, the signs of (18) are known

$$\frac{dg_1}{df_1} > 0 ; g_1 < F(f_1)
\frac{dg_1}{df_1} < 0 ; g_1 > F(f_1)$$
Region 1 (19a)

$$\frac{dg_{2}}{df_{2}} < 0 ; g_{2} < F(f_{2})$$

$$\frac{dg_{2}}{df_{2}} > 0 ; g_{2} > F(f_{2})$$
Region 2 (19b)

Also, from equation (18) and equations (13a,b), it follows that

$$g_{i} = \begin{cases} > 0 & , i = 1 \\ < 0 & , i = 2 \end{cases}$$
 (19c,d)

since $F(f_i)$ is monotone increasing.

The behavior of g will depend on the behavior of f, hence the limit cycle for g cannot precede that of f. Moreover, after f has reached its limit cycle, g need not have yet achieved its limit cycle. At $f(\theta_{\infty})$, g could be in any of three regions of the phase plane, viz., $g < F_1(f_1(n\theta_0)_{\infty}) \equiv F_1$, $g > F(f_2(j\theta_0)_{\infty}) \equiv F_2$ and $g \in [F_1, F_2]$. If $g > F_2(< F_1)$, then from the limit cycle behavior of f and equations (19a,b) g must decrease (increase) until $g \in (F_1, F_2)$. Because of the uniqueness of solution for first order ODEs and the uniqueness of extrema in each region, g will approach a limit cycle bounded by F_1 and F_2 .

Asymptotic Limits and Time Averages

As in the first order case, the first asymptotic limit used as an initial condition over a time θ_0 must give the other asymptotic limit. For f, the initial condition appears twice as shown by equations (14d,e), hence the solution for $f_1(n\theta_0)_{\infty}$ and $f_2(j\theta_0)_{\infty}$ gives quadratics. With persistent analysis, one root can be shown to be negative in both cases. The resultant asymptotic limits are

$$f_2(n\theta_0)_{\infty} = \frac{-c_8 + \sqrt{c_8^2 - 4c_9c_{10}}}{2c_9}$$
 (20a)

$$f_1(j\theta_0)_{\infty} = \frac{-c_{11} + \sqrt{c_{11}^2 - 4c_{12}c_{13}}}{2c_{12}}$$
 (20b)

where

$$c_8 = \phi_1(1-c_{15}) + \phi_2(1+c_{15}) \tag{20c}$$

$$c_9 = \phi_3(1-c_{15}) + \phi_4(1+c_{15})$$
 (20d)

$$c_{10} = c_1(c_1^2 - c_2^2)(1 - c_{15})$$
 (20e)

$$c_{11} = \phi_5 + \phi_6 - 2K_3c_1c_1 + f_{SS_1}(1 + c_3c_{15})$$
 (20f)

$$c_{12} = 2K_3^2(1-c_{14})f_{SS_1}(1+c_3c_{15}) + 2K_3c_1(1-c_{15})$$
 (20g)

$$c_{13} = -c_1c_1 + c_2 + c_3c_1 + c_2 + c_3c_1$$
 (20h)

$$\phi_1 = 2K_3c_1^2c_{14} + 2K_3c_1^2 + K_3(1-c_{14})(c_1^2-c_2^2)$$
 (20i)

$$\varphi_2 = K_3 c_1 c_2 (2 - 4c_{14}) \tag{20j}$$

$$\phi_3 = 2K_3^2 c_1(1+c_{14}) \tag{20k}$$

$$\varphi_4 = 2K_3^2c_2(1-c_{14}) \tag{201}$$

$$\phi_5 = K_3(1-c_{14})f_{SS_1}[c_1+c_2 + c_3c_{15}(c_1-c_2)]$$
 (20m)

$$\phi_6 = c_1[c_1+c_2 - c_{15}(c_1-c_2)] \tag{20n}$$

$$c_{14} = e^{-C_1\theta_0}$$
, $c_{15} = e^{-C_2\theta_0}$ (200)

The assymptotic limits for b are

$$b_1(n\theta_0)_{\infty} = \frac{\psi_8[\theta_0,\alpha(n\theta_0)_{\infty}] - \psi_9[\theta_0,\bar{\alpha}(j\theta_0)_{\infty}]e^{C_4\theta_0}}{2 \sinh(C_4\theta_0)}$$
(21a)

$$b_2(j\theta_0)_{\infty} = \frac{\psi_8[\theta_0,\alpha(n\theta_0)_{\infty}]e^{C_4\theta_0} - \psi_9[\theta_0,\bar{\alpha}(j\theta_0)_{\infty}]}{2 \sinh(C_4\theta_0)}$$
(21b)

$$\psi_{8}[\xi,\alpha] = K_{1}f_{SS_{1}}\left[\frac{1}{c_{+}}\sum_{j=0}^{\infty}\psi_{1}(\xi,j,\alpha) + c_{3}\psi_{2}(\xi,\alpha)\right]$$
 (21c)

$$\psi_{9}[\xi,\bar{\alpha}] = K_{1}c_{1}\bar{\alpha}\psi_{4}(\xi,\bar{\alpha}) \tag{21d}$$

The assymptotic limits for d are

$$d_{1}(n\theta_{0})_{\infty} = \frac{-\psi_{10}[\theta_{0},\alpha(n\theta_{0})_{\infty}]-\psi_{11}[\theta_{0},\bar{\alpha}(j\theta_{0})_{\infty}]e^{\theta_{0}}}{2 \sinh(\theta_{0})}$$
(22a)

$$d_{2}(j\theta_{0})_{\infty} = \frac{-\psi_{10}[\theta_{0},\alpha(n\theta_{0})_{\infty}]e^{\theta_{0}}-\psi_{11}[\theta_{0},\bar{\alpha}(j\theta_{0})_{\infty}]}{2 \sinh(\theta_{0})}$$
(22b)

$$\psi_{10}[\xi,\alpha] = \frac{K_3 f_{SS_1}^2}{c_2} \left[-c_2 (1-e^{-\xi}) + 2(1+c_3) \sum_{\ell=1}^{\infty} \psi_{\ell}(\xi,\ell,\alpha) + (1+c_3) \sum_{\ell=2}^{\infty} (\ell-1) \psi_{\ell}(\xi,\ell,\alpha) \right]$$
(22c)

$$\psi_{11}[\xi,\bar{\alpha}] = \frac{c_1(-\bar{\alpha})^{1/c_1}}{K_3(c_1-1)/c_1} \sum_{k=0}^{\infty} (\ell+1)\psi_7(\xi,k,\alpha)$$
 (22d)

The time averages are obtained by integrating the concentration functions with respect to time over one cycle and dividing by the cycle time. The mathematics are straightforward but laborious. With dedication we obtain

$$\vec{f} = \frac{1}{2\theta_0} \left\{ \frac{1}{K_3} \ln \left[\frac{1 + K_3 \bar{\alpha} (j\theta_0)_{\infty} c_{14}}{1 + K_3 \bar{\alpha} (j\theta_0)_{\infty}} \right] + \frac{f_{SS}}{c_2} \left[\ln \left\{ \frac{1/c_{15} - \alpha (n\theta_0)_{\infty}}{1 - \alpha (n\theta_0)_{\infty}} \right\} + c_3 \ln \left\{ \frac{1 - \alpha (n\theta_0)_{\infty} c_{15}}{1 - \alpha (n\theta_0)_{\infty}} \right\} \right] \right\}$$
(23)

$$5 = \frac{\psi_{12} + \psi_{13}}{2\theta_0} \tag{24a}$$

$$\psi_{12} = \frac{b_1(n\theta_0)_{\infty}}{c_4} (1 - e^{-c_4\theta_0}) + K_1 f_{SS_1} \left[c_3 \psi_{14} + \frac{1}{c_4} \sum_{j=0}^{\infty} \psi_{15}(j) \right]$$
 (24b)

$$\psi_{13} = \frac{b_2(j\theta_0)_{\infty}}{c_4} (1 - e^{-c_4\theta_0}) - K_1 c_1 \bar{a}(j\theta_0)_{\infty} \psi_{17}$$
 (24c)

$$\psi_{14} = \begin{cases} \frac{\alpha(n\theta_0)_{\infty}}{c_4 - c_2} \sum_{j=0}^{\infty} \psi_{16}(j) & ; c_6 \text{ finite} \\ \frac{\alpha(n\theta_0)_{\infty}}{c_2} \left[\frac{c_{15} \ln[1 - \alpha(n\theta_0)_{\infty} c_{15}]}{c_2} + \frac{\ln[1 - \alpha(n\theta_0)_{\infty}] - \ln[1 - c_{15}\alpha(n\theta_0)_{\infty}}{\alpha(n\theta_0)_{\infty} c_2} + \right] \\ \theta_0 c_{15} - \frac{c_{15} \ln[1 - \alpha(n\theta_0)_{\infty}]}{c_2} & ; c_6 = \infty \end{cases}$$
(24d)

$$\psi_{16}(j) = \begin{cases} \frac{\alpha(n\theta_0)^{j}_{\infty}}{c_6 j + 1} & \left\{ \frac{1 - c_{15}^{(j+1)}}{(j+1)c_2} - \left[\frac{1 - e^{-c_4 \theta_0}}{c_4} \right] \right\}; c_6 j \neq -1 \\ \frac{\alpha(n\theta_0)^{j}_{\infty}}{c_4} & \left(c_4 - c_2 \right) \left[\frac{1 - e^{-c_4 \theta_0}}{c_4} - \theta_0 e^{-c_4 \theta_0} \right]; c_6 j = -1 \end{cases}$$
(24e)

$$\psi_{15}(j) = \begin{cases} \frac{\alpha(n\theta_0)^{j}}{c_5 j + 1} \begin{cases} \frac{1 - c_{15}^{j}}{c_2 j} ; j \neq 0 \\ \theta_0 ; j = 0 \end{cases} - \frac{1 - e^{-c_4 \theta_0}}{c_4} ; c_5 j \neq -1 \\ \alpha(n\theta_0)^{j}_{\infty} \left[\frac{1 - e^{-c_4 \theta_0}}{c_4} - \theta_0 e^{-c_4 \theta_0} \right] ; c_5 j = -1 \end{cases}$$
(24f)

$$\psi_{17} = \begin{cases} \frac{1}{K_{1}(K_{2}-1)} \sum_{\ell=0}^{\infty} \psi_{18}(\ell) & ; K_{2} \neq 1 \\ \frac{c_{14}}{c_{1}^{2}} \ln \left[\frac{1+K_{3}\bar{\alpha}(j\theta_{0})_{\infty}}{1/c_{13}+K_{3}\bar{\alpha}(j\theta_{0})_{\infty}} - \frac{1}{c_{1}^{2}K_{3}\bar{\alpha}(j\theta_{0})_{\infty}} \ln \left[\frac{1+K_{3}\bar{\alpha}(j\theta_{0})_{\infty}c_{14}}{1+K_{3}\bar{\alpha}(j\theta_{0})_{\infty}} \right]; K_{2}=1 \end{cases}$$
(24g)

$$\psi_{18}(\ell) = \begin{cases} \left[\frac{-K_{3}\bar{\alpha}(j\theta_{0})_{\infty}}{c_{7}\ell + 1} \right]^{\ell} & \left[\frac{1-c_{14}^{(\ell+1)}}{(\ell+1)c_{1}} - \frac{1-e^{-c_{4}\theta_{0}}}{c_{4}} \right]; c_{7}\ell \neq -1 \\ \\ \left[-K_{3}\bar{\alpha}(j\theta_{0})_{\infty} \right]^{\ell} & \frac{K_{1}(K_{2}-1)}{c_{4}} & \left[\frac{1-e^{-c_{4}\theta_{0}}}{c_{4}} - \theta_{0}e^{-c_{4}\theta_{0}} \right]; c_{7}\ell = -1 \end{cases}$$
(24h)

$$\bar{d} = \frac{\psi_{19} + \psi_{20}}{2\theta_0}$$
 (25a)

$$\psi_{19} = d_{1}(n\theta_{0})_{\infty}(1-e^{-\theta_{0}}) - \frac{K_{3}f_{SS1}^{2}}{c_{2}} \left\{ c_{2}[1-\theta_{0}-e^{-\theta_{0}}] + 2(1+c_{3}) \sum_{\ell=1}^{\infty} \psi_{21}(\ell) + (1+c_{3})^{2} \sum_{\ell=2}^{\infty} (\ell-1)\psi_{21}(\ell) \right\}$$
(25b)

$$\psi_{21}(l) = \alpha (n\theta_0)_{\infty}^{l} c_2 \frac{1}{lc_2-1} \frac{1-e^{lc_2\theta_0}}{lc_2} + e^{-\theta_0}-1$$
 (25c)

$$\psi_{20} = d_2(j\theta_0)_{\infty}(1-e^{-\theta_0}) - \frac{c_1[-\bar{\alpha}(j\theta_0)_{\infty}]^{1/c_1}}{K_3^{(c_1-1)/c_1}} \sum_{m=0}^{\infty} (m+1)\psi_{22}(m)$$
 (25d)

$$\psi_{22}(m) = \frac{c_1[-\bar{\alpha}(j\theta_0)_{\infty}K_3]}{(m+2)c_1-1} \begin{bmatrix} \frac{1-e^{-(m+2)c_1\theta_0}}{(m+2)c_1} + e^{-\theta_0} - 1 \end{bmatrix}$$
(25e)

$$\alpha(n\theta_0)_{\infty} = \frac{2K_3f_1(n\theta_0)_{\infty} + c_1 - c_2}{2K_3f_1(n\theta_0)_{\infty} + c_1 + c_2}$$
(25f)

and

$$\bar{\alpha}(j\theta_0)_{\infty} = \frac{-f_2(j\theta_0)_{\infty}}{K_3 f_2(j\theta_0)_{\infty} + c_1}$$
(25g)

CALCULATIVE RESULTS

All of the solutions presented are exact analytic solutions.

Unfortunately, the complexity of the results has frustrated all efforts to draw a priori conclusions. This reduces the analysis of the results to the examination of the trends calculated from the analytic expressions. Numerical simulation of the process was performed as a check. The analytic predictions match the numerical simulation with deviations on the order of the accuracy of the simulation technique using the IMSL subroutine DVOGER.

Table 1 shows the predicted enhancement of the time average outlet concentrations over the corresponding steady state outlet concentrations. As mentioned in the section on the method of comparison, the comparisons for f and d are made with the periodic residence time equal to that of the steady state (nonperiodic) process, while b is compared with the optimum steady state b_s [8].

TABLE 1. Enhancement of time average periodic concentrations over steady state concentrations. Approximation to consecutive reactions when $K_3{\simeq}0$. Approximation to second order reaction when $K_1{\simeq}0$, $K_2{\simeq}0$.

# 1	F- 	1 1 1 1 1 1 1 1 1 1 1 1 1 1 1 1 1 1 1	# 1 1 1 1 1 1 1 1 1 1 1 1 1 1 1 1 1 1 1	2)	(^c ₁ -c _{ss})/c _{ss} ·100	00		1. 1. 1. 1. 1. 1. 1. 1. 1. 1. 1. 1. 1. 1	•	• • • • • • • • • • • • • • • • • • •	2)	(C ₁ -C _{SS})/C _{SS} -100	•100
بر	K ₂	κ.	0 :	-	٩	P	ж	, K	, K	0.0	٠	p	Р
-	-	-	Τ.	070	070	.347	<i>-</i>	-	Ģ	Ξ.	.007	031	;
<u>-</u> :	-	-	-	- 4.02	- 4.02	19.4	-	-	0ر	-	.014	004	:
<u>.</u> :	-	-	10.	-10.7	-10.7	51.7	<u>-</u> :	-	0ر	.01	.007	900	;
.0	-	-	- .	073	-66.4	8.97	-	10.	۶	- .	.007	-34.1	;
.0		-	-	65	9.99-	79.3	<u>-</u>	.01	0ء	-	.014	-34.1	;
10.	-	-	10.	11	9.99-	95.0	<u>-</u>	.01	<u>2</u>	10.	.007	-34.1	:
<u>-</u> :	10.	-	-	070	-24.9	.35	.00	-	۲.0	- .	0	-81.7	1
<u>-</u> :	10.	-	-	- 4.02	-27.9	19.4	.01	-	٠٠	-	0	-81.7	:
-	10.	-	10.	-10.7	-32.9	51.7	٠٠.	-	0-	10.	0	-81.7	;
-:	-	.01	-	520	520	.45	٥٠	9	-	٦.	007	;	60.
-	-	10.	-	-12.4	-12.4	10.7	ۍ	٠0	-	_:	67	;	7.4
-:	-	10.	10.	-21.5	-21.5	18.5	5	9	-	10	- 5.5	;	61.0
10.	10.	-	-	073	-84.2	8.96	3	9	-	-	90	;	Ξ.
10.	10.	-	-	65	-84.3	79.3	ۍ	9	٦.	-	- 4.1	;	9.9
10.	10.	<u>.</u> :	10.	11	-84.3	95.2	3	0ر	٦.	10.	-16.7	;	27.0
-:	10.	10.	-	52	-33.0	.46	3	9	10.	٦.	46	:	.40
-	10.	10.	-	-12.4	-41.0	10.7	3	9	10.	-	-12.0	;	4.4
<u>-</u> :	10.	10.	10.	-21.5	-47.1	18.5	3	0ر	10.	.01	-24.0	:	8.9
10.	10.	10.	τ.	67	-83.4	8.73							
10.	10.	10.	-	- 4.96	-84.1	64.6							
10.	10.	10.	10.	- 5.84	-84.2	0.97							

Several trends can be distinguished from the data. Except for very small deviations in the case of consecutive reactions, conversion is enhanced for all of the constants examined. Frustrating the objective of the study is the result that periodic operation appears to be always detrimental to the yield of intermediate b. The only encouraging result is that the time average concentration of d is enhanced for all of the constants examined. The drop in f ranges from 0-21.5%, while b drops 0-84.3%. d, however, is enhanced by as much as 95% over the steady state.

d is most enhanced when the kinetic constants favor the formation of b and c. This is logical, since the rate of formation of d is second order in f, while the formation of b is first order in f. By increasing the feed concentration, the amount of f in the reactor is increased. The rate of reaction of d grows as the square of that for b, hence production of d should rise. If, however, the kinetic constants already favor the formation of d, then mostly d would be formed without cycling, making the possible enhancement small.

The effect of cycling on enhancement increases as the period θ_0 increases. The influence of large θ_0 is shown in Figure 2. Notice the concentrations spend a large fraction of their time close to the respective steady state for the region. This configuration approaches a single CSTR with feed concentration equal to twice that of the steady state process being compared, operated for one half the total length of time.

The approximation to consecutive kinetics where $K_3\sim 0$ has two distinctive characteristics. First, there is virtually no enhancement in f (Table 1). The apparent loss of production of b comes about because this comparison is made against the optimum b_s . When compared to the steady state with the same residence time as the periodic process, the

periodic time averages closely match b_s . Second, there is no change in enhancement (b or f) as θ_0 is varied. Both of these trends should be expected, since the consecutive system is completely linear.

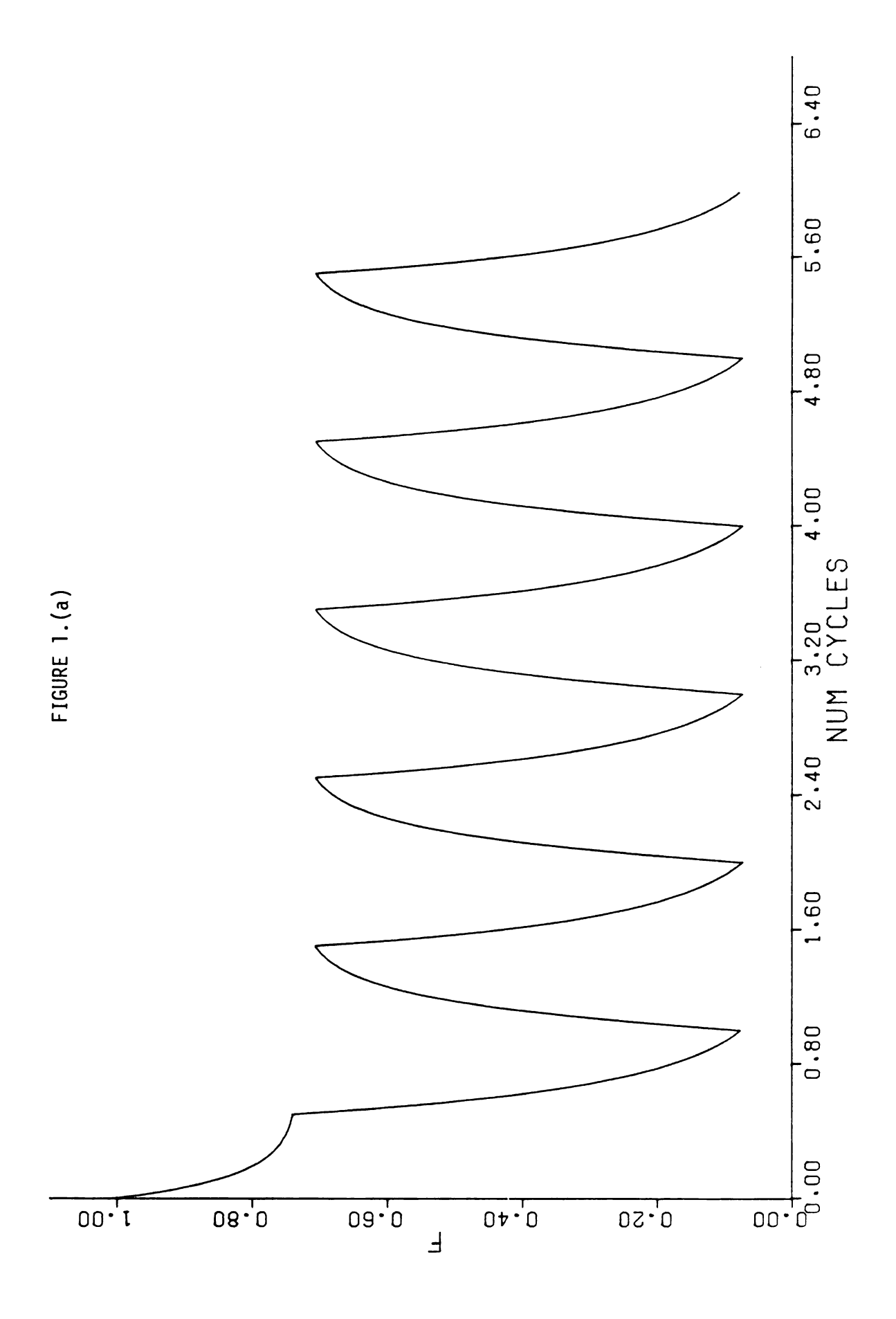
Figures 1, 2, and 3 show the system behavior for 3 different combinations of kinetic constants and cycling frequencies. Figure 1 is a case of intermediate cycling frequency with θ_0 = 1. Figure 2 shows a system which gives 51% enhancement of d. This is slow cycling, with θ_0 = 10. As mentioned, the concentrations are near their respective steady states most of the time. It is also interesting that the trajectory in the b-f phase plane need not stay close to the locus of steady states. This behavior is expected for quasi-steady state operation where the change in the process input occurs so slowly that the system always stays near the steady state corresponding to the inlet condition. The rapid switching of feed concentration, however, makes this case different from quasi-steady state.

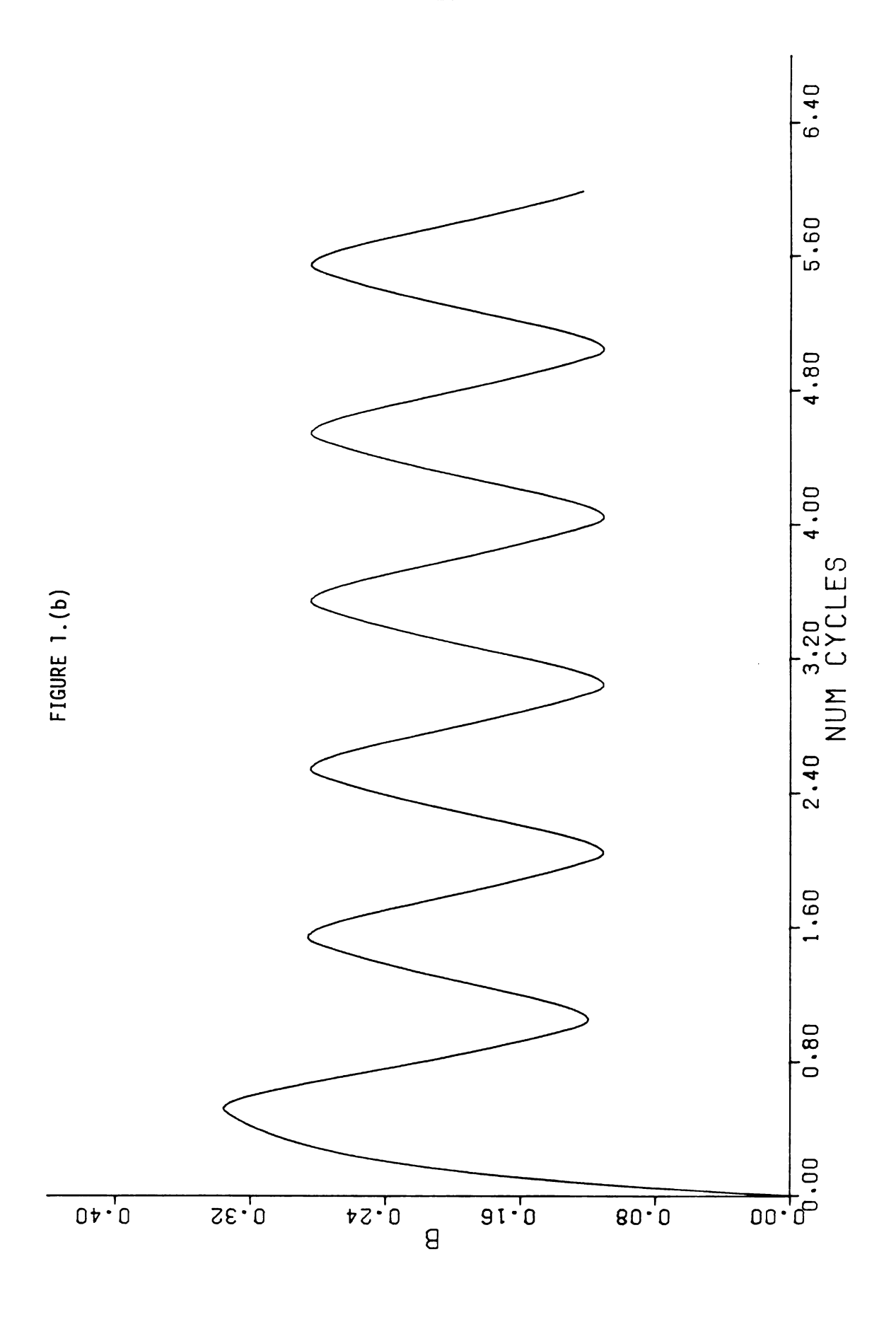
Figure 3 shows a case of rapid cycling with θ_0 = .3. The concentrations are rapidly changing most of the time, and many cycles are required for the system to approach a limit cycle. The magnitudes of the oscillations are small compared to slower cycling.

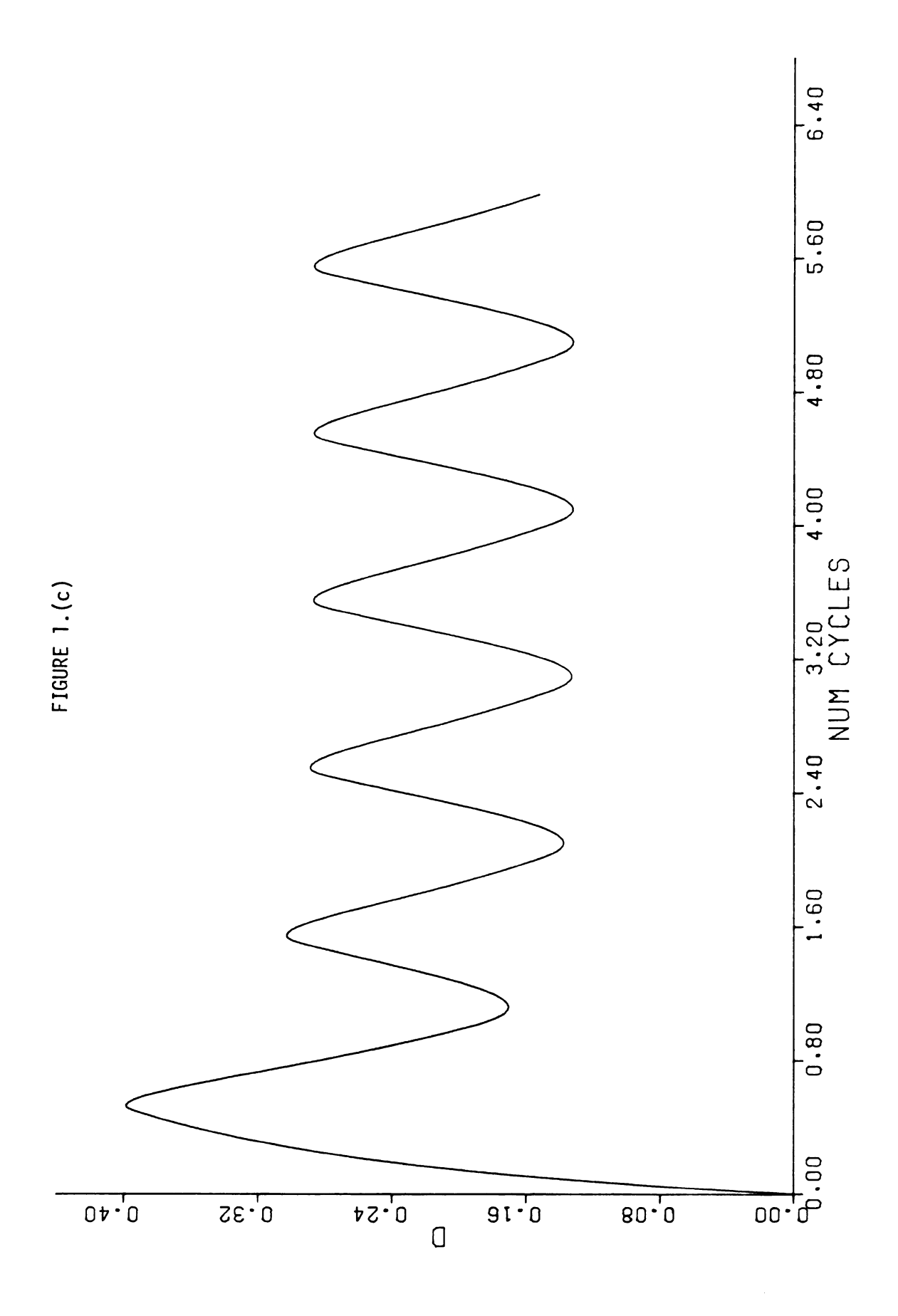
CONCLUSIONS

The analytic expressions for time average outlet concentrations resulting from square wave cycling of feed concentration to an isothermal CSTR with Van de Vusse kinetics are apparently too complicated to yield qualitative a priori predictions. Analysis of trends resulting from various system constants shows that time average concentrations of f and b appear always less than the corresponding steady state concentrations. Time average of f compares with the steady state process having the same residence time as the periodic process while the time average of b is

FIGURE 1.(a-d) Behavior of the Van de Vusse system for a case of intermediate cycling frequency. $K_1 = K_2 = K_3 = 1$, $\theta_0 = 1$.







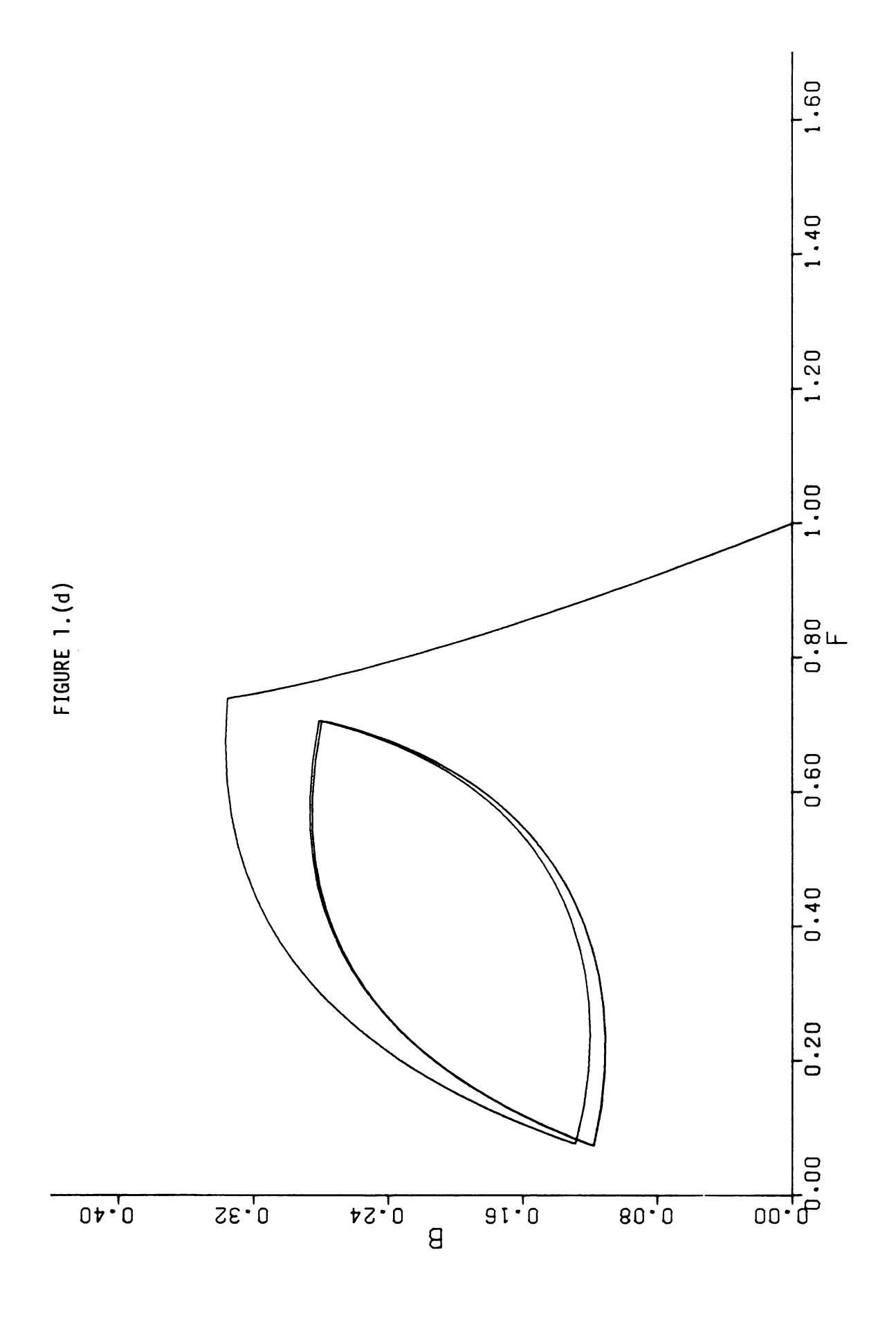
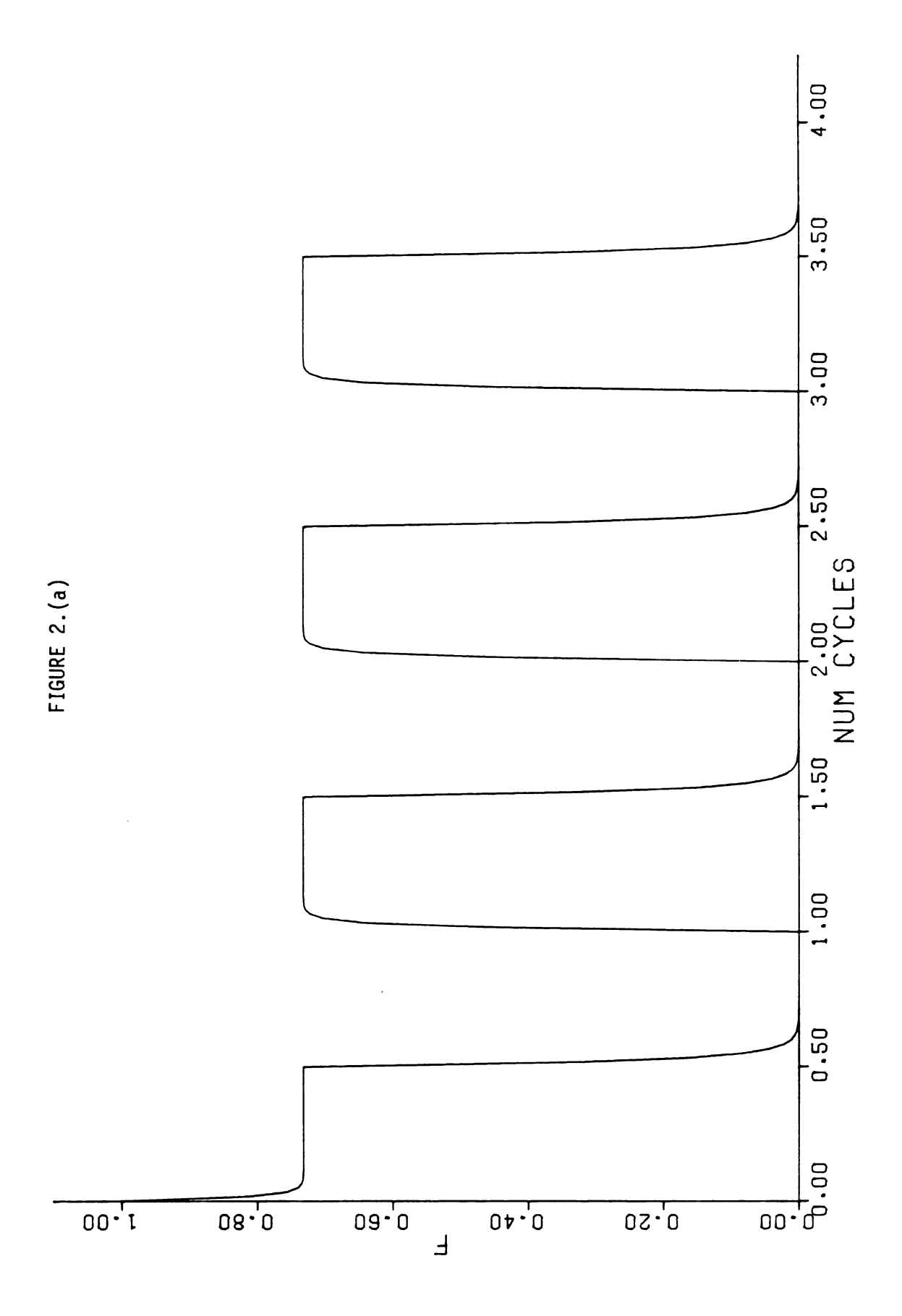
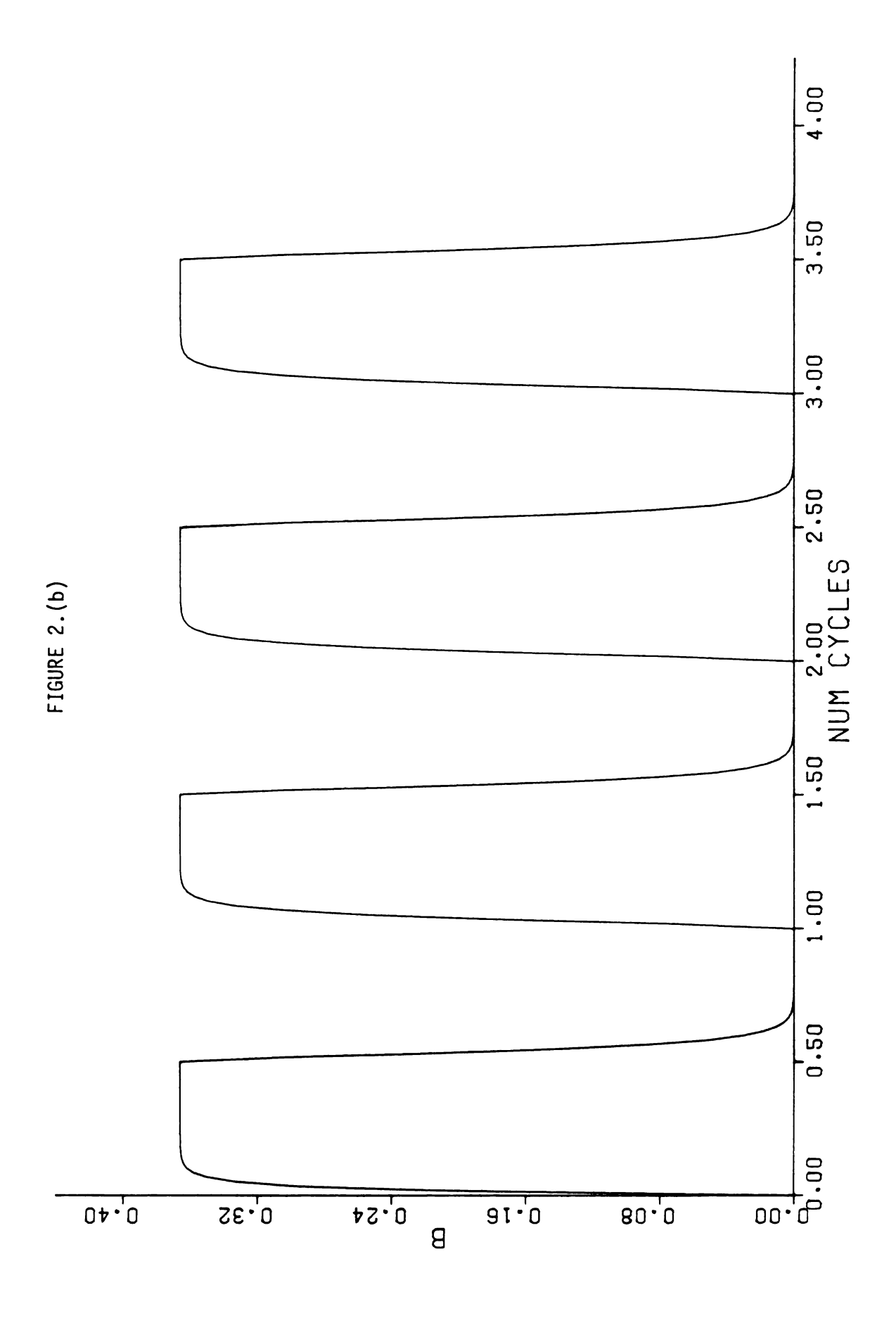
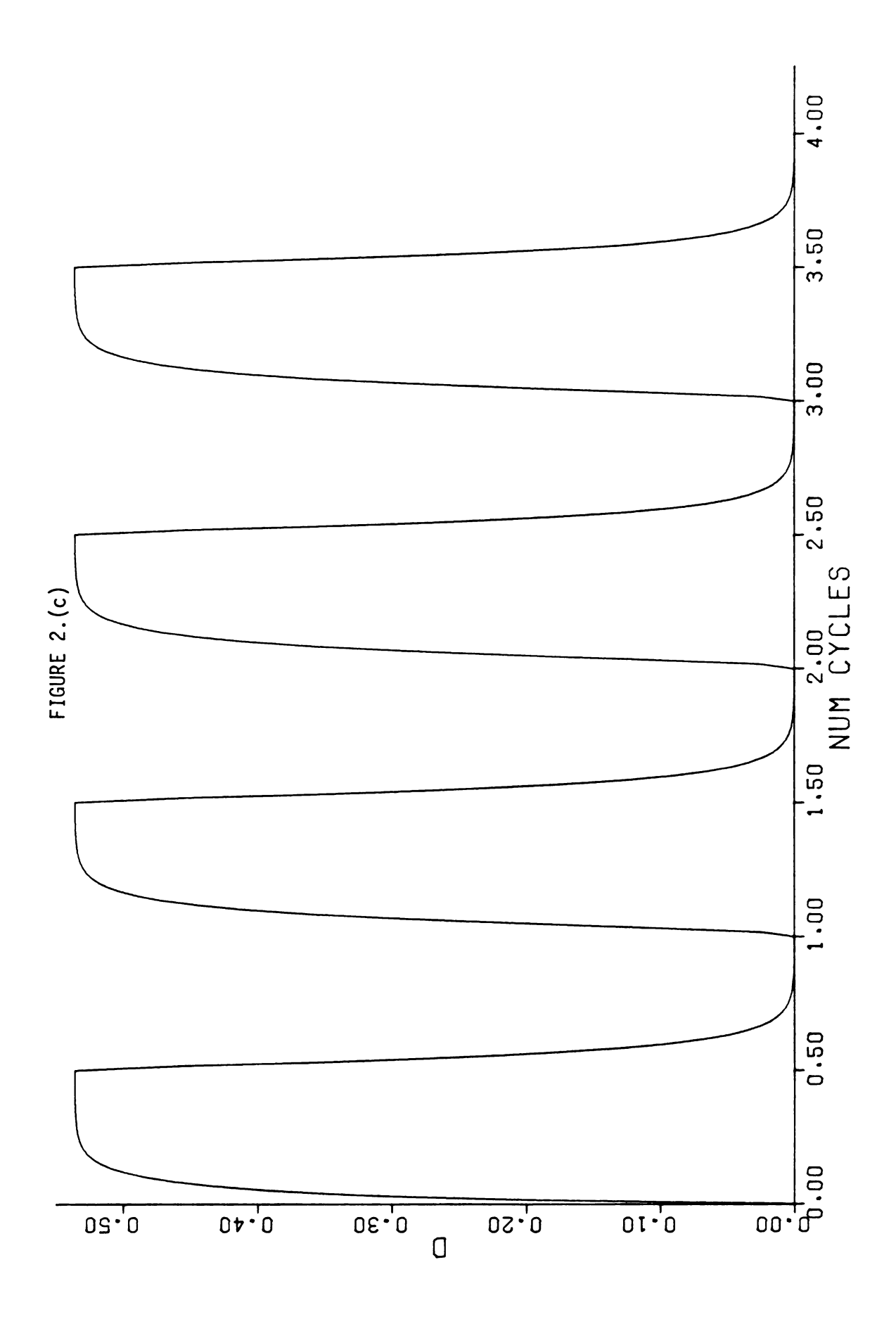


FIGURE 2.(a-d) Behavior of the Van de Vusse system for a case of slow cycling frequency. K_1 = K_2 = K_3 = 1, θ_0 = 10.







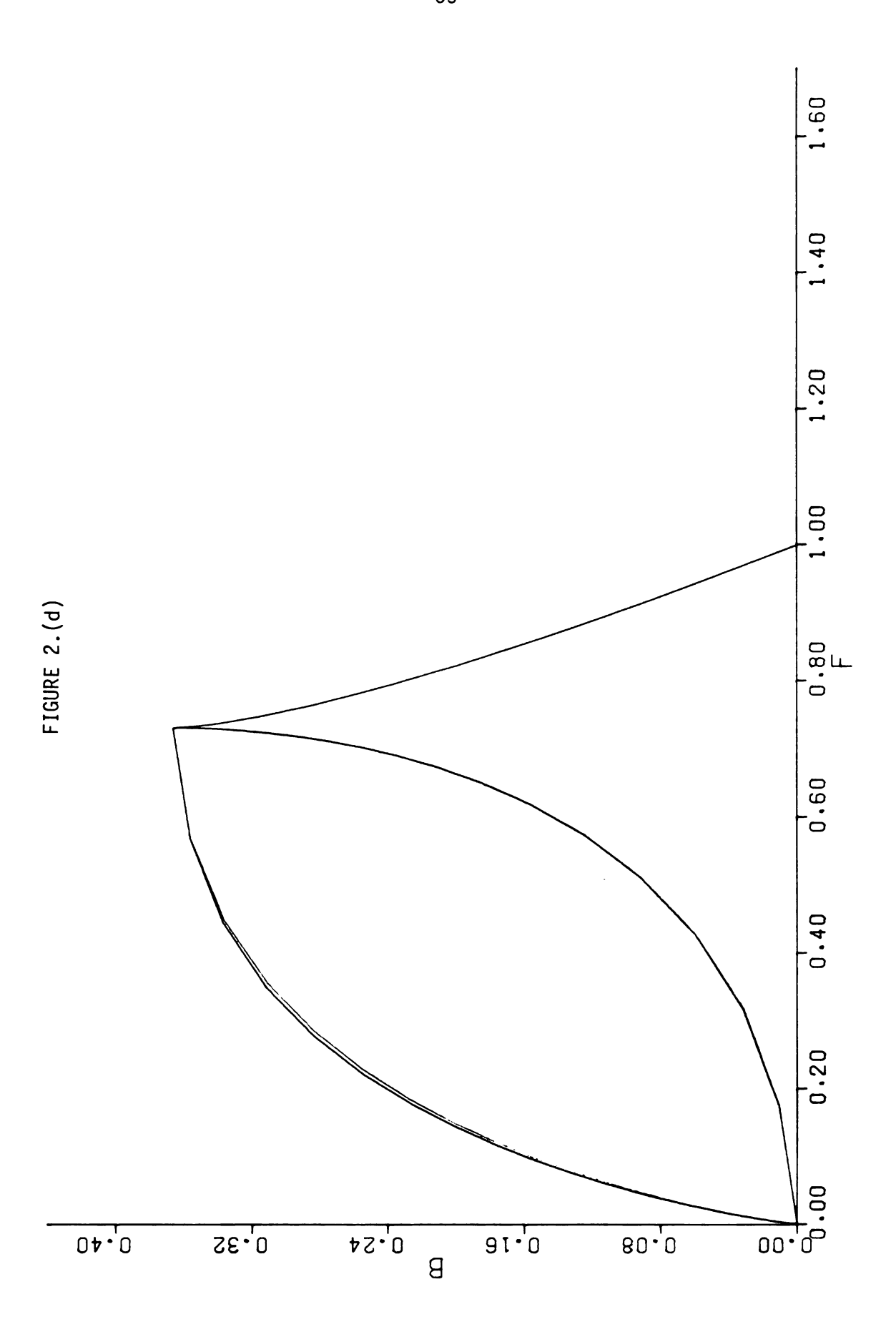
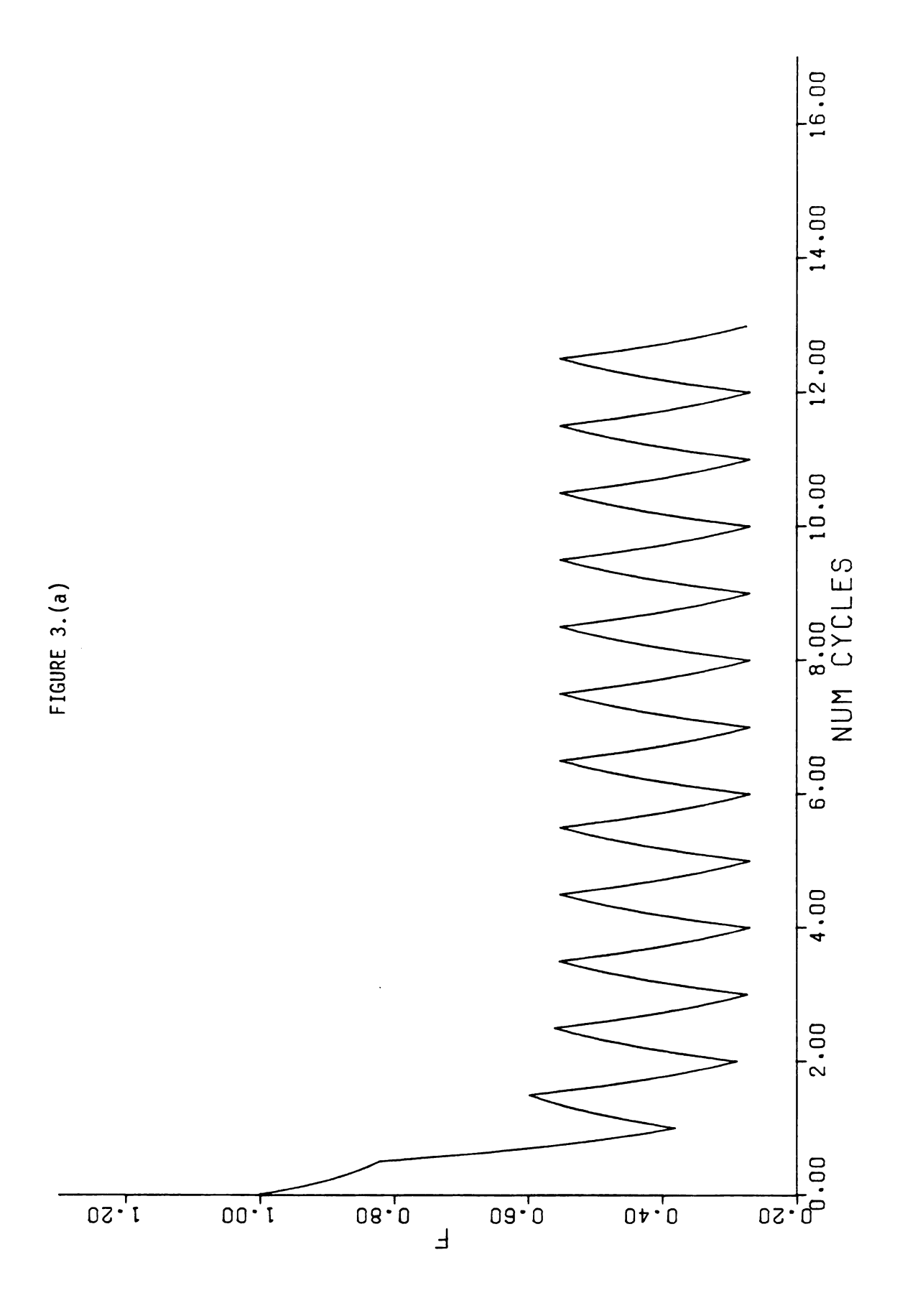
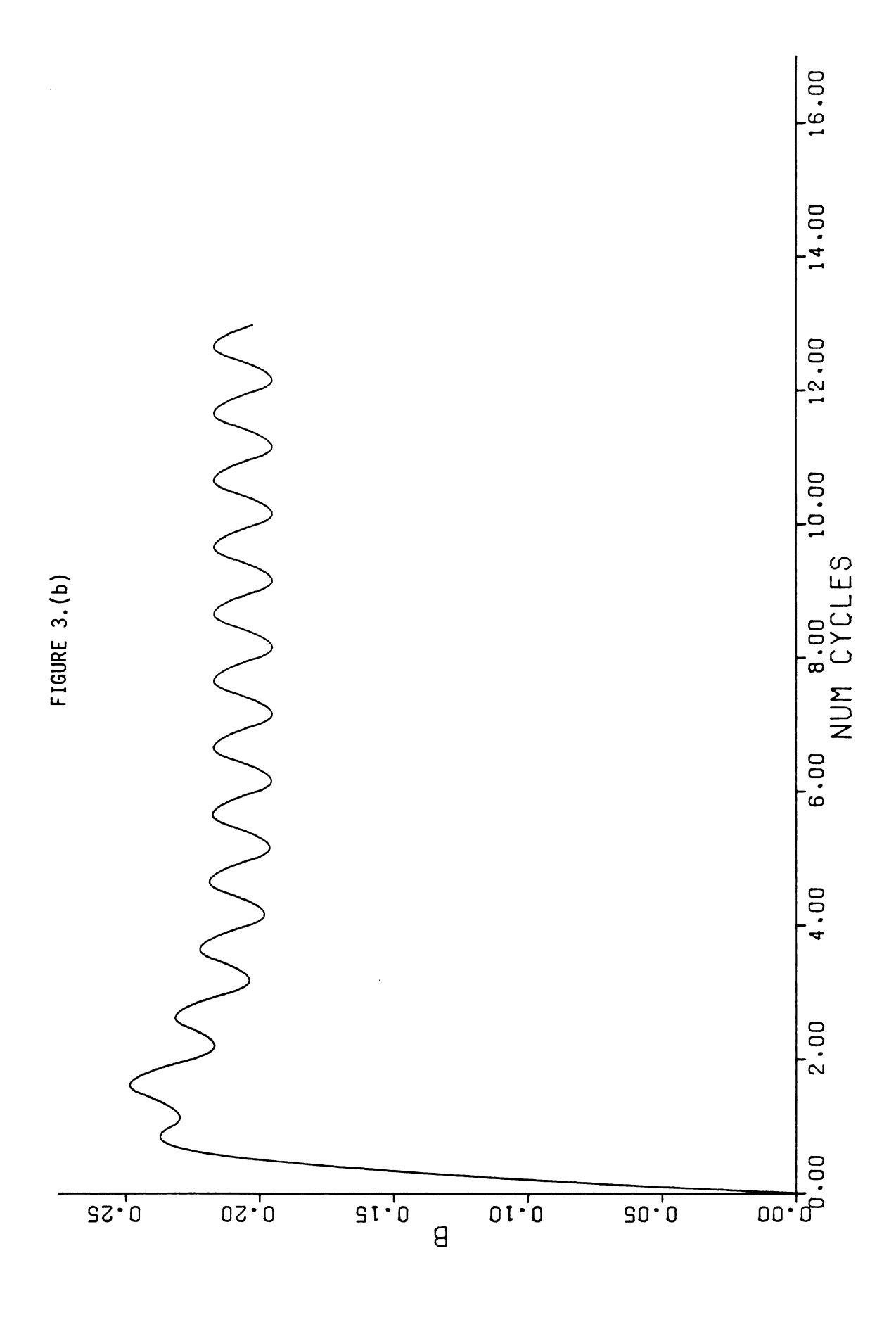
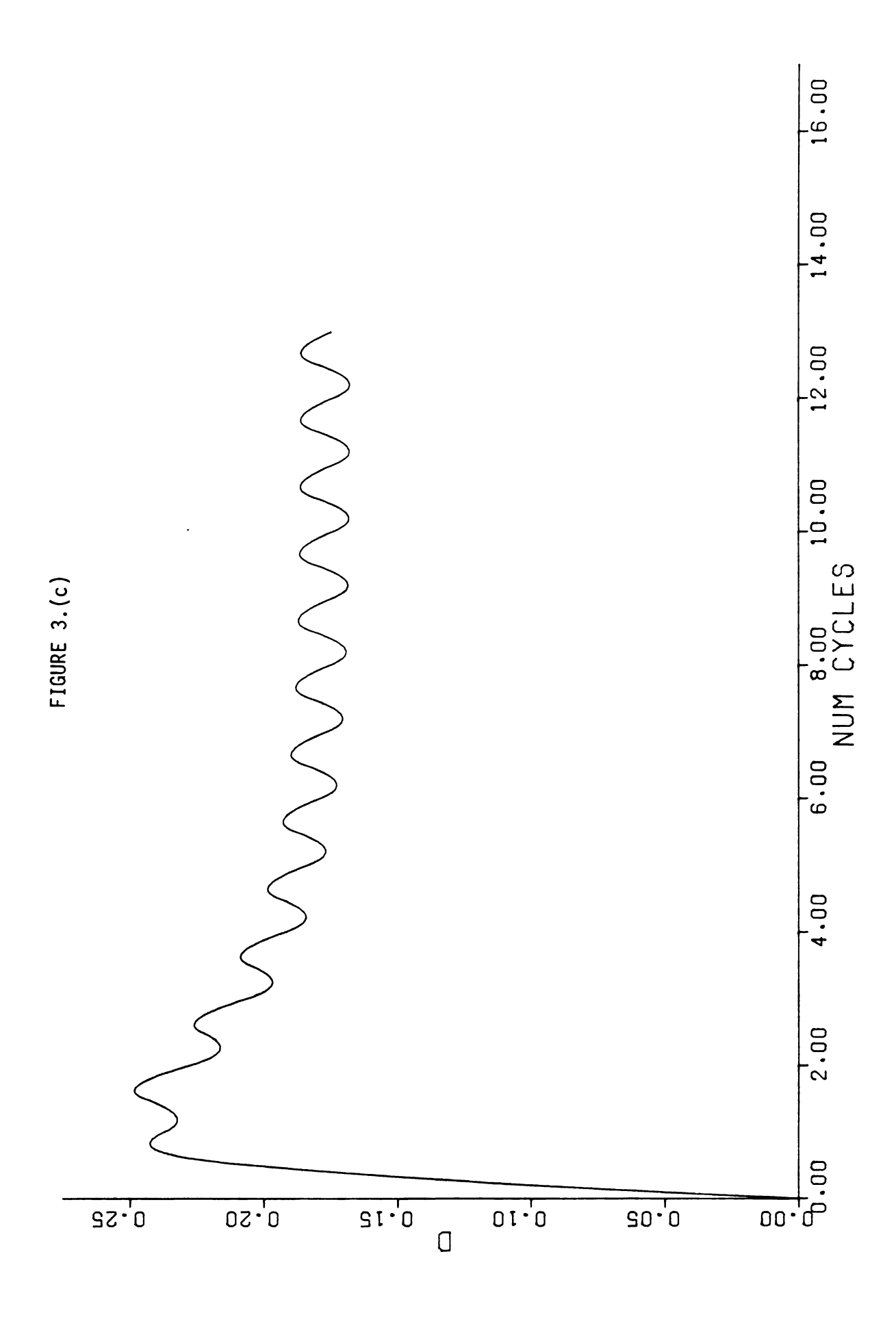
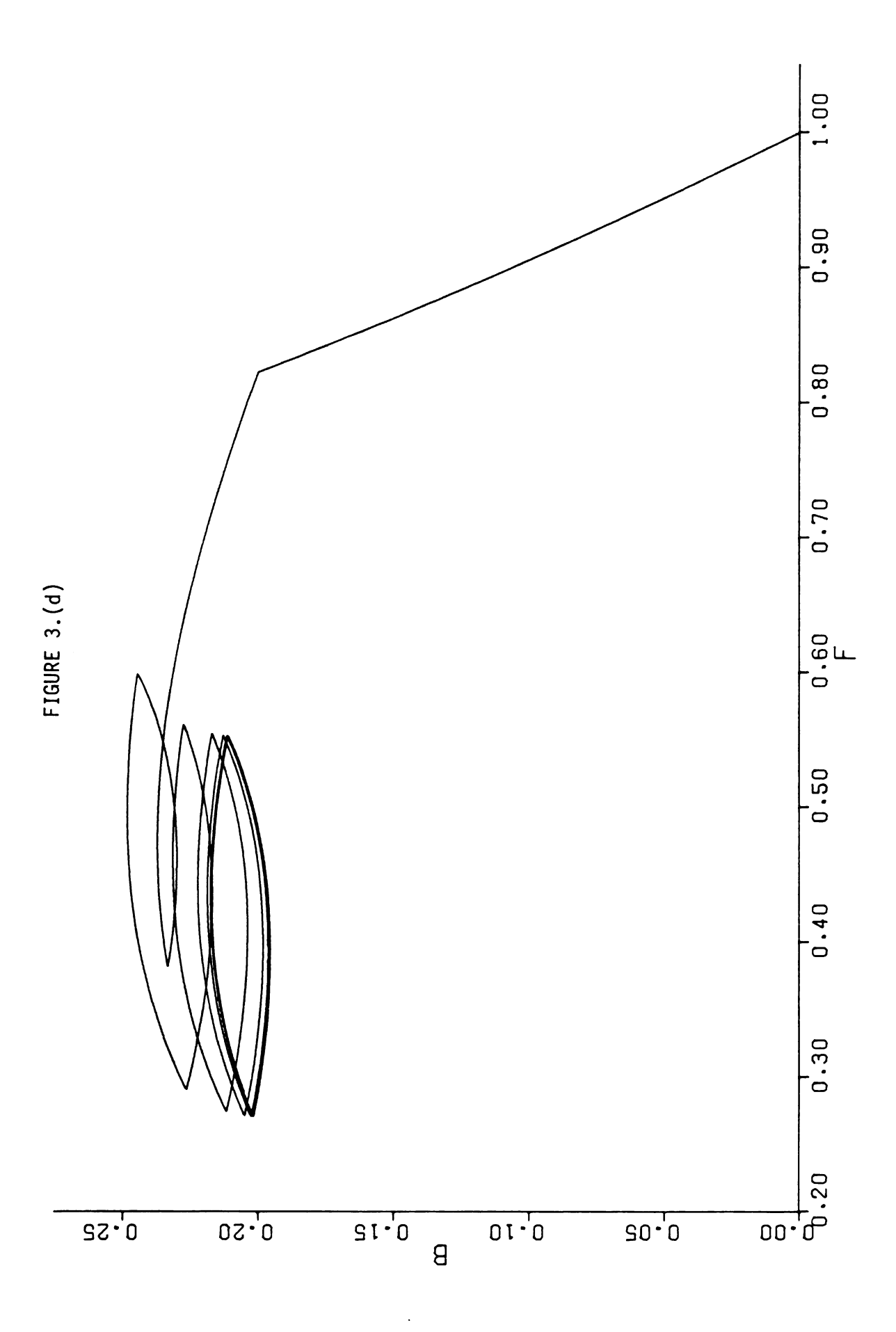


FIGURE 3.(a-d) Behavior of the Van de Vusse system for a case of rapid cycling frequency. K_1 = K_2 = K_3 = 1, θ_0 = .3.









always compared with the optimum steady state. Time average concentration of d appears always greater than the corresponding steady state with residence time equal to the periodic process. The subcase of consecutive kinetics shows no change under periodic operation. The subcase of second order kinetics has its product distribution shifted toward d and away from f. Hence square wave cycling of feed concentration appears detrimental whenever b is desired, and the optimum steady state process should be used. When d is desired, square wave cycling of feed concentration can give enhancement close to 100% over steady state operation.

Periodic operation of porous catalytic systems is only beginning to be explored [9] [10] [11] [12]. The interaction of diffusion within a catalyst pellet with cycled feed concentration to the bathing medium adds a new dimension to the problems so far considered. The coupling of the mass balances for the medium and the catalyst pellet, combined with a complex kinetics makes this a challenging problem, and it is currently being studied by these authors.

CHAPTER 2

PERIODIC SINUSOIDAL FEED CONCENTRATION TO A HOMOGENEOUS ISOTHERMAL CSTR WITH A VAN DE VUSSE REACTION NETWORK

Chemical reactors operated under forced periodic operation sometimes give time average outlet concentrations which differ from the corresponding steady state concentrations. This is generally observed when the governing mass balances contain a non-linear term, either from non-linear kinetics, or, for non-isothermal systems, from the exponential temperature dependence of one or more kinetic rate constants. A good deal of theoretical research in this area has focused on kinetic schemes in which conversion is the only economically important criterion, probably because this approach avoids the complicated expressions which result from more complex kinetics. Conversion can usually be increased, however, by simply using a larger reactor at steady state, and this provides a much simpler remedy.

A potential application of periodic reactor operation is in complex kinetics for which the yield of a desired intermediate product exhibits an absolute steady state maximum. A simple example is the consecutive reaction $A \rightarrow B \rightarrow C$. More difficult problems, which are considered here, are the kinetics scheme proposed by Van de Vusse $A \rightarrow B \rightarrow C$ and $2A \rightarrow D$, and the consecutive-parallel reactions $A \rightarrow B \rightarrow C$ and $A \rightarrow D$, in both of which the desired product is the intermediate B.

Douglas and coworkers have done a substantial amount of work on isothermal systems in this area. Douglas and Rippin [1] considered a sinusoidal feed concentration input to an isothermal CSTR with a second order, irreversible reaction. Using numerical simulation, they were able to show a very small increase in conversion for small amplitude variations in feed composition. Douglas [2] considered the same problem using a perturbation approach in which he introduced an arbitrary perturbation parameter. He was able to show good agreement of his analytical and numerical work, reinforcing the conclusions in [1]. Dorawala and Douglas [3] considered both parallel and consecutive reactions, using a sinusoidal flow

rate disturbance. They were able to show small (.3%, .02%) improvements in yield over the steady state system. Other investigators [4,5,6,7,10] have looked at different aspects of forced periodic operation of reactors.

Bailey [8] provides a review of work through 1973.

We have presented [13] analysis of the Van de Vusse system taking place in an isothermal CSTR under square wave cycling of the feed concentration. The results presented there were exact analytic predictions of the time average outlet concentrations which, unfortunately, frustrated all efforts to draw a priori conclusions as to the direction of change. In this work, using a very accurate approximation, we are able to draw a priori conclusions as to the direction of change of the time average concentrations from the steady state concentrations. This is most valuable, since it gives the relative effectiveness of cycling independent of the system constants, without resorting to numerical calculations.

THE METHOD OF COMPARISON

In order to make a meaningful comparison of steady state operation to periodic operation, several conditions must be observed.

(1) Residence time: For those products for which steady state operation can be made as effective as desired by simply using a longer residence time (for example, the reactant A in both the consecutive-parallel and Van de Vusse schemes), the comparison is based on the same residence time for both periodic and steady state operation. For those products which exhibit an absolute maximum concentration with respect to residence time in steady state mode, the periodic residence time which produces the largest time average concentration is used. Any increase over the steady state maximum, regardless of residence time, is clearly beneficial.

- (2) Equal time average molar flow rates of reactant species into the reactor must be used in periodic and steady state mode.
- (3) Initial transients are ignored. For the steady state mode, only the steady state concentrations are considered. For the periodic mode, time averages are taken only after the effluent concentrations achieve a stable repetitive cycle (limit cycle).
 - (4) Volumetric flow rate does not vary with time in the periodic process.

CONSECUTIVE PARALLEL REACTIONS

Basic Equations

For consecutive parallel reactions taking place in an isothermal CSTR, the transient mass balances for A and B are:

$$qA_{f} - qA - (k_1+k_3)AV = V \frac{dA}{dt}$$
 (1a)

$$qB_{f} - qB - (k_{2}B - k_{1}A)V = V \frac{dB}{dt}$$
 (1b)

Here we take the feed concentration of B to be zero. The disturbance of the inlet concentration of reactant is given by

$$A_{f} = A_{o} [1 + \varepsilon \sin(\omega t)]$$
 (2)

where ϵ is a parameter adjustable between zero and one and ω is the frequency of the input disturbance. Introducing the dimensionless variables:

$$f \equiv \frac{A}{A_0}$$
, $b \equiv \frac{B}{A_0}$, $\tau \equiv \frac{V}{Q}$, $\theta \equiv \frac{t}{\tau}$, $\Lambda \equiv \omega \tau$ (3)

and substituting equation (2) gives for equations (1)

$$\frac{df}{d\theta} + [1 + \tau(k_1 + k_3)]f = 1 + \varepsilon \sin \Lambda\theta$$
 (3a)

$$\frac{db}{d\theta} + (1 + \tau k_2)b = \tau k_1 f \tag{3b}$$

with initial conditions

$$\theta = 0$$
: $f = f(0)$; $b = 0$ (3c)

Analytic Solutions

The solutions to (3) are easily found to be

$$f(\theta) = \frac{1}{a_{22}} + \frac{\epsilon \{a_{22} \sin \Lambda \theta - \Lambda \cos \Lambda \theta\}}{a_{22}^2 + \Lambda^2} + a_{31} \exp(-a_{22}\theta)$$
 (4)

$$b(\theta) = \tau k_1 \left[\frac{1}{a_{11}a_{12}} + \frac{\varepsilon}{(a_{22}^2 + \Lambda^2)(a_{11}^2 + \Lambda^2)} \left[(a_{11}a_{22} - \Lambda^2) \sin \Lambda \theta - A_{11}a_{22} \right] + \left\{ a_{31}\theta \exp(-a_{11}\theta); a_{11} = a_{12} \right\} + a_{32}\exp(-a_{11}\theta)$$

$$\frac{a_{31}\exp(-a_{22}\theta)}{a_{31}\exp(-a_{22}\theta)}; a_{11} \neq a_{12}$$

where

$$a_{22} \equiv 1 + \tau(k_1 + k_3); \ a_{11} \equiv 1 + \tau k_2; \ a_{31} \equiv f(0) - \frac{1}{a_{22}} + \frac{\varepsilon \Lambda}{a_{22}^2 + \Lambda^2}$$
 (6a)

$$a_{32} = -\tau k_1 \left[\frac{1}{a_{11}a_{12}} + \frac{\varepsilon \Lambda(a_{11}+a_{12})}{(a_{22}^2+\Lambda^2)(a_{11}^2+\Lambda^2)} + \begin{cases} 0 & ; a_{11} = a_{12} \\ \frac{c}{a_{11}-a_{22}} & ; a_{11} \neq a_{12} \end{cases} \right]$$
 (6b)

The solutions are periodic with the same frequency as the input disturbance.

Evaluation of Enhancement

The time average limit cycle concentrations are found by taking the limits of (4) and (5) as θ becomes large, integrating over one cycle, and dividing by the cycle time $\Lambda/2\pi$. The terms containing the constants in both equations vanish as θ becomes large, and the contributions from the integrals of the sin and cos terms are zero, giving the time average reactant concentrations

$$\overline{f} = \frac{1}{a_{22}} \tag{7a}$$

$$\delta = \frac{\tau k_1}{a_{11}a_{22}} \tag{7b}$$

The right hand sides of equations (7) are just the steady state values of f and b corresponding to ε = 0. Hence we see that for consecutive-parallel reactions, sinusoidal forcing of the inlet concentration gives time average outlet concentrations equal to the corresponding steady state values.

VAN DE VUSSE KINETICS

Basic Equations

The reaction scheme

$$k_1$$
 k_2 k_3 $A \rightarrow B \rightarrow C$, $A + A \rightarrow D$

was proposed by Van de Vusse [9] as a simple example that defied general reactor selection guidelines. The transient mass balances for this kinetics in an isothermal CSTR are

$$V \frac{dA}{dt} = qA_f - qA - k_1VA - k_3VA^2$$
 (8a)

$$V \frac{dB}{dt} = qB_f - qB - k_2VB + k_1VA$$
 (8b)

$$V \frac{dC}{dt} = qC_f - qC + k_2BV$$
 (8c)

$$V \frac{dD}{dt} = qD_f - qD + k_3A^2V$$
 (8d)

Imposing the condition in (2) and using the dimensionless variables in (3) and $b_f = c_f = d_f = 0$ we obtain

$$\frac{df}{d\theta} + c_1 f + \frac{c_2}{2} f^2 = 1 + \varepsilon \sin \Lambda\theta$$
 (9a)

$$\frac{db}{d\theta} + c_4b = \tau k_1 f \tag{9b}$$

$$\frac{dc}{d\hat{r}} + c = \tau k_2 b \tag{9c}$$

$$\frac{dd}{d\theta} + d = \tau k_3 A_0 f^2 \tag{9d}$$

where

$$c_1 \equiv (1+\tau k_1), c_2 \equiv 2\tau k_3 A_0, c_3 \equiv [c_1^2+2c_2]^{1/2}, c_4 \equiv (1+\tau k_2)$$
 (10)

with initial conditions

$$\theta = 0$$
: $f = f(0), b = 0, c = 0, d = 0$ (11)

Perturbation Solution

An analytic solution to (9a) is apparently not possible. In order to develop an approximate one, the solution is assumed to be composed of a non-periodic term and a sum of periodic terms:

$$f(\theta) = F_1(\theta) + \varepsilon P_1(\theta) + \varepsilon^2 P_2(\theta)$$
 (12)

This imposes the restriction on (9a) that ϵ be small enough so that term on the order of ϵ^3 are negligible. Substituting (12) into (9a) and collecting terms of like order in ϵ gives the following three differential equations:

$$\frac{dF_1}{d\theta} + c_1 F_1 + \frac{c_2}{2} F_1^2 = 1 \tag{13a}$$

$$\frac{dP_1}{d\hat{c}} + \{c_1 + c_2F_1\}P_1 = \sin \Lambda\theta$$
 (13b)

$$\frac{dP_2}{d\hat{c}} + \{c_1 + c_2F_1\}P_2 = -P_1^2$$
 (13c)

Note that the zero order equation returns the transient mass balance for an unperturbed (ϵ =0) feed.

The solutions to equations (13) are straightforward but are fairly tedious. Defining for convenience the steady state values corresponding to $\epsilon = 0$:

$$f_s = \frac{(c_3 - c_1)}{c_2}, b_s = \frac{\tau k_1 f_s}{c_4}, c_s = \frac{\tau^2 k_1 k_2 f_s}{c_4}, d_s = \tau k_3 A_0 f_s^2$$
 (14)

we obtain [11] for the solutions to equations [13]

$$F_1(\theta) = f_s + \frac{2c_3\alpha e^{-c_3\theta}}{c_2(1-\alpha e^{-c_3\theta})}$$
 (15a)

$$P_{1}(\theta) = \frac{1}{(1-\alpha e^{-C_{3}\theta})^{2}} \{ \psi_{1}(\theta) - 2\alpha \psi_{2}(\theta) + \alpha^{2} \psi_{3}(\theta) + I_{1}e^{-a\theta} \}$$
 (15b)

$$P_{2}(\theta) = \frac{1}{(1-\alpha e^{-C_{3}\theta})^{2}} \{I_{2}e^{-a\theta} - \psi_{4}(\theta) + \psi_{5}(\theta) - \psi_{6}(\theta)\}$$
 (15c)

where

$$\psi_1(\theta) = \frac{a \sin \Lambda \theta - \Lambda \cos \Lambda \theta}{a^2 + \Lambda^2}$$
 (15d)

$$\psi_2(\theta) = e^{-C_3\theta} \frac{(a-C_3) \sin \Lambda\theta - \Lambda \cos \Lambda\theta}{(a-C_3)^2 + \Lambda^2}$$
 (15e)

$$\psi_3(\theta) = e^{-2c_3\theta} \left[\frac{(a-2c_3) \sin \Lambda\theta - \Lambda \cos \Lambda\theta}{(a-2_3)^2 + \Lambda^2} \right]$$
 (15f)

$$\psi_{4}(\theta) = \sum_{i=0}^{\infty} (i+1)\alpha^{i} \{\psi_{7}(i,\theta) + \psi_{8}(i,\theta) - \psi_{9}(i,\theta)\}$$
 (15g)

$$\psi_{7}(i,\theta) = \sum_{\ell=1}^{5} (-1)^{\ell+1} \left[\beta_{\ell} + \frac{\eta_{\ell} \lambda_{\ell}, i}{2\Lambda}\right] \left[\frac{e^{-c_{3}(\ell+i-1)\theta}}{\lambda_{\ell}^{2}, i + 4\Lambda^{2}}\right] \left[\sin \Lambda\theta \left(\lambda_{\ell}, i \sin \Lambda\theta - 2\Lambda \cos \Lambda\theta\right) + \left\{\frac{2\Lambda^{2}}{\lambda_{\ell}, i}; \lambda_{\ell}, i \neq 0 \\ 2\Lambda^{2}\theta e^{-a\theta}; \lambda_{\ell}, i = 0\right\}\right]$$

$$(15h)$$

$$\psi_{\theta}(\mathbf{i},\theta) = \sum_{\ell=1}^{5} (-1)^{\ell+1} \gamma_{\ell} \left[\frac{e^{-c_{3}(\ell+i+1)\theta}}{\lambda^{2} \ell, \mathbf{i}^{+4\Lambda^{2}}} \right] \left[\cos \Lambda\theta (\lambda_{\ell}, \mathbf{i} \cos \Lambda\theta + 2\Lambda \sin \Lambda\theta) \right]$$

$$+ \left\{ \begin{array}{l} \frac{2\Lambda^2}{\lambda_{\ell,i}}; & ,i \neq 0 \\ 2\Lambda^2 \theta e^{-a\theta}, \lambda_{\ell,i} = 0 \end{array} \right\}$$
(15i)

$$\psi_{9}(i,\theta) = \sum_{\ell=1}^{5} (-1)^{\ell+1} \frac{\eta_{\ell} e^{-c_{3}(\ell+i-1)\theta}}{2\Lambda} \sin^{2} \Lambda \theta$$
 (15j)

$$\psi_{5}(\theta) = 2I_{1} \sum_{i=0}^{\infty} (i+1)\alpha^{i} \left\{ \sum_{\ell=1}^{3} (-1)^{\ell+1} \frac{e^{-[a+c_{3}(\ell+i-1)]\theta}}{(\lambda_{\ell,i}-a)^{2} + \Lambda^{2}} \psi_{10}(i,\ell,\theta) \right\}$$
(15k)

$$\psi_{10}(i,\ell,\theta) = \nu_{\ell} \left[(\lambda_{\ell,i}^{-a}) \sin \Lambda \theta - \Lambda \cos \Lambda \theta \right] - \sigma_{\ell} \left[(\lambda_{\ell,i}^{-a}) \cos \Lambda \theta + \Lambda \sin \Lambda \theta \right]$$
 (151)

$$\psi_{6}(\theta) = I_{1}^{2} \sum_{i=0}^{\infty} (i+1)\alpha^{i} \frac{e^{-(a+c_{3}i)\theta}}{a+c_{3}i}$$
(15m)

and

$$\alpha = \frac{c_2 f(0) + c_1 - c_3}{c_2 f(0) + c_1 + c_3}, \quad a = c_3, \quad \lambda_{\ell, i} = c_3 (2 - \ell - i)$$
 (15n)

$$\beta_1 = \bar{a}_1^2, \ \beta_2 = 2\bar{a}_1\bar{b}_1, \ \beta_3 = 2\bar{a}_1\bar{c}_1 + \bar{b}_1^2, \ \beta_4 = 2\bar{b}_1\bar{c}_1, \ \beta_5 = \bar{c}_1^2$$
 (15p)

$$\gamma_1 = \bar{a}_2^2, \ \gamma_2 = 2\bar{a}_2\bar{b}_2, \ \gamma_3 = 2\bar{a}_2\bar{c}_2 + \bar{b}_2^2, \ \gamma_4 = 2\bar{b}_2\bar{c}_2, \ \gamma_5 = \bar{c}_2^2$$
 (15q)

$$\eta_1 = 2\bar{a}_1\bar{a}_2$$
, $\eta_2 = 2(\bar{a}_1\bar{b}_2 + \bar{a}_2\bar{b}_1)$, $\eta_3 = 2(\bar{a}_1\bar{c}_2 + \bar{b}_1\bar{b}_2 + \bar{c}_1\bar{a}_2)$,

$$\eta_4 = 2(\bar{b}_1\bar{c}_2 + \bar{b}_2\bar{c}_1)$$
, $\eta_5 = 2\bar{c}_1\bar{c}_2$ (15r)

$$v_1 = \bar{a}_1, v_2 = \bar{b}_1, v_3 = \bar{c}_1$$
 (15s)

$$\sigma_1 = \overline{a}_2, \ \sigma_2 = \overline{b}_2, \ \sigma_3 = \overline{c}_2$$
 (15t)

$$\bar{\mathbf{a}}_1 = \mathbf{a}\alpha_1, \ \bar{\mathbf{a}}_2 = \Lambda\alpha_1$$
 (15u)

$$\overline{b}_1 = 0; \ \overline{b}_2 = 2\alpha \alpha_2 \Lambda \tag{15v}$$

$$\bar{\mathbf{c}}_1 = -\alpha^2 \alpha_3 \mathbf{c}_3, \ \bar{\mathbf{c}}_2 = \alpha^2 \alpha_3 \Lambda \tag{15w}$$

$$\alpha_1 = \alpha_3 = (a^2 + \Lambda^2)^{-1}, \quad \alpha_2 = 1/\Lambda^2$$
 (15x)

Evaluation of the constants I_1 and I_2 requires the use of the initial condition as well as the differential equations. Since $F_1(0) = f(0)$ for all ε , we have $P_1(0) + \varepsilon P_2(0) = 0$. Setting $\theta = 0$ in equations (13b), (13c) gives relations between $P_1(0)$, $P_2(0)$ and $P_1(0)$, $P_2(0)$. Eliminating $P_1(0)$, $P_2(0)$, and $P_2(0)$ gives $P_1(0) = 0$, from which $P_2(0) = 0$. Since P_1 only contains I_1 , and P_2 only contains I_2 , their values are readily found to be

$$I_1 = 2\alpha\psi_2(0) - \psi_1(0) - \alpha^2\psi_3(0)$$
 (15y)

$$I_2 = \psi_4(0) - \psi_5(0) + \psi_6(0)$$
 (15z)

The Solutions to b, c, and d

In solving the differential equations for b, c, and d, no assumptions about the form of the solutions were made. For b, the expression for f derived above was substituted directly into the differential equation and solved. Because of the complexity of the square of the full solution for f, the full transient solution for d was not obtained. The limiting d equation $(\theta \rightarrow \infty)$ was obtained by first taking the limit of f as $\theta \rightarrow \infty$, squaring the limiting form, and using that form in the differential equation for d. The b equation was used directly in the differential equation to find the solution to c. As a consistency check, the limiting c equation was evaluated by the limiting method used to find the d equation, and this result was compared with the limit as $\theta \rightarrow \infty$ of the full c solution. As expected, the two forms showed perfect agreement.

The full transient b solution, which in comparison makes the solution of f look easy, turns out to be of the form

$$b(\theta) = \tau k_1 \{B_1(\theta) + \varepsilon P_3(\theta) + \varepsilon^2 P_4(\theta) - e^{-C_4 \theta} I_3\}$$
 (16)

where

$$B_1(\theta) = \frac{f_S}{C_L} + \frac{2c_3}{C_2} \psi_{11}(\theta)$$
 (17a)

$$\psi_{11}(\theta) = \begin{cases} \sum_{j=0}^{\infty} \alpha^{j+1} & \psi_{12}(\theta,j) ; c_3 \neq c_4 \\ j=0 & \\ \frac{\alpha}{c_3} & e^{-c_3\theta} & \ln[e^{c_3\theta} - \alpha] ; c_3 = c_4 \end{cases}$$
 (17b)

$$\psi_{12}(\theta, \mathbf{j}) = \begin{cases} \frac{1}{c_5} e^{(c_5 - c_4)\theta} ; & c_5 \neq 0 \\ \theta e^{-c_4 \theta} ; & c_5 = 0 \end{cases}$$
 (17c)

$$c_5 = c_4 - (j+1)c_3$$
 (17d)

and

$$P_{3}(\theta) = \sum_{i=0}^{\infty} (i+1)\alpha^{i} \left\{ \sum_{k=1}^{3} \left[-1 \right]^{k+1} \frac{e^{-c_{3}(k+i-1)\theta}}{\omega_{k,i}^{2} + \Lambda^{2}} \psi_{13}(k,i,\theta) \right] + I_{1}\psi_{14}(i,\theta) \right\}$$
(18a)

$$\psi_{13}(\ell,i,\theta) = (\mu_{\ell}\omega_{\ell,i} - \bar{\mu}_{\ell}\Lambda)\sin\Lambda\theta + (\Lambda\mu_{\ell} + \bar{\mu}_{\ell}\omega_{\ell,i})\cos\Lambda\theta$$
 (18b)

$$\psi_{14}(i,\theta) = \begin{cases} \frac{e^{-(c_3i+a)\theta}}{c_4-c_3i-a} ; & c_4 \neq c_3i+a \\ \theta e^{-c_4\theta} & \vdots & c_6 = c_3i+a \end{cases}$$
 (18c)

$$\omega_{\ell,i} = c_4 - c_3(\ell+i-1) \tag{18d}$$

$$\mu_1 = \bar{a}_1, \ \mu_2 = \bar{b}_1, \ \mu_3 = \bar{c}_1$$
 (18e)

and

$$\bar{\mu}_1 = \bar{a}_2, \; \bar{\mu}_2 = \bar{b}_2, \; \bar{\mu}_3 = \bar{c}_2$$
 (18f)

$$P_{+}(\theta) = I_{2} \tilde{\Sigma}_{\alpha}^{k} (k+1) \psi_{15}(k,\theta) + \tilde{\Sigma}_{15}^{\infty} \tilde{\Sigma}_{15}(i+1) (k+1) \alpha^{i+k} \psi_{16}(k,i,\theta)$$

$$k=0 \qquad k=0 \qquad i=0$$
(19a)

where

$$\psi_{15}(k,\theta) = \begin{cases} \frac{e^{-(a+c_3k)\theta}}{c_4-a-c_3k} ; c_4 \neq a+c_3k \\ \theta e^{-c_4\theta} ; c_4 = a+c_3k \end{cases}$$
(19b)

$$\psi_{16}(k,i,\theta) = \sum_{\ell=1}^{5} (-1)^{\ell+1} \left\{ \frac{\eta_{\ell}}{2\Lambda} \psi_{17}(k,\ell,i,\theta) - \psi_{18}(k,\ell,i,\theta) \right\} + 2I_{1}\sum_{\ell=1}^{3} (-1)^{\ell+1}$$

$$\psi_{19}(\mathbf{k}, \ell, \mathbf{i}, \theta) - I_1^2 \psi_{20}(\mathbf{k}, \mathbf{i}, \theta)$$
 (19c)

$$\psi_{17}(k,\ell,i,\theta) = \begin{cases} \frac{e^{\left[\zeta_{1}(k,\ell,i)-c_{4}\right]\theta}}{\zeta_{1}(k,\ell,i)^{2}+4\Lambda^{2}} & \psi_{21}(k,\ell,i,\theta); & \zeta_{1}(k,\ell,i)\neq 0 \\ e^{-c_{4}\theta} & \left[\frac{\theta}{2} - \frac{\sin 2\Lambda\theta}{4\Lambda} \right]; & \zeta_{1}(k,\ell,i) = 0 \end{cases}$$
(19d)

$$\psi_{21}(\mathbf{k},\ell,\mathbf{i},\theta) = \frac{2\Lambda^2}{\zeta_1(\mathbf{k},\ell,\mathbf{i})} + \sin \Lambda\theta [\zeta_1(\mathbf{k},\ell,\mathbf{i})\sin \Lambda\theta - 2\Lambda\cos \Lambda\theta]$$
 (19e)

$$\psi_{1\theta}(\mathbf{k},\mathbf{l},\mathbf{i},\theta) = \begin{cases} \frac{e^{\left[\zeta_{1}(\mathbf{k},\mathbf{l},\mathbf{i})-c_{4}\right]\theta}}{\zeta_{5}(\mathbf{l},\mathbf{i})} \left[\frac{\psi_{22}(\mathbf{k},\mathbf{l},\mathbf{i},\theta)}{\zeta_{1}(\mathbf{k},\mathbf{l},\mathbf{i})^{2}+4\Lambda^{2}} + \psi_{25}(\mathbf{k},\mathbf{l},\mathbf{i},\theta)\right]; \zeta_{1}(\mathbf{k},\mathbf{l},\mathbf{i})\neq 0 \\ \frac{e^{-c_{4}\theta}}{\zeta_{5}(\mathbf{l},\mathbf{i})} \left\{\psi_{26}(\mathbf{l},\mathbf{i},\theta) ; \lambda_{\mathbf{l},\mathbf{i}}\neq 0 \\ \psi_{27}(\mathbf{l},\mathbf{i},\theta) ; \lambda_{\mathbf{l},\mathbf{i}}=0 \right\} \zeta_{1}(\mathbf{k},\mathbf{l},\mathbf{i})=0 \end{cases}$$

$$(19f)$$

$$\psi_{22}(k,\ell,i,\theta) = \zeta_{4}(\ell,i)\psi_{21}(k,\ell,i,\theta) + \gamma_{\ell}\lambda_{\ell,i}\psi_{23}(k,\ell,i,\theta) + \psi_{24}(k,\ell,i,\theta)$$
 (19g)

$$\psi_{23}(\mathbf{k},\ell,\mathbf{i},\theta) = \frac{2\Lambda^2}{\zeta_1(\mathbf{k},\ell,\mathbf{i})} + \cos\Lambda\theta[\zeta_1(\mathbf{k},\ell,\mathbf{i})\cos\Lambda\theta + 2\Lambda \sin\Lambda\theta]$$
 (19h)

$$\psi_{24}(\mathbf{k},\ell,\mathbf{i},\theta) = \Lambda \zeta_2(\ell,\mathbf{i}) [\zeta_1(\mathbf{k},\ell,\mathbf{i}) \sin 2\Lambda\theta - 2\Lambda \cos 2\Lambda\theta]$$
 (19i)

$$\psi_{25}(k,\ell,i,\theta) = 2\Lambda^{2}\zeta_{3}(\ell,i) \begin{cases} \frac{1}{\lambda_{\ell,i}\zeta_{1}(k,\ell,i)} ; \lambda_{\ell,i} \neq 0 \\ \psi_{28}(k,\ell,i,\theta) ; \lambda_{\ell,i} = 0 \end{cases}$$

$$(19j)$$

$$\psi_{26}(k,\ell,i,\theta) = \begin{cases}
\frac{e^{-a\theta}}{\zeta_{1}(k,\ell,i)-a} \left[\theta - \frac{1}{\zeta_{1}(k,\ell,i)-a}; \zeta_{1}(k,\ell,i) \neq a\right] \\
\frac{\theta^{2}}{2} e^{-\zeta_{1}(k,\ell,i)\theta}; \zeta_{1}(k,\ell,i) = a
\end{cases}$$

$$\psi_{26}(\ell,i,\theta) = \zeta_{4}(\ell,i)\left[\frac{\theta}{2} - \frac{\sin 2\Lambda\theta}{4\Lambda}\right] + \gamma_{\ell}\lambda_{\ell,i}\left[\frac{\theta}{2} + \frac{\sin 2\Lambda\theta}{4\Lambda}\right]$$
(19k)

$$-\frac{\zeta_{2}(\ell,i)}{2}\cos 2\Delta\theta + \frac{2\Lambda^{2}}{\lambda_{0,1}}\zeta_{3}(\ell,i)\theta$$
 (191)

$$\psi_{27}(\ell,i,\theta) = \frac{\zeta_2(\ell,i)}{2} \cos 2\Lambda\theta - \frac{2\Lambda^2\zeta_3(\ell,i)}{a} e^{-a\theta} \left[\theta + \frac{1}{a}\right]$$
 (19m)

$$\psi_{19}(k,\ell,i,\theta) = \frac{e^{-[a+c_3(k+\ell+i-1)]\theta} \left[\psi_{29}(k,\ell,i,\theta) - \psi_{30}(k,\ell,i,\theta) \right]}{(\lambda_{\ell,i}-a)^2 + \Lambda^2} \left[\psi_{29}(k,\ell,i,\theta) - \psi_{30}(k,\ell,i,\theta) \right]}$$
(19n)

$$ψ_{29}(k, \ell, i, \theta) = [ν_{\ell}(λ_{\ell, i} - a) - σ_{\ell}Λ] [(ζ_1(k, \ell, i) - a) sinΛθ - ΛcosΛθ] (19p)$$

$$\psi_{30}(\mathbf{k},\ell,\mathbf{i},\theta) = \left[\nu_{\ell}\Lambda + \sigma_{\ell}(\lambda_{\ell,\mathbf{i}} - \mathbf{a})\right] \left[(\zeta_{1}(\mathbf{k},\ell,\mathbf{i}) - \mathbf{a})\cos\Lambda\theta + \Lambda\sin\Lambda\theta\right]$$
(19q)

$$\psi_{20}(k,i,\theta) = \begin{cases} \frac{e^{-[a+c_{3}(i+k)]\theta}}{(a+c_{3}i)[c_{4}-a-c_{3}(i+k)]} ; & c_{4} \neq a + c_{3}(i+k) \\ \frac{\theta e^{-c_{4}\theta}}{(a+c_{3}i)} ; & c_{4} = a + c_{3}(i+k) \end{cases}$$
(19r)

and

$$\zeta_{1}(k,\ell,i) = c_{4}-c_{3}(k+\ell+i-1)$$
 (19s)

$$\zeta_{2}(\ell, \mathbf{i}) = \gamma_{\hat{\ell}} - \beta_{\hat{\ell}} - \frac{\eta_{\hat{\ell}} \lambda_{\hat{\ell}, \mathbf{i}}}{2\Lambda}$$
 (19t)

$$\zeta_{3}(\ell,i) = \gamma_{\ell} + \beta_{\ell} + \frac{\eta_{\ell} \lambda_{\ell,i}}{2\Lambda}$$
 (19u)

$$\zeta_{4}(\ell,i) = \lambda_{\hat{k},i} \left(\beta_{\hat{k}} + \frac{\eta_{\hat{k}}\lambda_{\hat{k},i}}{2\Lambda}\right)$$
 (19v)

$$\zeta_5(\hat{x}, i) = \lambda_{\hat{x}, i}^2 + 4\Lambda^2$$
 (19w)

The double summation appearing in equation (19a) is a condensation of a quadruple summation which occurs when the term $1/(1-\alpha e^{-c_3\theta})$ is written in series form and squared. The constant of integration I_3 was found by setting $\theta=0$ and $b(\theta=0)=0$. The result is simply

$$I_3 = B_1(0) + \varepsilon P_3(0) + \varepsilon^2 P_4(0)$$
 (20)

The simplicity of equation (20) belies the triple summations which it contains.

The full transient solution for $c(\theta)$ was evaluated by substitution of equations (16)-(20) into (9c) and integrating. The result is almost twice as lengthy as $b(\theta)$. It was used here as a check to the limiting form $(\theta \rightarrow \infty)$ of $c(\theta)$ found by using the limiting form of $b(\theta)$ in the differential equation. Because the full transient c equation is almost twice as lengthy as $b(\theta)$, and because we are largely interested in the limiting behavior of the components, it is not included here.

Limit Cycle Forms

From the perspective of analyzing process performance, we are interested in looking at the behavior of the system over a long time period. It can be seen from equations (15)-(19) that both $f(\theta)$ and $b(\theta)$ consist of sin and cos terms, many of which are damped out as $\theta \rightarrow \infty$ (this is easier to see when the equations are written on one line; however, this requires a sheet of paper almost 12 feet long). As $\theta \rightarrow \infty$ all of the exponentials become zero or one, and the only θ dependence remaining arises from the trigonometric functions. The functions oscillate regularly, and both functions complete one cycle in the longest period of their component functions, $2\pi/\Lambda$. Moreover, since $c(\theta)$ and $d(\theta)$ are obtained by integrating an exponential times either $f^2(\theta)$ or $b(\theta)$, both $c(\theta)$ and $d(\theta)$ will retain the cyclic properties of $f(\theta)$ and $b(\theta)$.

$$F_1(\theta_m) = f_g \tag{21a}$$

$$P_1(\theta_{\infty}) = \frac{a \sin \Lambda\theta - \Lambda \cos \Lambda\theta}{a^2 + \Lambda^2}$$
 (21b)

$$P_{2}(\theta_{\infty}) = -\frac{\beta_{1} + \frac{\eta_{1}\lambda_{1,0}}{2\Lambda}}{\lambda_{1,0}^{2} + 4\Lambda^{2}} \quad \sin \Lambda\theta (\lambda_{1,0} \sin \Lambda\theta - 2\Lambda \cos \Lambda\theta) + \frac{2\Lambda^{2}}{\lambda_{1,0}}$$

$$-\frac{\gamma_1}{\lambda_{1,0}^2+4\Lambda^2}\cos \Lambda\theta(\lambda_{1,0}\cos \Lambda\theta+2\Lambda\sin \Lambda\theta)+\frac{2\Lambda^2}{\lambda_{1,0}}+\frac{\eta_1\sin^2\Lambda\theta}{2\Lambda}$$
 (21c)

$$B_1(\theta_{\infty}) = \frac{b_s}{\tau k_1}$$
 (22a)

$$P_{3}(\theta_{\infty}) = \frac{(\mu_{1}\omega_{1}, 0 - \overline{\mu}_{1}\Lambda)\sin \Lambda\theta - (\Lambda\mu_{1} + \overline{\mu}_{1}\omega_{1}, 0)\cos \Lambda\theta}{\omega_{1}^{2}, 0 + \Lambda^{2}}$$
(22b)

$$P_{\downarrow}(\theta_{\infty}) = \frac{\eta_{1}\left[\frac{2\Lambda^{2}}{c_{\downarrow}} + c_{\downarrow}\sin^{2}\Lambda\theta - \Lambda\sin2\Lambda\theta\right]}{2\Lambda(c_{\downarrow}^{2} + 4\Lambda^{2})} - \frac{\psi_{31}(\theta)}{\lambda_{1,0}^{2} + 4\Lambda^{2}}$$
(22c)

$$\psi_{31}(\theta) = \chi_1 + \psi_{33}(\theta) \tag{22d}$$

$$\psi_{33}(\theta) = \frac{\zeta_2(1,0)\{\Lambda[(\lambda_{10}+c_4)\sin 2\Lambda\theta - 2\Lambda\cos 2\Lambda\theta] - c_4\lambda_{10}\sin^2 \Lambda\theta\}}{c_4^2}$$
(22e)

The limiting forms of the c and d equations are:

$$c(\theta_{\infty}) = c_{s} + \tau^{2}k_{1}k_{2}[\varepsilon P_{5}(\theta_{\infty}) + \varepsilon^{2}P_{6}(\theta_{\infty})]$$
 (23a)

where

$$P_{5}(\theta_{\infty}) = \frac{\psi_{34} \sin \theta - \psi_{35} \cos \theta}{(\omega_{1,0}^{2} + \Lambda^{2}) (1 + \Lambda^{2})}$$
(23b)

$$P_6(\theta_{\infty}) = \psi_{36} + \psi_{37} \sin^2 \Lambda\theta + \psi_{38} \sin 2\Lambda\theta$$
 (23c)

and

$$d(\theta) = d_{s} + \tau k_{3} A_{0} \left[\varepsilon P_{7}(\theta_{\infty}) \ \varepsilon^{2} P_{8}(\theta_{\infty}) \right]$$
 (23d)

$$P_7(\theta_{\infty}) = \frac{2f_s[(a-\Lambda^2)\sin\Lambda\theta-\Lambda(1+a)\cos\Lambda\theta]}{(a^2+\Lambda^2)(1+\Lambda^2)}$$
(23e)

$$P_{8}(\theta_{\infty}) = \psi_{41}\sin^{2}\Lambda\theta - \psi_{42}\sin^{2}\Lambda\theta + \psi_{43}$$
 (23f)

where

$$\psi_{34} = (\mu_1 \omega_{1,0} - \bar{\mu}_1 \Lambda) - \Lambda (\Lambda \mu_1 + \bar{\mu}_1 \omega_{1,0})$$
 (23q)

$$\psi_{35} = \Lambda(\mu_1 \cup_{1,0} - \bar{\mu}_1 \Lambda) + (\Lambda \mu_1 + \bar{\mu}_1 \omega_{1,0})$$
 (23h)

$$\psi_{36} = \chi_3 + \frac{2\Lambda}{(1+4\Lambda^2)} \left[\Lambda(\chi_4 + \chi_2) + \chi_5 \right]$$
 (23i)

$$\psi_{37} = \frac{1}{1+4\Lambda^2} \left[\chi_4 - 4\Lambda \chi_5 - \frac{4\Lambda^2 \chi_2}{(\lambda_{1,0}^2 + 4\Lambda^2)} \right]$$
 (23j)

$$\psi_{38} = \frac{1}{1+4\Lambda^2} \left[\frac{4\Lambda^3 \chi_2}{(\lambda_{1,0}^2 + 4\Lambda^2)} - \Lambda \chi_4 - \chi_5 \right]$$
 (23k)

$$\psi_{41} = \frac{\left(a^2 - \Lambda^2\right) - 4a\Lambda^2}{\left(a^2 + \Lambda^2\right)^2} + 2f_{S} \left[\chi_{45} - 4\Lambda\psi_{46}\right]$$
(231)

$$\psi_{42} = \frac{\left[(a^2 - \Lambda^2) + a \right] \Lambda}{\left(a^2 + \Lambda^2 \right)^2} + 2f_s \left[\psi_{45} \Lambda + \psi_{46} \right]$$
(23m)

$$\psi_{43} = \frac{\Lambda^2 (1 + 2a^2 + 2\Lambda^2 + 2a) + 2f_s[2\Lambda^2 \psi_{45} + 2\Lambda \psi_{46}]}{(1 + 4\Lambda^2)} + 2f_s \psi_{44}$$
 (23n)

$$\psi_{4,4} = \frac{-1}{(\lambda_1^2, 0^{+4}\Lambda^2)} \left[\frac{2\Lambda^2 \zeta_3(1,0)}{\lambda_1, 0} + \gamma_1 \lambda_1, 0 \right]$$
 (23p)

$$\psi_{45} = \frac{\eta_1}{2\Lambda} + \frac{\lambda_{1,0}}{\lambda_{1,0}^2 + 4\Lambda^2} \zeta_2(1,0)$$
 (23q)

$$\psi_{46} = \frac{\Lambda}{\lambda_{1,0}^2 + 4\Lambda^2} \zeta_2(1,0) \tag{23r}$$

$$\chi_1 = \frac{2\Lambda^2 \zeta_3(1,0)}{c_4} \left(\frac{\lambda_{1,0}}{c_4^2 + 4\Lambda^2} + \frac{1}{\lambda_{1,0}} \right) + \frac{c_4 \gamma_1 \lambda_{1,0}}{c_4^2 + 4\Lambda^2}$$
 (23s)

$$\chi_2 = \frac{\zeta_2(1,0)}{c_+^2 + 4\Lambda^2}$$
 (23t)

$$\chi_3 = \frac{\Lambda \eta_1}{c_4 (c_4^2 + 4\Lambda^2)} - \frac{\chi_1}{\lambda_{1,0} + 4\Lambda^2}$$
 (23u)

$$\chi_4 = \frac{\mathbf{c}_4 \eta_1}{2\Lambda (\mathbf{c}_4^2 + 4\Lambda^2)} + \frac{\mathbf{c}_4 \lambda_1, 0 \chi_2}{(\lambda_1, 0 + 4\Lambda^2)}$$
 (23v)

$$\chi_5 = \frac{\Lambda(\lambda_1, 0 + C_4)\chi_2}{\lambda_1, 0 + 4\Lambda^2} + \frac{\eta_1}{2(C_4^2 + 4\Lambda^2)}$$
 (23w)

All four equations are limit cycles with longest period $2\pi/\Lambda$. In each case the first order correction term (ϵ^1) is composed of first powers of $sin\Lambda\theta$ and $cos\Lambda\theta$. The second order corrections (ϵ^2) , contain $sin^2\Lambda\theta$, $sin2\lambda\theta$ and constants.

Analysis of Time Average Concentrations

The time average concentrations are found by integrating the concentration functions over one period and dividing by the length of the period. The longest period appearing in an equation determines its overall period, which here is $2\pi/\Lambda$ for all four equations. Notice that since the first

order terms are all composed of sines and cosines of $\Lambda\theta$, their integral over one period is zero. Hence the first order terms taken alone do not give a time average concentration which differs from the steady state concentration.

Similarly, the $\sin 2\Lambda\theta$ terms which appear in the second order (ϵ^2) terms have a zero integral over one cycle. However, the $\sin^2 \! \Lambda\theta$ term yields a constant when integrated, and this combined with the constants appearing in the second order terms allow the time average concentrations to take on a value different from the steady state.

Considering the complexity of the full transient solutions, the values of the time average concentrations, with dedicated manipulation, can be put into remarkably simple forms. After integration and simplification, we obtain for the time averages:

$$\bar{f} = f_S - \frac{\varepsilon^2}{2a(a^2 + \Lambda^2)}$$
 (24a)

$$\bar{b} = b_{s} - \frac{\tau k_{1} \Lambda \epsilon^{2} \left[\left(a^{2} + \Lambda^{2} \right) c_{4}^{2} a^{2} + 2 \Lambda^{4} \left(a^{2} + c_{4}^{2} + 4 \Lambda^{2} \right) \right]}{\left(\lambda_{1}^{2}, 0 + 4 \Lambda^{2} \right) \left(a^{2} + \Lambda^{2} \right)^{2}}$$
(24b)

$$\bar{c} = c_s - \frac{\varepsilon^2 \tau^2 k_1 k_2 (\gamma_1 + \beta_1)}{2c_4 \lambda_1, 0}$$
 (24c)

$$\bar{d} = d_S + \varepsilon^2 \tau k_3 A_0 \frac{2c_1 + (c_2 - 2)c_3}{2ac_2(a^2 + \Lambda^2)}$$
 (24d)

All of the time average concentrations are less than the steady state except \bar{d} , which varies depending on the magnitude of the constants c_1 , c_2 , c_3 . Qualitatively, it appears that only when c_1 and c_2 are both small will \bar{d} be less than d_s .

From these results, it is clear that if B or C is the desired product, sinusoidal fluctuation of the feed concentration (when ϵ^3 is negligible) is detrimental to product formation. If D is desired, then for moderate

values of c_1 and c_2 , the average concentration of D from the reactor may be greater under sinusoidal concentration perturbation than at steady state. The magnitude of any enhancement can be calculated from equation (24d).

If B is desired, then our aim is to exceed the maximum steady state b. However, \bar{b} is always less than b_s at the same residence time. Since b_s at any residence time is less than or equal to the maximum steady state b_s we are guaranteed that the steady state process is more effective. The objective of enhancing the yield b in Van de Vusse kinetics by a small $(\epsilon^3 \approx 0)$ sinusoidal perturbation of the feed can never be achieved.

NUMERICAL RESULTS

The heuristic nature of the perturbation solution to $f(\theta)$ requires verification. Since equations (9) are not highly non-linear, they are easily integrated numerically with high accuracy. In this case the solution to equations (9) was simulated using the IMSL subroutine DVOGER on MSU's Control Data Corporation Cyber 170 model 750 computer. The results are presented in terms of the dimensionless groups τk_1 , k_2/k_1 , $\tau k_3 A_0$, Λ , and ε . The initial conditions used for all calculations were f(0) = 1 and b(0) = c(0) = d(0) = 0.

In the formation of the perturbation solution, the assumption was made that terms on the order of ε^3 were negligible. However, for some kinetic constants the solution gives reasonable accuracy for ε up to the physical maximum of ε =1 (since ε >1 requires the feed concentration to be negative). The equations used to evaluate the perturbation solutions were the full transient solutions for f and b, equations (15), (16)-(19), and the limit cycle forms of c and d, equations (23). The perturbation solutions were found to show good agreement with the numerical simulation for the values $\tau k_1 = k_2/k_1 = \tau k_3 A_0 = \Lambda = 1$. These values of

the constants will be used as a starting point to show how the deviation of the approximate solution from numerical simulation changes with the various system constants.

Figures 1 and 2 show the results for the constants $\tau k_1 = k_2/k_1 = \tau k_3 A_0 = \Lambda = 1$. For $\epsilon = .1$ and $\epsilon = 1$. Figures le and 2e show the b-f phase plane. As expected, the limit cycle is much larger for a larger perturbation. Virtually all of the calculations of concentration vs time showed behavior qualitatively similar to that in Figures 1 and 2.

Figures 3 and 4 and parts e and f of Figures 1 and 2 show the percent deviation of the approximate solution from the numerical solution for ϵ values of .1, .25, .75 and 1. The error increases significantly with ϵ , but for ϵ =1 remains within about ±15% except for periodic spikes. The spikes are caused by a relatively constant error when the value of the function itself gets small enough for the error to be significant. Considering the initial assumption that ϵ^3 is negligible, the agreement is quite surprising.

Figures 5 and 6 show the sensitivity of the solution accuracy to increasing $\tau k_3 A_0$ to 5. The agreement is still good for ϵ = .25, but increases sharply for ϵ = .75. Figures 7 and 8 show the error for $\tau k_1 = k_2/k_1 = 5$. Even for ϵ = .75, the error remains small, showing a small sensitivity to these two constants.

Figures 9 and 10 show what happens when $\tau k_1 = k_2/k_1 = \tau k_2 A_0 = 5$. The error increases sharply even from $\tau k_1 = k_2/k_1 = 1$; $\tau k_3 A_0 = 5$, which already showed a substantial error. Hence, although the solution accuracy always deteriorates as $\tau k_3 A_0$ is increased, the effect of τk_1 and k_2/k_1 may be large or small.

Finally, the effect of increasing Λ is shown in Figures 11 and 12. Decreasing Λ is shown in Figures 13 and 14. The error remains small

except for Λ = .2 and ϵ = .75, where the d equation spikes up to almost twice the numerical simulation. Why this should occur for this slow cycling is not clear.

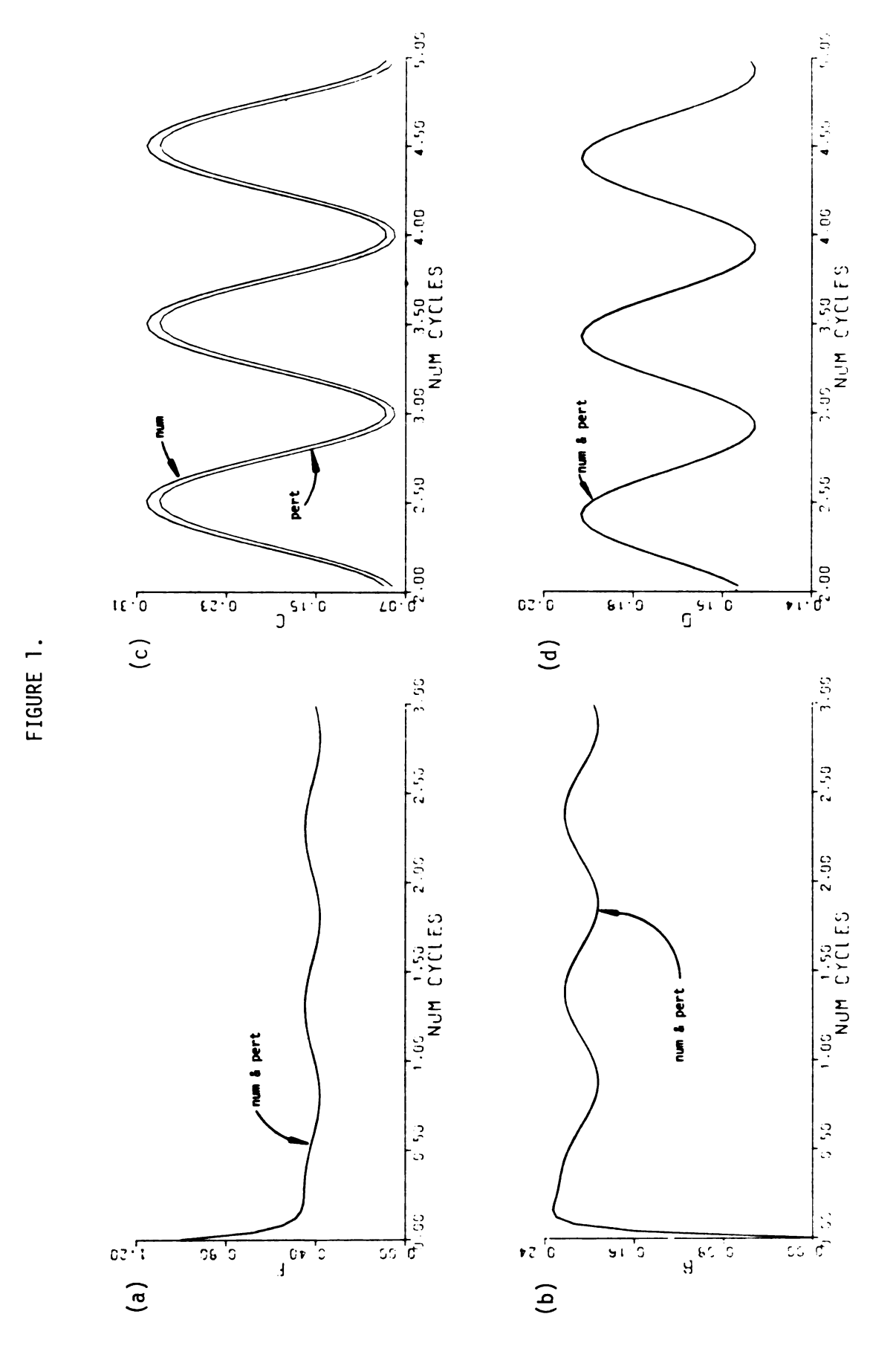
Notice that in many cases, the initial response of the perturbation solution to f drops below the numerical simulation, giving a sharp downward spike in the error. The b solution initially tends to climb above the numerical, giving a sharp upward spike in the error. Exactly why this occurs is certainly not clear from the huge equations, but the perturbation solution apparently cannot follow the rapid changes in the initial region. It may be that higher order terms contain higher harmonics which are quickly damped, hence they could add (or subtract) an initial spurt to the solution before they die out. It may also be due in part to the initial inaccuracy in the numerical simulation, since a fixed step size is required to obtain the time average concentration by integration of the numerical simulation.

A typical plot over 3 cycles required about 1.5 central processing seconds on the CDC 170 model 750. This involves about 90 evaluations of the b and f equations which totalled an average of about .15 CP seconds, or 10% of the total computing time. A reasonable estimate is at least 1.0 CP seconds were required for the numerical simulation, with the remainder used to evaluate c and d. Hence, the perturbation solution, while much more laborious to program, runs much more efficiently in spite of the triple summations that must be evaluated in each call.

The evaluation of enhancement by numerical simulation requires that the differential equations be solved and then integrated over time, in this case an average of about 1 cp second for each set of constants.

The predictions from the perturbation expansion, equations (24), are much simpler, requiring a small fraction of the time and memory. Hence

FIGURE 1.(a-g) Behavior of Van de Vusse system for $\tau k_1 = k_2/k_1 = \tau k_3 A_0 = \Lambda = 1$, $\epsilon = .1$.



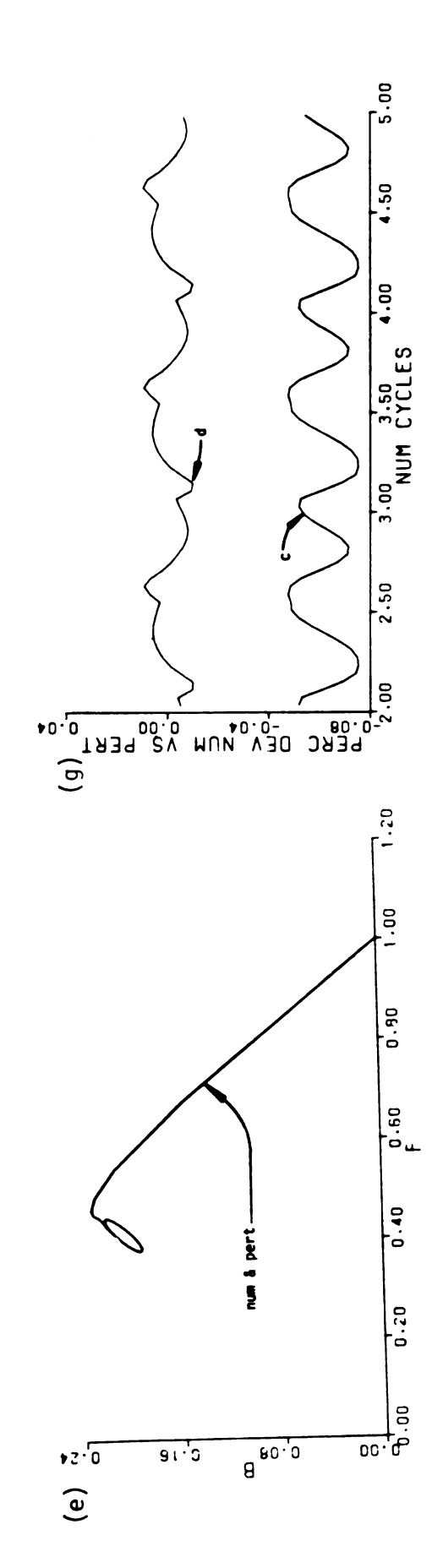


FIGURE 1 - continued

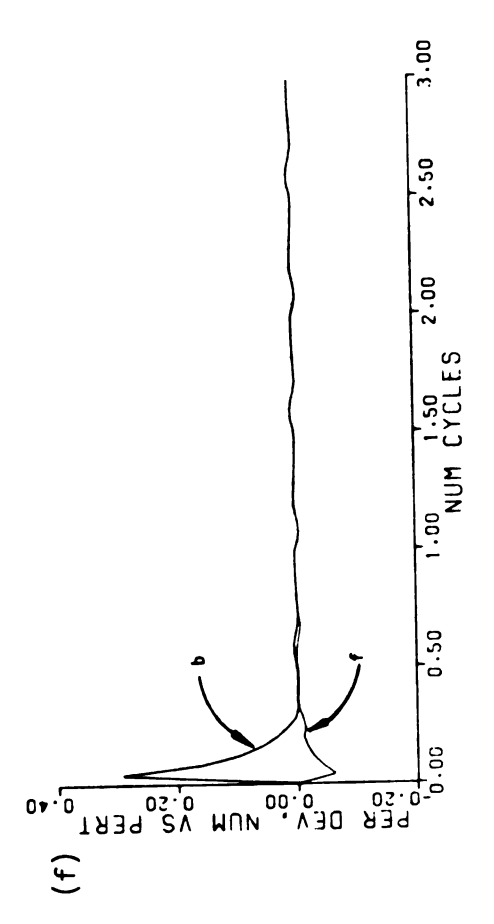
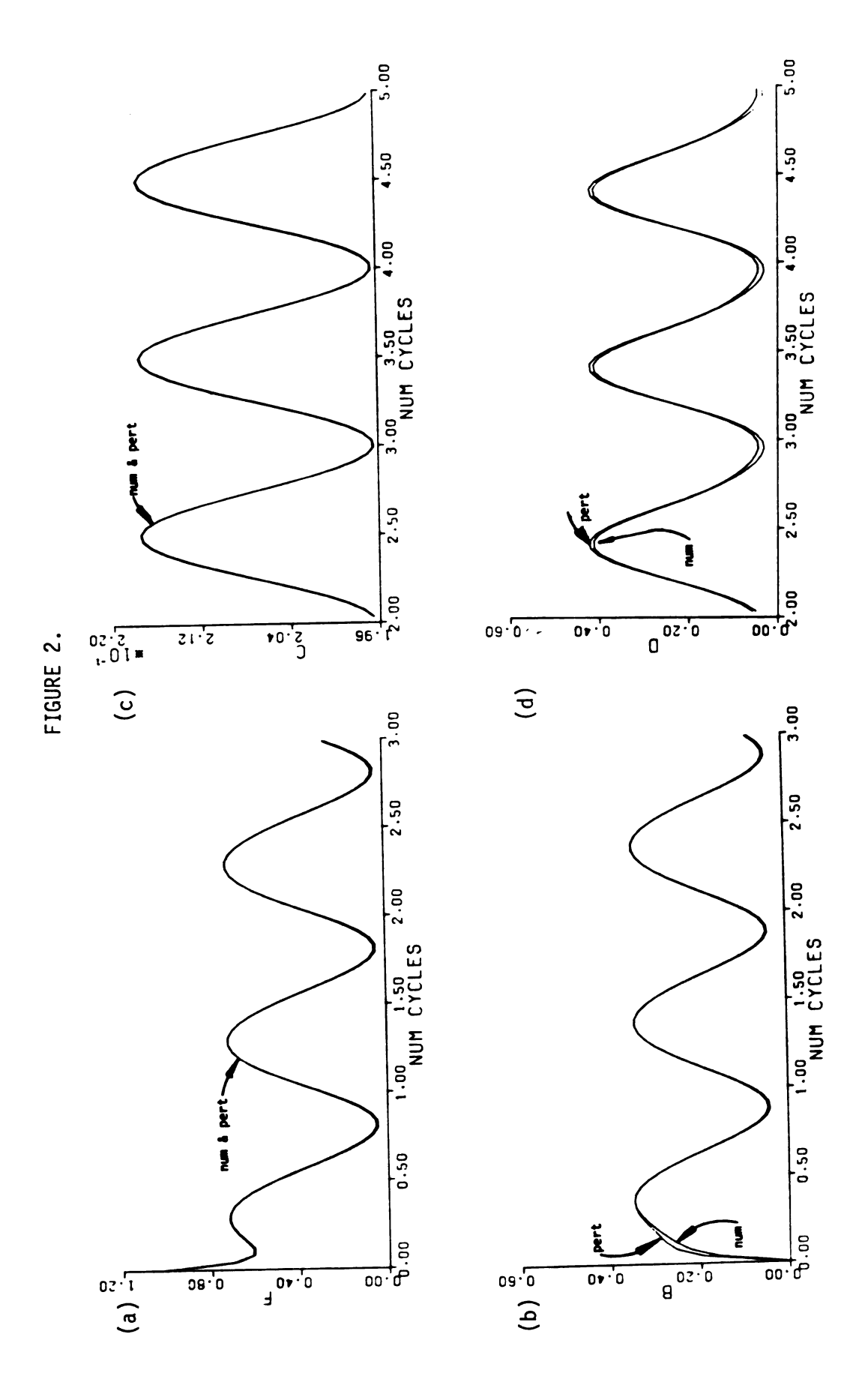
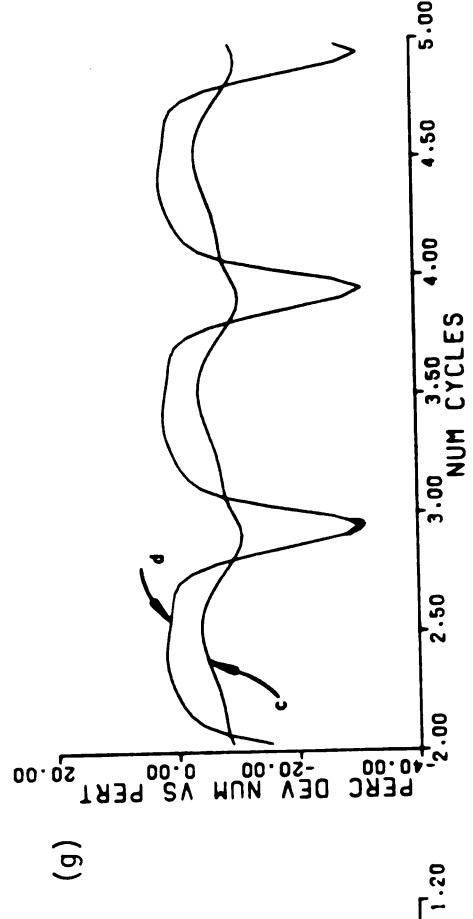
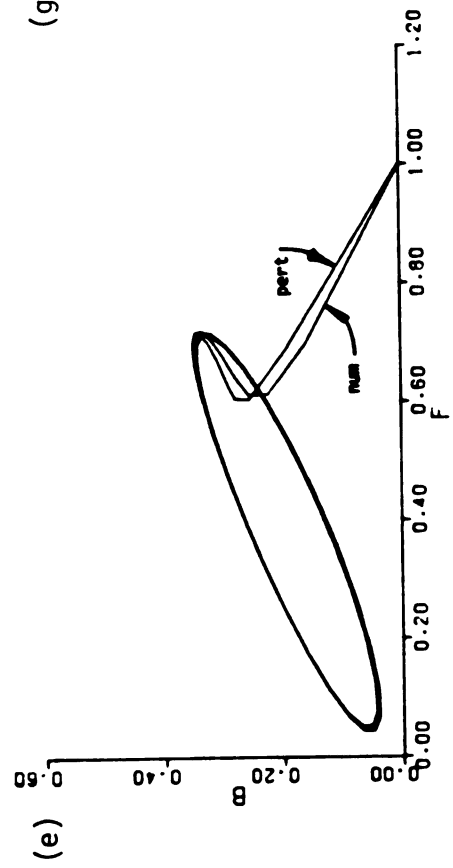


FIGURE 2.(a-g) Behavior of Van de Vusse system for $\tau k_1 = k_2/k_1 = \tau k_3 A_0 = \Lambda = 1$, $\epsilon = 1$.







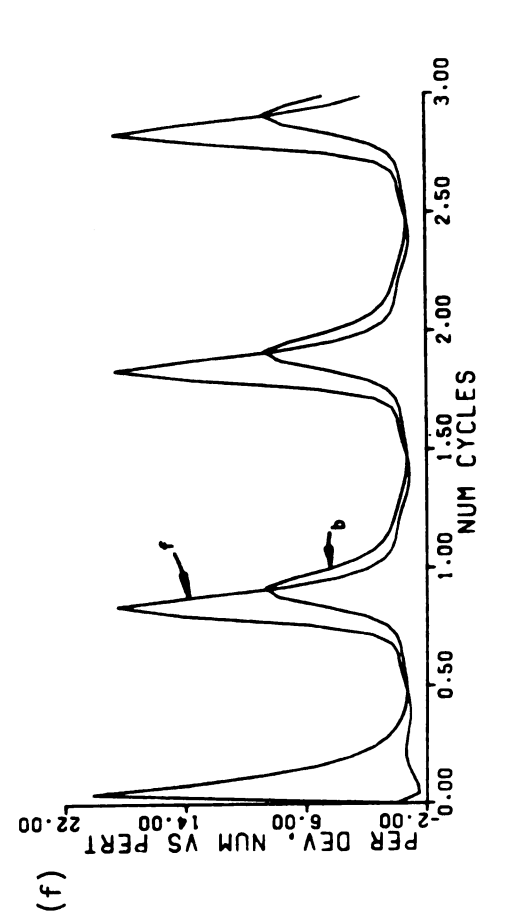
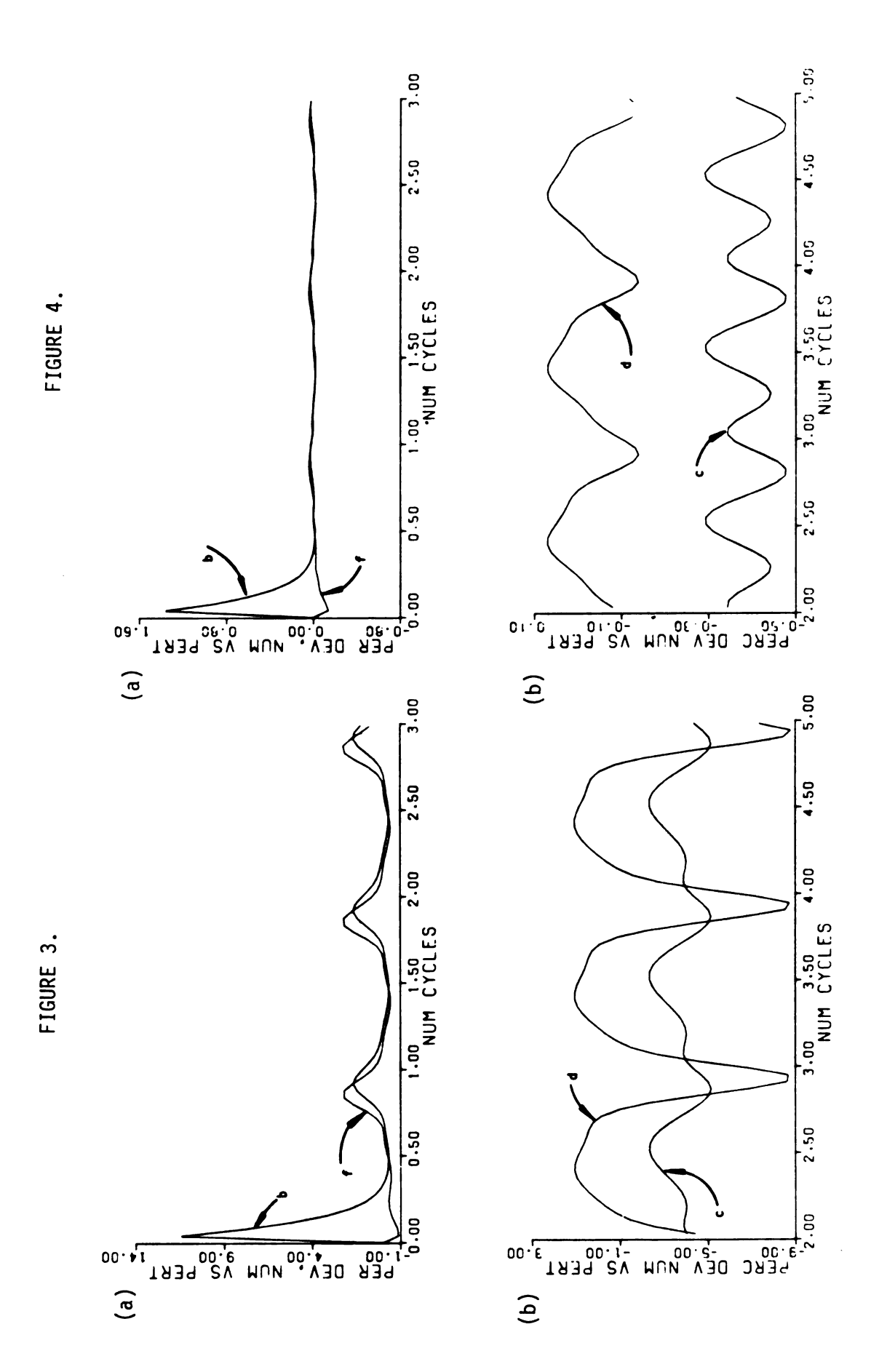
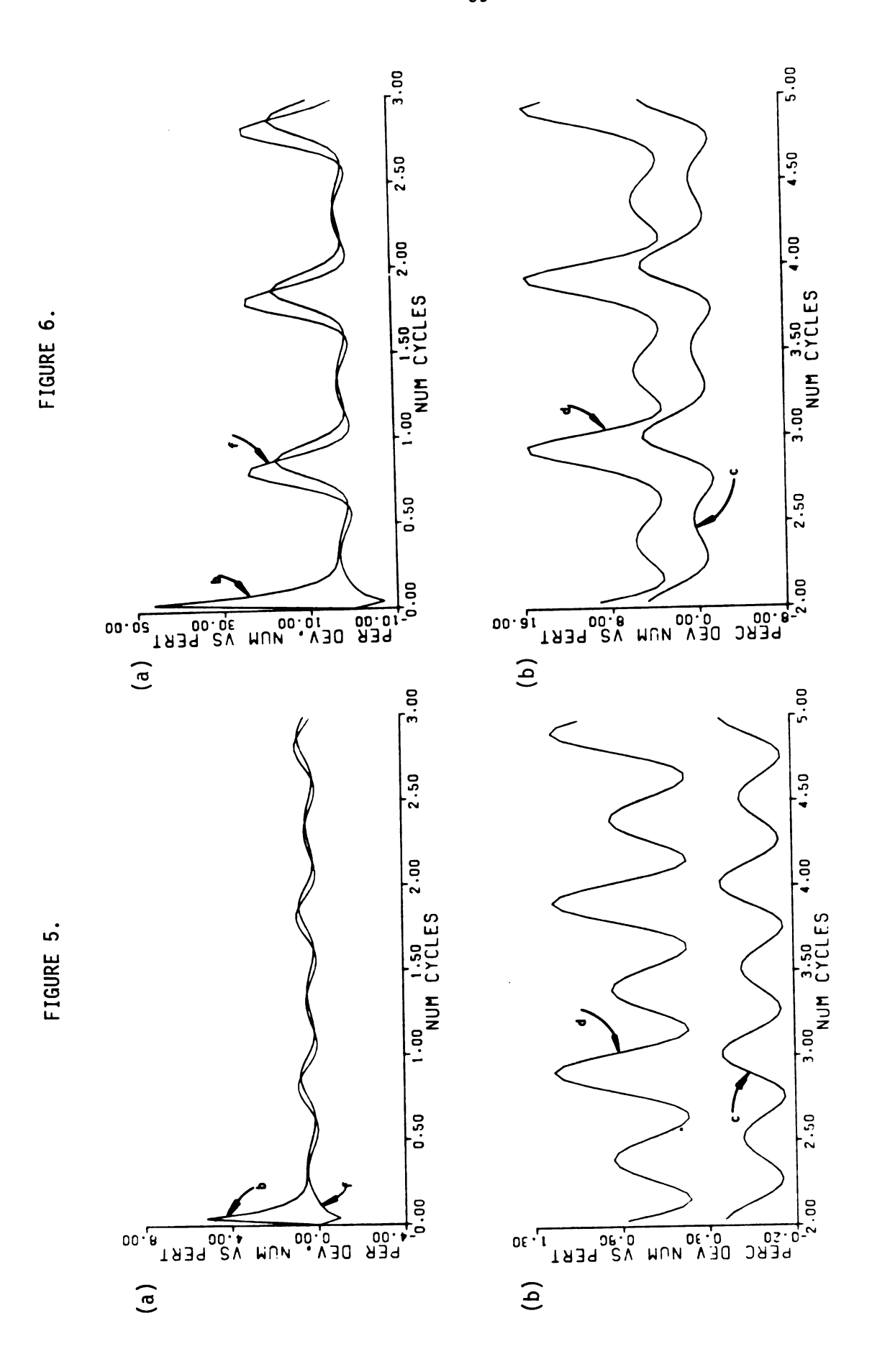


FIGURE 2 - continued

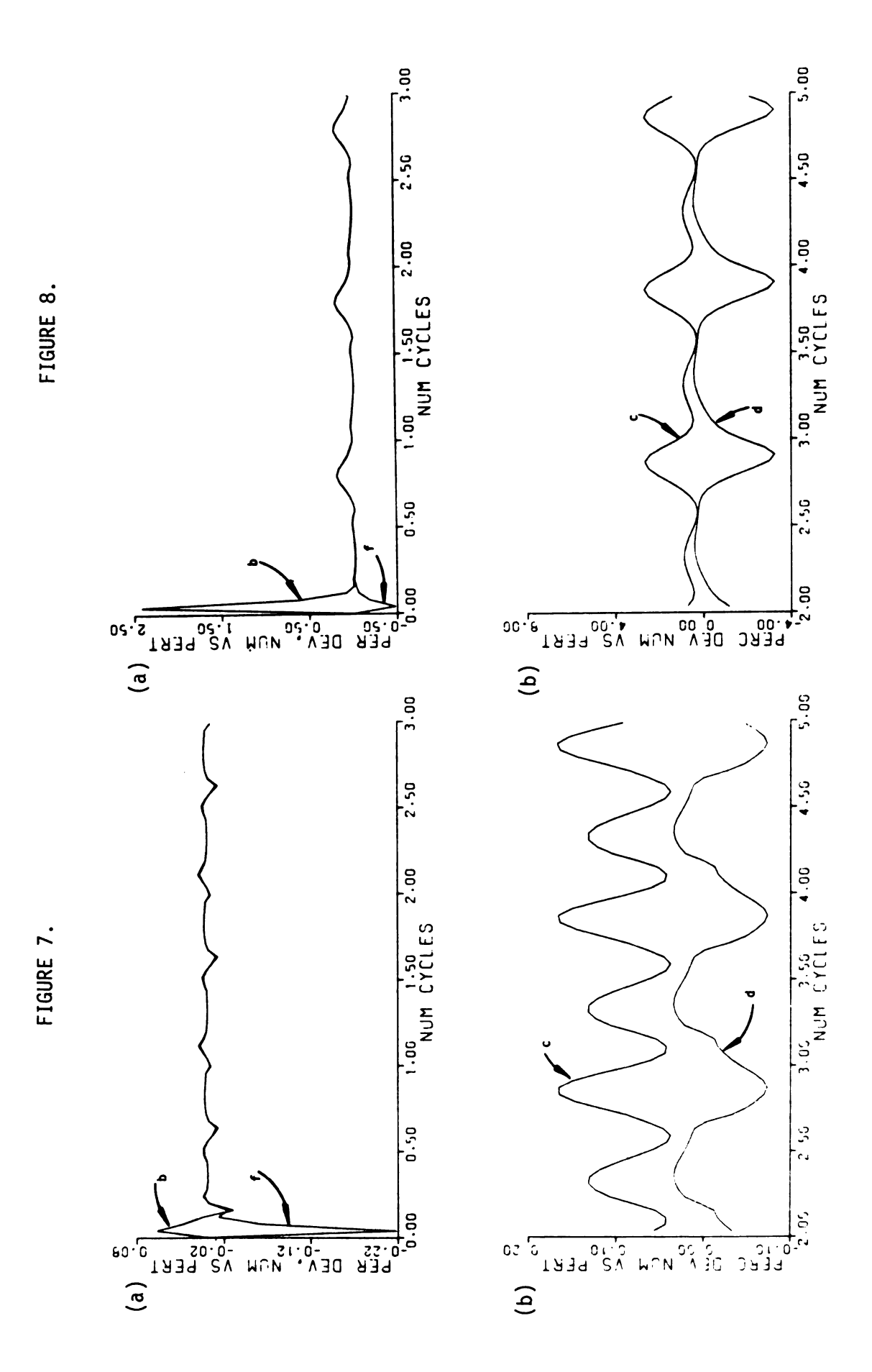
- FIGURE 3.(a-b) Behavior of Van de Vusse system for $\tau k_1 = k_2/k_1 = \tau k_3 A_0 = \Lambda = 1$, $\epsilon = .75$.
- FIGURE 4.(a-b) Behavior of Van de Vusse system for $\tau k_1 = k_2/k_1 = \tau k_3 A_0 = \Lambda = 1$, $\epsilon = .25$.



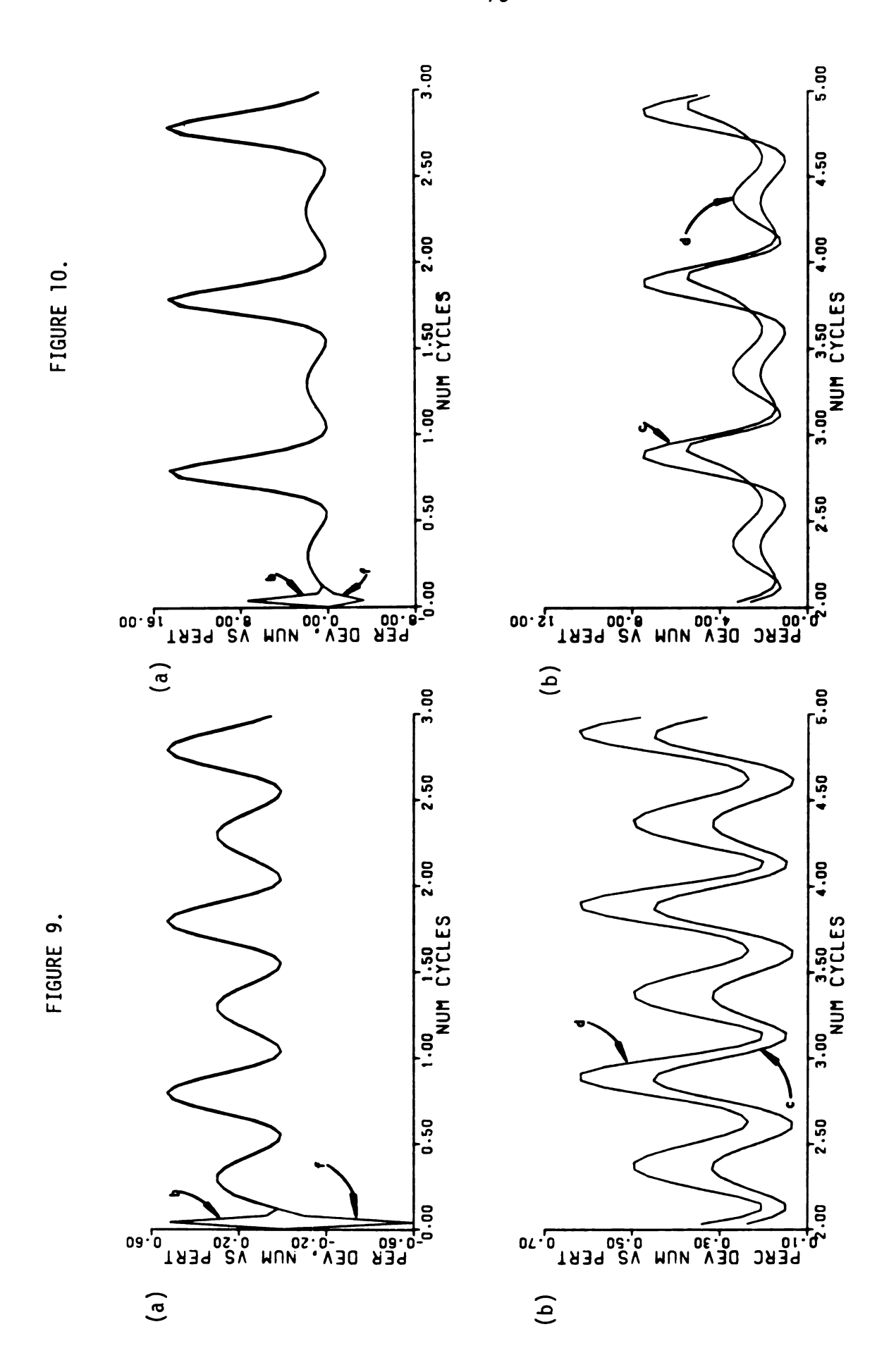
- FIGURE 5.(a-b) Deviation of perturbation solution from numerical simulation for Van de Vusse system $\tau k_1 = k_2/k_1 = 1$ $\tau k_3 A_0 = 5$ $\Lambda = 1$ $\epsilon = .25$. % error = ($C_{pert} C_{num}$)/ C_{num} 100.
- FIGURE 6.(a-b) Deviation of perturbation solution from numerical simulation for Van de Vusse system $\tau k_1 = k_2/k_1 = 1$ $\tau k_3 A_0 = 5$ $\Lambda = 1$ $\epsilon = .75$. % error = $(C_{pert} C_{num})/C_{num}$ 100.



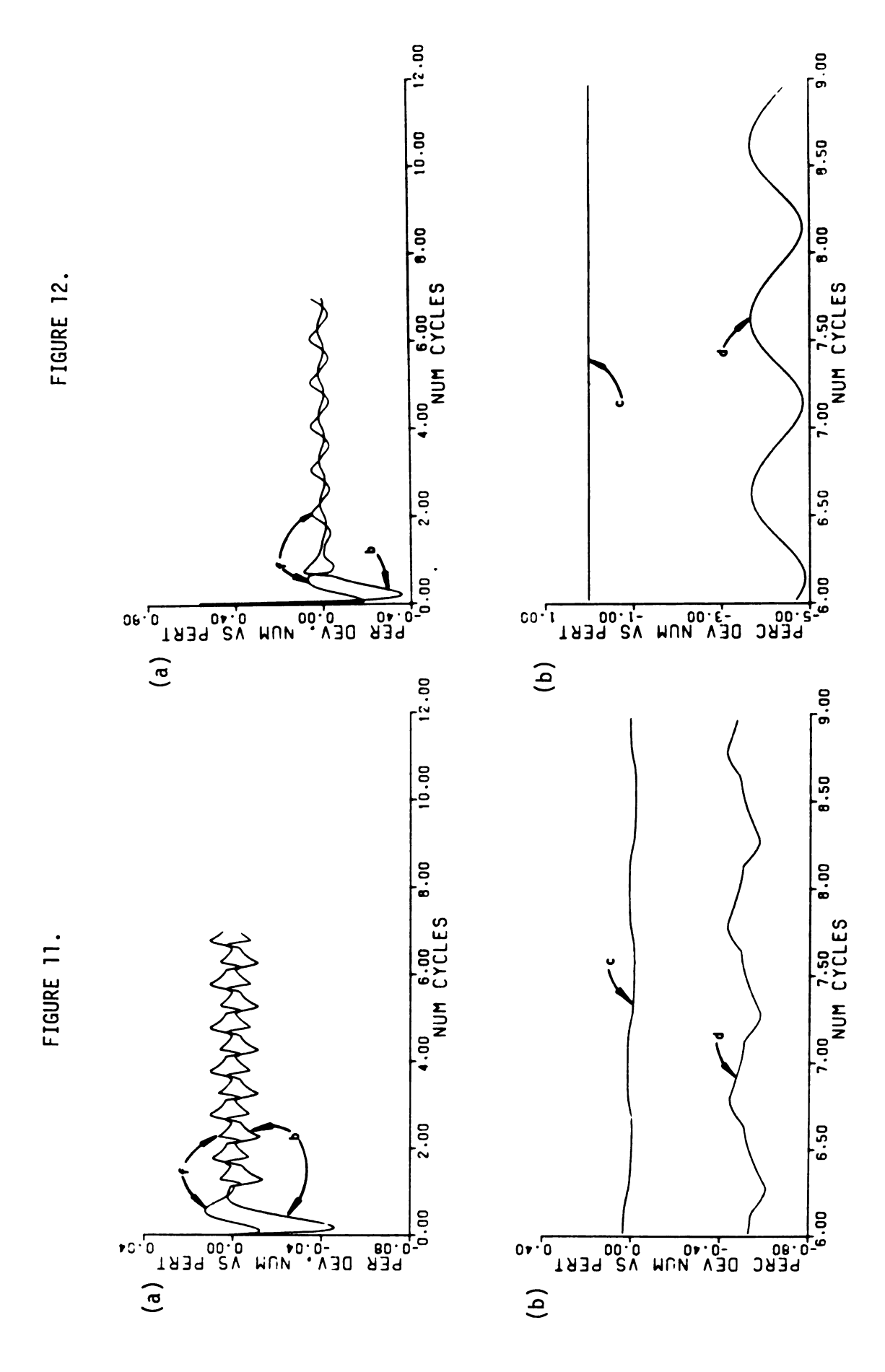
- FIGURE 7.(a-b) Deviation of perturbation solution from numerical simulation for Van de Vusse system $\tau k_1 = k_2/k_1 = 5$ $\tau k_3 A_0 = 1$ $\Lambda = 1$ $\epsilon = .25$. % error = $(C_{pert} C_{num})/C_{num}$ 100.
- FIGURE 8.(a-b) Deviation of perturbation solution from numerical simulation for Van de Vusse system $\tau k_1 = k_2/k_1 = 5$ $\tau k_3 A_0 = 1$ $\Lambda = 1$ $\epsilon = .75$. % error = $(C_{pert} C_{num})/C_{num}$ 100.



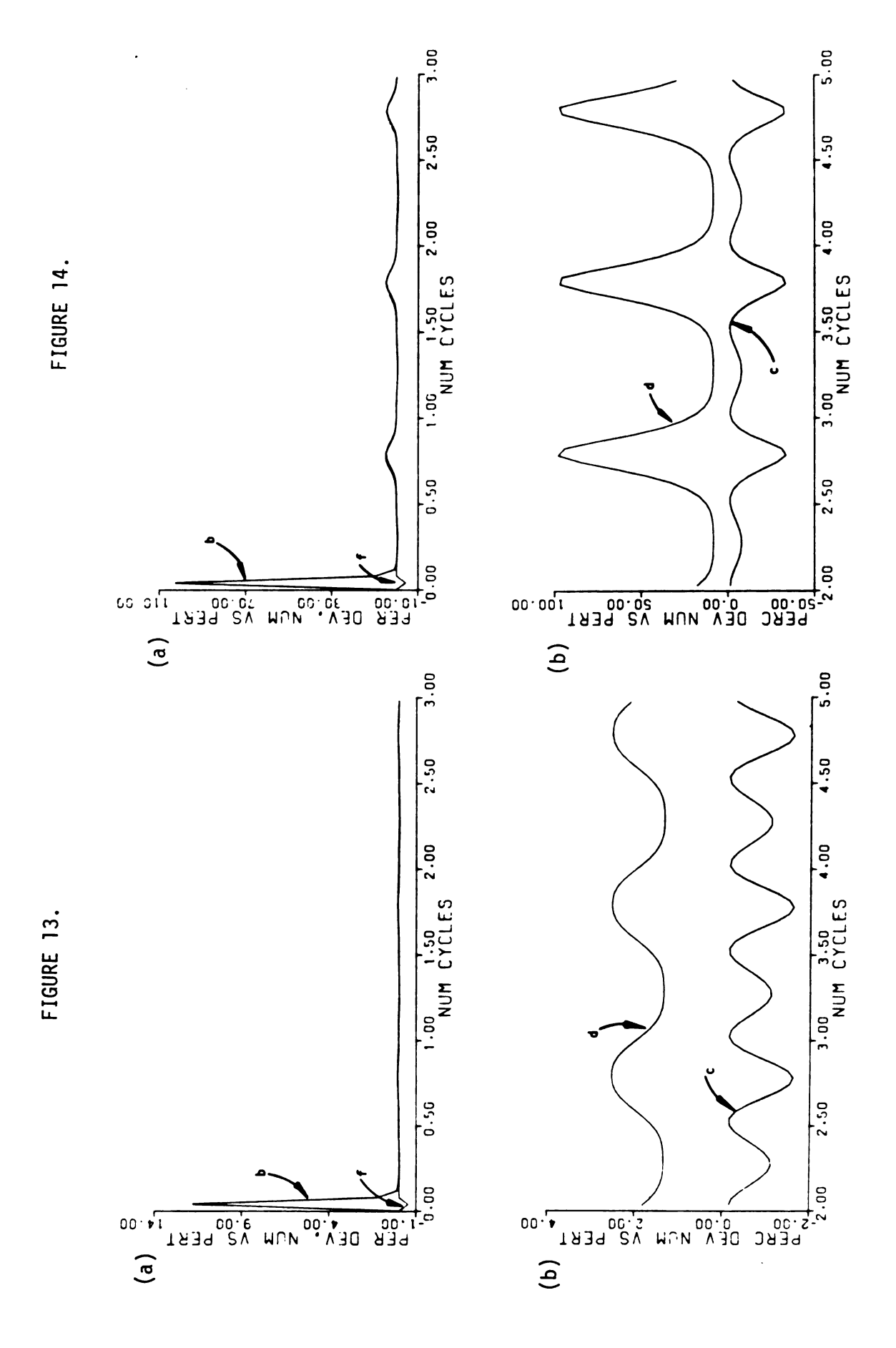
- FIGURE 9.(a-b) Deviation of perturbation solution from numerical simulation for Van de Vusse system $\tau k_1 = k_2/k_1 = \tau k_3 A_0 = 5$ $\Lambda = 1$ $\epsilon = .25$. % error = (Cpert Cnum)/Cnum:100.
- FIGURE 10.(a-b) Deviation of perturbation solution from numerical simulation for Van de Vusse system $\tau k_1 = k_2/k_1 = \tau k_3 A_0 = 5$ $\Lambda = 1$ $\epsilon = .75$. % error = ($C_{pert} C_{num}$)/ C_{num} ·100.



- FIGURE 11.(a-b) Deviation of perturbation solution from numerical simulation for Van de Vusse system $\tau k_1 = k_2/k_1 = \tau k_3 A_0 = 1$ $\Lambda = 5$ $\epsilon = .25$. % error = $(C_{pert} C_{num})/C_{num}$:100.
- FIGURE 12.(a-b) Deviation of perturbation solution from numerical simulation for Van de Vusse system $\tau k_1 = k_2/k_1 = \tau k_3 A_0 = 1$ $\Lambda = 5$ $\epsilon = .75$. % error = $(C_{pert} C_{num})/C_{num}$:



- FIGURE 13.(a-b) Deviation of perturbation solution from numerical simulation for Van de Vusse system $\tau k_1 = k_2/k_1 = \tau k_3 A_0 = 1$ $\Lambda = .2$ $\epsilon = .25$. % error = $(C_{pert} C_{num})/C_{num}$ 100.
- FIGURE 14.(a-b) Deviation of perturbation solution from numerical simulation for Van de Vusse system $\tau k_1 = k_2/k_1 = \tau k_3 A_0 = 1$ $\Lambda = .2$ $\epsilon = .75$. % error = $(C_{pert} C_{num})/C_{num}$ 100.



the perturbation solution gives an accurate and convenient prediction of the time average system behavior.

Table 1 shows the predictions from the perturbation solutions for those values of the system constants which appear in the figures. The first 4 columns give the percent error in the average concentrations calculated from equations (24) when compared to the numerical simulation. The largest error is 5.43%, including all the cases where the error in the functions themselves were large. The second four columns give the predicted enhancement in concentration. Again, \vec{f} , \vec{c} , and \vec{d} compare to the steady state with the same residence time as the periodic process while \vec{b} compares to the optimum steady state \vec{b} given by DeVera and Varma [12].

Several trends can be discerned from the data in Table 1. These are very similar to the behavior of the Van de Vusse system under square wave feed concentration [13]. As with square wave cycling, the effect of periodic operation on the time averages increases as the period of the feed disturbance increases, or as Λ decreases. This trend implies that the most effective cycling for this case is quasi-steady state cycling, where the process input changes very slowly. In that case, the process responds quickly enough to always be near the steady state corresponding to the instantaneous value of the input. If the effects of cycling are desirable, it may be more advantageous to run several steady state processes in parallel, since the performance of a quasi-steady state process can be approached in this manner.

The form of the analytic expressions (24) show that conversion is always enhanced, yields of b and c are diminished, and yield of d is almost always enhanced. These a priori conclusions reinforce the same trends in the data for the square wave feed, although a priori predictions were not possible in that case.

TABLE 1. Percent deviation of approximate time average concentrations [equations (24)] from numerically simulated time average concentrations; percent enhancement of approximate time average concentrations over steady state concentrations.

_:
ė
፭
2

b b c c c c c c c c c c c c c c c c c c	0 0 0 0 0 0 0 0 0 0 0		• • • • • • • • • • • • • • • • • • •	0 0 0 0 0 0 0 0 0 0 0 0 0 0 0 0 0 0 0	Percent D	eviation,	ercent Deviation, Č _{i,num} vs Či,pert	. Ci.pert	Per	Percent Enhancement**	ancement	*
					(Či,per	t ^{-Ĉ} i,num	(Či,pert -Či,num)/Či,num	100	, <u>,</u> ,	(č, pert-ci,s)/	د. ا	. 100
1k1	k,/k1	k, A _o	<	ω	84 -	و	ıu	Р	.	٩	U	P
-		-	-	<u>-</u>	0000	.013	00(13	0002	047	061	047	228
_:	<u>-</u> :	-	-	. 25	0008	082	0008	00.1	297	378	297	1.43
-	-	_:	-	.75	064	769.	064	.266	-2.66	-3.40	-2.66	12.8
-	-:		-	-	213	1.17	213	.792	-4.74	-6.05	-4.74	22.9
-:	-	5.	-	.25		177	357	692	088		088	1.31
<u>-</u> :	-	5.	-	. 75		-2.02	-3.69	-5.50	792		792	11.8
5.	5.	-	-	.25		121	0000	.002	074	-65.9	074	2.74
5.	5.		-	.75		-1.10	0008	.024	668	-65.8	668	24.7
5.	5.	5.	-:	.25		279	198	381	049	-64.8	049	2.39
5.	5.	5.	<u>-</u> :	.75		-2.60	-1.85	-2.75	445	-64.7	445	21.5
-	-	_:	5.	.25	0001	0002	015	027	081	081	081	.390
-	_:	_:	5.	.75		002	010	040	727	727	727	3.51
-	-	_:	.2	.25	001	.597	001	900.	331	928	331	1.60
_:	<u>-</u> :	-	.2	.75	106	5.43	106	.432	-2.98	-8.35	-2.98	14.4

*C_j - f, b, c, or d

^{**}f, c, d compare to steady state with same residence time as periodic--b compares to optimum steady state b [12].

One other trend is observed which also appeared in square wave cycling. The effects of periodic operation were most pronounced when the kinetic constants favor the formation of B over the formation of D. This is in fact logical. If the kinetic constants favor the formation of D, then little B or C would be produced, making it impossible to sizeably shift the product distribution from B and C toward D.

CONCLUSION

Sinusoidal concentration fluctuations to an isothermal CSTR with either consecutive parallel or Van de Vusse kinetics is ineffective in increasing the yield of intermediate product B, or the output of product c. For Van de Vusse kinetics, however, output of the side product D can be sizeably enhanced by up to 25% by such an input disturbance. The perturbation solution given above provides a convenient and calculationally simple method of approximating the time average output of the reactor.

CHAPTER 3

PERIODIC SQUARE WAVE FEED CONCENTRATION TO AN ISOTHERMAL CSTR WITH A VAN DE VUSSE REACTION OCCURRING IN POROUS SLAB CATALYST PARTICLES

Periodic operation of chemical reactors has its most significant impact in the area of heterogeneously catalyzed systems, which are by far most important from an industrial viewpoint. The complexity of the mathematics evolving from the treatment of such systems, however, is immense. For this reason, research in this area has either relied heavily on extreme simplifying assumptions, has used approximate or numerical approaches, or both.

Bailey has explored the theoretical aspects of periodically operated catalytic processes. His early work emphasized a control oriented approach to the topic and neglected diffusional or mass transfer effects entirely [1,2,3,4,5,6]. His later work considers a less idealized case in which a porous catalyst pellet is examined under the influence of a periodic boundary condition [7,8]. He was able to show increases in selectivity using numerical and approximate analytic techniques.

Others have studied similar problems from a theoretical viewpoint.

Oruzheinkov et al. [9] used an approach similar to the early work of

Bailey and concluded that selectivity in a non-porous catalyst could be
improved by periodic operation. Rice and coworkers [10,11] looked at the
transient, non-periodic behavior of a porous catalyst both with and
without external mass transfer limitations. Experimental work in the area
has centered on problems in which diffusional effects are absent [12,13,14],
with the exception of Unni, et al., who showed an increase in conversion
from concentration cycling [15].

The Model

Unlike the other models, e.g., Bailey, we consider here a case where the perturbation is caused by an external forcing function. A CSTR in which porous catalyst pellets are contained is fed with a stream whose

concentration varies in a square wave. The pellets are considered to be one-dimensional. A complex reaction network named after

$$A \stackrel{k_1}{\rightarrow} B \stackrel{k_2}{\rightarrow} C$$

$$A + A \stackrel{k}{\rightarrow} D$$

takes place on the active surface within the catalyst with no reaction volume change. The diffusivities of the various species may be unequal but are considered constant. Mass transfer coefficients are assumed equal for all species. Adsorption-desorption effects are lumped into effective rate constants which give the rate of surface reaction in terms of the adjacent fluid phase concentrations. Diffusional resistance within the pellet is considered important and an external mass transfer resistance is included. Components A and B will be considered.

The Basic Equations

Two mass balances are involved for each component: the balance with the catalyst slab and the balance on the fluid medium in which the particles are bathed, which will be referred to as the bulk phase. For component A in the slab we have

$$D_{e_{\Lambda}} \frac{\partial^2 A}{\partial x^2} - k_1 A - k_3 A^2 = \frac{\partial A}{\partial t}$$
 (1a)

and the in the bulk phase

$$q \hat{A}_f(t) - q\hat{A} - D_{e_A} \frac{\partial A}{\partial x} (x=L,t) An_p = V \epsilon \frac{d\hat{A}}{dt}$$
 (1b)

with boundary conditions

$$\hat{A}(t=0)=0$$
; $A(x,t=0)=0$; $\frac{\partial A}{\partial x}(x=0)=0$; $D_{e_A} \frac{\partial A}{\partial x}(x=L)=k_g[\hat{A}-A(x=L)]$ (1c)

For component B in the slab,

$$D_{\mathbf{e}_{\mathbf{B}}} \frac{\partial^{2} \mathbf{B}}{\partial \mathbf{x}^{2}} + k_{1} \mathbf{A} - k_{2} \mathbf{B} = \frac{\partial \mathbf{B}}{\partial \mathbf{t}}$$
 (2a)

and in the bulk

$$q\hat{B}_f - q\hat{B} - D_{e_R} \frac{\partial B}{\partial t} (x=L,t)An_p = V_{\epsilon} \frac{d\hat{B}}{dt}$$
 (2b)

and boundary conditions

$$\hat{B}(t=0)=0$$
; $B(x,t=0)=0$; $\frac{\partial B}{\partial x}(x=0)=0$; $D_{e_{R}}\frac{\partial B}{\partial x}(x=1)=k_{g}[\hat{B}-B(x=1)]$ (2c)

Defining the following dimensionless variables,

$$\phi = \sqrt{\frac{k_1 L^2}{D_e_A}}; \quad \zeta \equiv \frac{X}{L}; \quad u \equiv \frac{A}{A_o}; \quad K_3 \equiv \frac{k_3 A_o}{k_1}$$
 (3a)

$$e \equiv \frac{tD_{e_A}}{L}$$
; $b \equiv \frac{B}{A_0}$; $\kappa_2 \equiv \frac{k_2}{k_1}$; $h = \frac{D_{e_A}}{D_{e_B}}$ (3b)

$$\Phi \equiv \frac{V \in D_{\mathbf{e}_{A}}}{qL^{2}} \quad \beta \equiv \frac{D_{\mathbf{e}_{A}} n_{\mathbf{p}_{A}}}{qL} \quad \nu \equiv \frac{kgL}{D_{\mathbf{e}_{A}}}$$
 (3c)

$$\hat{\mathbf{u}} = \frac{\hat{\mathbf{A}}}{\mathbf{A}_{\mathbf{0}}} \qquad \hat{\mathbf{b}} = \frac{\hat{\mathbf{B}}}{\mathbf{A}_{\mathbf{0}}} \tag{3d}$$

the mass balances can be made dimensionless as follows

$$\frac{\partial^2 u}{\partial \xi^2} - \phi^2 \left[u + K_3 u^2 \right] = \frac{\partial u}{\partial \theta} \tag{4a}$$

$$\hat{\mathbf{u}}_{\mathbf{f}} - \hat{\mathbf{u}} - \beta \frac{\partial \mathbf{u}}{\partial \xi} (\xi = 1, \theta) = \Phi \frac{d\hat{\mathbf{u}}}{d\theta}$$
 (4b)

with dimensionless boundary conditions

$$\hat{\mathbf{u}}(\theta=0); \ \mathbf{u}(\xi,\theta=0)=0; \ \frac{\partial \mathbf{u}}{\partial \xi} \ (\xi=0)=0; \ \frac{\partial \mathbf{u}}{\partial \xi} \ (\xi=1) = \nu[\hat{\mathbf{u}}-\mathbf{u}(\xi=1)] \tag{4c}$$

for b

$$\frac{\partial^2 b}{\partial \xi^2} + \phi^2 h \left[u - K_2 b \right] = h \frac{\partial b}{\partial \theta}$$
 (5a)

$$\hat{\mathbf{b}}_{\mathbf{f}} - \hat{\mathbf{b}} - \frac{\beta}{\mathbf{h}} \frac{\partial \mathbf{b}}{\partial \xi} (\xi = 1, \theta) = \Phi \frac{\partial \hat{\mathbf{b}}}{\partial \theta}$$
 (5b)

with boundary conditions

$$\hat{\mathbf{b}}(\theta=0)=0; \ \mathbf{b}(\xi,\theta=0)=0; \ \frac{\partial \mathbf{b}}{\partial \xi} \ (\xi=0)=0; \ \frac{\partial \mathbf{b}}{\partial \xi} \ (\xi=1)=\mathbf{h} \vee [\hat{\mathbf{b}}-\mathbf{b}(\xi=1)] \tag{5c}$$

Equations (4) are coupled but independent of equations (5); equations (5) are unidirectionally coupled to equations (4).

The periodic forcing function of interest is the square wave

$$u_{f} = \begin{cases} 0; t \in [0, \pi/\Lambda) \\ u_{f}(t+2\pi/\Lambda) = u_{f}(t); b_{f} = 0 \end{cases}$$

$$(6)$$

$$2; t \in [\pi/\Lambda, 2\pi/\Lambda)$$

There is no intermediate b in the feed. The steady state anologs of equations (4) and (5) are obtained by setting the time derivatives equal to zero and letting $\mathbf{u_f}$ equal one.

Of the 4 steady state and 4 transient equations, only the steady state counterparts of the reactant balances (4) were found amenable to solution. The solution to $u(\xi)$ takes on one of three simple forms depending on whether $u(\xi=0) >< = 1/2K_3$, or $1/2K_3 > 1$. Since the evaluation of $u(\xi=0)$ requires a knowledge of the solution form, it is convenient to determine the value of $\phi_0(=\sqrt{\phi_0^2})$ which corresponds to $u(\xi=0) = 1/2K_3$. By maximum principles and the uniqueness of solution, it can be shown that $\frac{du(\xi=0)}{d\varphi} < 0$, so that the value of φ determines which form of the solution applies. The result is for $\varphi > \varphi_0$, or if $1/(2K_3)>1$

$$u(\xi) = c + (u_0 - c) dc^2 \{ \sqrt{\frac{K_3 \phi^2 (u_0 - c)}{6}} \xi \}$$
; $\phi > \phi_0$ (7a)

The value of u_0 is found for $\phi > \phi_0$ by solving the following equations simultaneously:

$$\sqrt{\frac{2K_3\phi^2}{3}} \sqrt{(u_1-u_0)(u_1-b)(u_1-c)} = \frac{v}{1+\beta v} [1-u_1]$$
 (7b)

$$u_1 = c + [u_0 - c] dc^2 \{ \sqrt{\frac{K_3 \varsigma^2 (u_0 - c)}{6}} \}$$
 (7c)

where

$$b_{+,c} = \frac{-(u_0 + 3/2K_3) \pm \sqrt{(u_0 + 3/2K_3)^2 - 4u_0(u_0 + 3/2K_3)}}{2}$$
 (7d)

The notation b_+,c_- in equation (7d) implies that b corresponds to the plus sign and c to the minus sign. For $\phi=\phi_0$, the solution takes on a simple form

$$u(\xi) = u_0\{1+3 \tan^2 (\frac{\xi_0}{2}\xi)\} ; \phi = \phi_0$$
 (8)

For \$<\$0

$$u(\xi) = u_0 + \frac{1 - cn[\sqrt{2K_3/3g^2} + \xi]}{1 + cn[\sqrt{2K_3/3g^2} + \xi]} \cdot A, \qquad \phi < \phi_0$$
 (9a)

Here, dc and cn are the Jacobian elliptic functions. Again u_0 is found for $\phi < \phi_0$ by the simultaneous solution of 2 equations, viz.,

$$u_1 = u_0 + \frac{1 - cn[\sqrt{2K_3}/3g^2 \phi]}{1 + cn[\sqrt{2K_3}/3g^2 \phi]} \cdot A$$
 (9b)

and equation (7b). The quantities needed for evaluation of (9b) are

$$A^2 = (b_1 - u_0)^2 + a_1^2$$
 (9c)

$$g = 1/\sqrt{A}, b_1 = \frac{b+c}{2}, a_1^2 = -\frac{(b-c)^2}{4}$$
 (9d)

where b and c are again defined by (7d).

When $1/(2K_3)>1$, ϕ_0 need not be calculated; otherwise the value of ϕ_0 is found by solving

$$\sqrt{\frac{2K_3}{3}} \ 2 \ \tan^{-1} \left[\sqrt{\frac{u_1 - 1/2K_3}{3/2K_3}} \right] \left[u_1 + 1/K_3 \right] \left[u_1 - 1/2K_3 \right]^{1/2} = \frac{v[1 - u_1]}{1 + \beta v}$$
 (10a)

for u_1 . The result is substituted into the following equation and solved for ϕ_0 :

$$u_1 = 1/2K_3\{1+3\tan^2(\frac{\phi_0}{2})\}$$
 (10b)

The bulk phase concentration is given by a simple algebraic relationship:

$$\hat{\mathbf{u}} = \frac{1 + \beta \nu \mathbf{u}(\xi=1)}{1 + \beta \nu} \tag{11}$$

The steady state counterparts to equations (5) can be solved by variation of parameters in combination with equations (7-10). However, the integrals arising from such a treatment contain expressions of the form $\int \frac{e^{at}}{\cos bt} dt$ or $\int \frac{e^{at}}{\cos^2 bt} dt$ which cannot be expressed in terms of a finite series of elementary functions or, to our knowledge, any infinite but convergent series. The periodic equations (4,5,6) are nonlinear partial differential equations and are presumed to have no exact solution. As of yet no applicable approximate solutions have been found, although such work is in progress.

NUMERICAL RESULTS

The steady state forms, which give second order ordinary differential equations (ODE's) with boundary values, were solved using the iterative McGuinness method [19]. The periodic forms were treated by the method of lines [20], in which the spatial derivatives are discretized, yielding a coupled system of ODE's with respect to time. These are solved simultaneously with the ODE governing the bulk phase concentration. All of the ODE's encountered were solved with the IMSL routine DGEAR using Adam's method.

The steady state solution for $u(\xi)$ was checked against numerical simulation and gave arbitrarily close agreement within the accuracy of DGEAR for all three solution regions. Thereafter, in all steady state

calculations, including the numerical simulation of $b(\xi)$, the analytic expression for $u(\xi)$ was used.

Table 1 summarizes the results of the numerical solution of the periodic process for square wave forcing. As can be seen for the results with h = 5., the accuracy of the results change dramatically with the number of spatial increments used. Close convergence of the results with increasing number of increments is elusive, because computing time increases very rapidly. In some cases as much as 125 CP seconds on MSU's Cyber 750 model 170 were needed to perform a simulation with 25 spatial increments.

Rows 1 and 2 of Table 1, marked Ref, give the results when all of the system constants are equal to one. Row 2 with 20 spatial increments is the more accurate and provides a reference against which the other results can be compared. In each case one constant was varied and all others were held fixed at one. The column on the left shows which constant was varied.

Figures 1 through 5 show the system behavior for the case where all constants are equal to one. There is an abrupt break in the slope of $\hat{u}(\theta)$ (Fig. 1), whereas $\hat{b}(\theta)$ (Fig. 2) shows no abrupt changes in slope. Figure 3 shows the phase plane for the bulk phase concentrations. Figures 4 and 5 show the concentration profiles within the pellet at five different points in the cycle. The horizontal sections on the right of each profile show the bulk phase concentrations. The diagonal lines connecting the values at the outside of the catalyst pellet to those in the bulk represent a physical gradient which imparts an impression of the concentration difference across the external boundary layer. It is interesting that the bulk phase behavior, Figures 1, 2, 3, is quite similar to that observed for the square wave forced homogeneous system [16].

FIGURE 1. Bulk phase reactant concentration vs. time for square wave cycling. $\phi=1$. $\nu=1$. $\beta=1$. $K_3=1$. h=1. $K_2=1$. $\Lambda=1$. $\psi=1$.

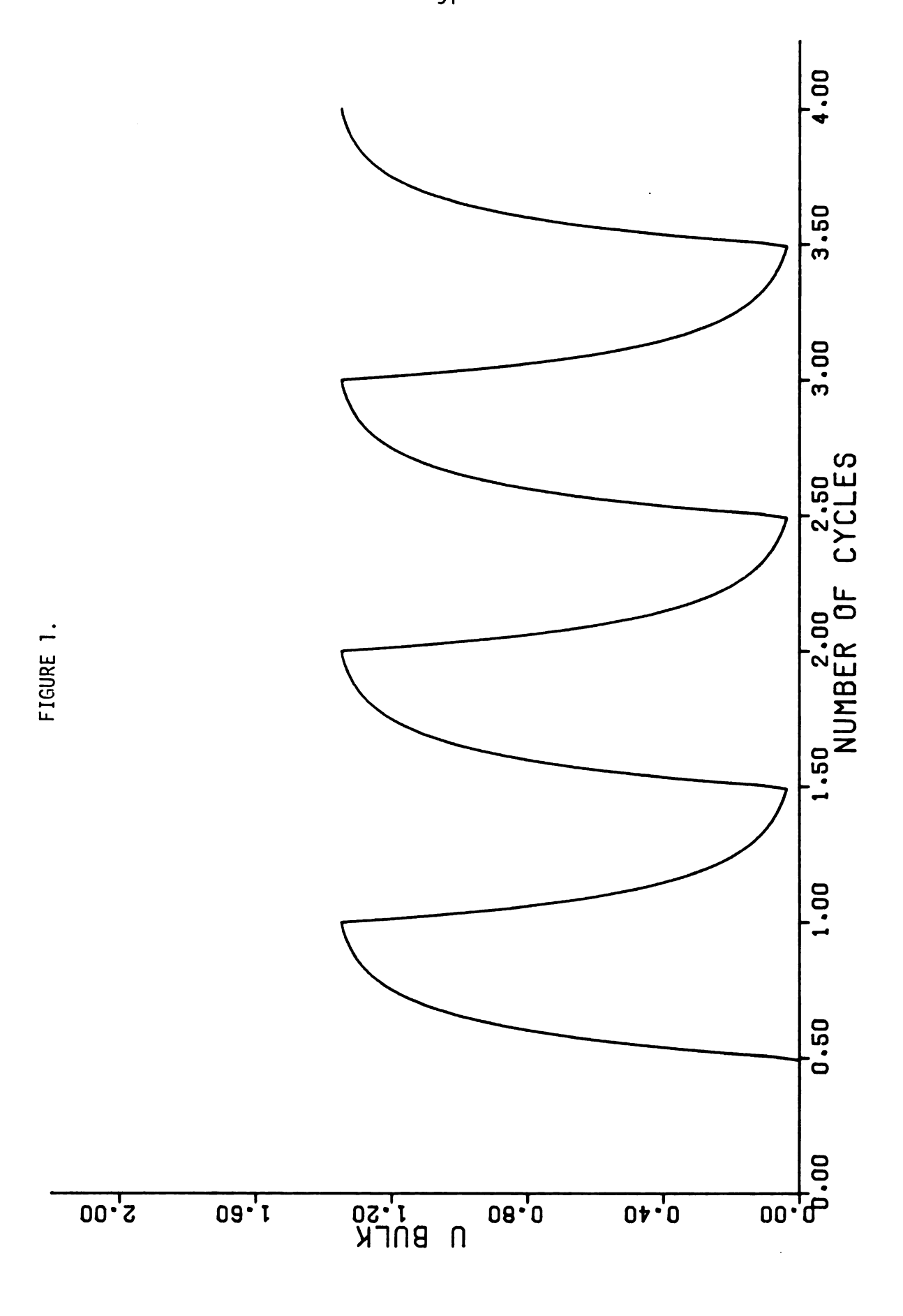


FIGURE 2. Bulk phase intermediate concentration vs time for square wave cycling. ϕ =1. ν =1. β =1. K_3 =1. h=1. K_2 =1. Λ =1. ψ =1.

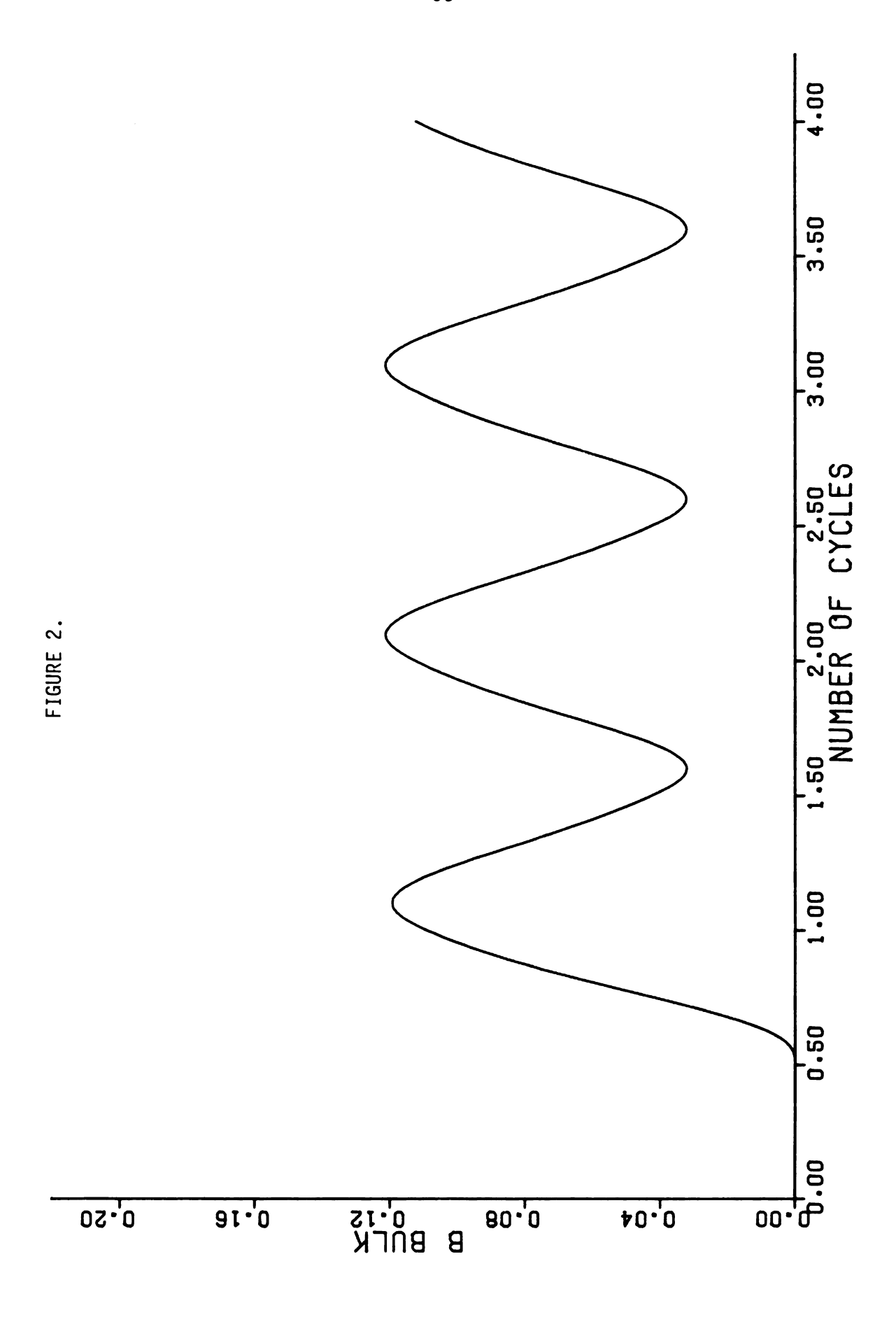


FIGURE 3. Bulk phase plane behavior for square wave cycling. ϕ =1. ν =1. β =1. K_3 =1. h=1. K_2 =1. Λ =1. ψ =1.

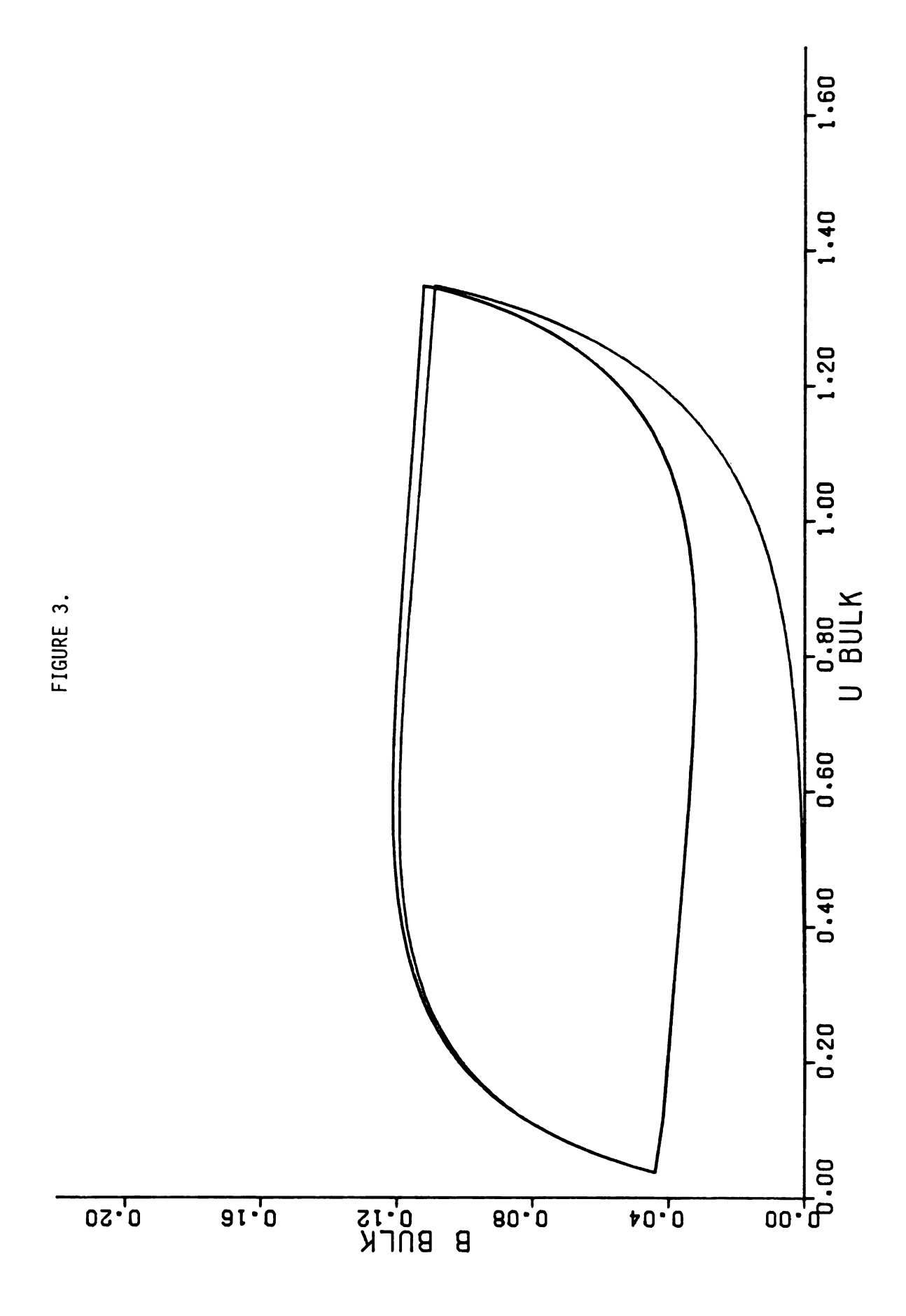


FIGURE 4. Reactant concentration profile within the pellet at five selected points in the limit cycle. ϕ =1. ν =1. β =1. K_3 =1. h=1. K_2 =1. Λ =1. ψ =1.

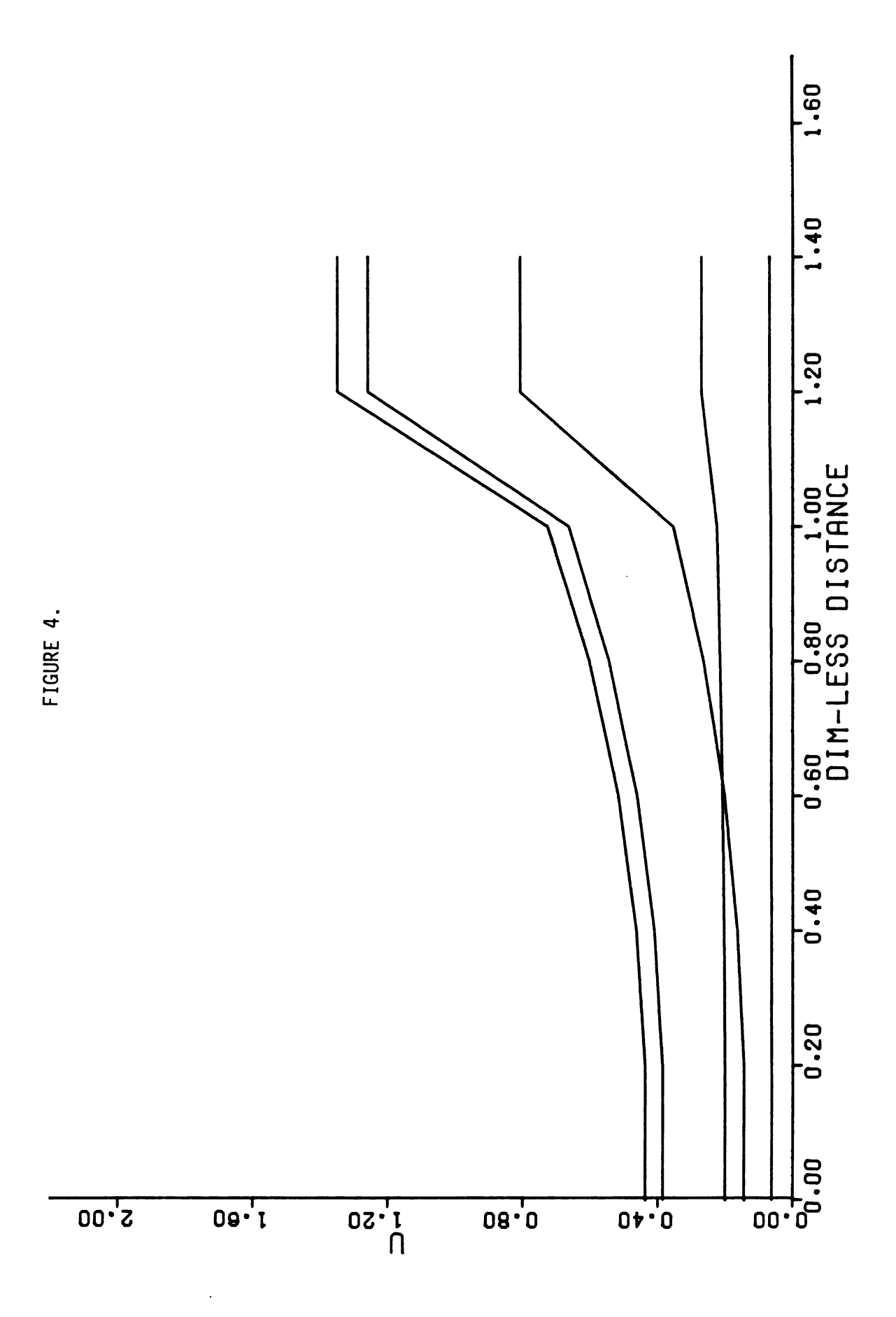


FIGURE 5. Intermediate concentration profile within the pellet at five selected pointed in the limit cycle. ϕ =1. ν =1. β =1. K_3 =1. h=1. K_2 =1. Λ =1. ψ =1.

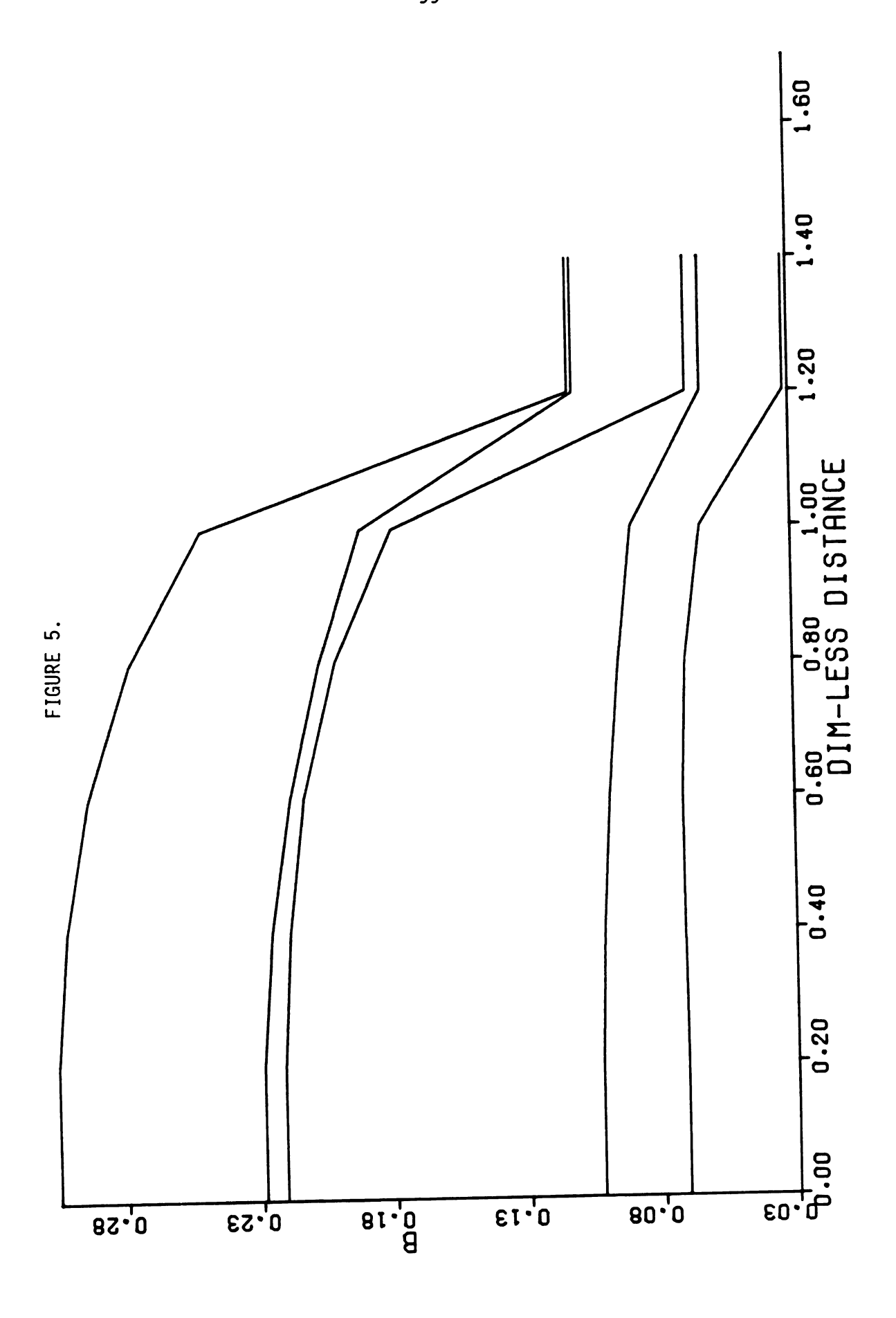


TABLE 1. Percent increase in time average of periodic bulk phase concentrations over steady state concentrations for square wave perturbation.

TABLE 1.

	¢	Б	ν	К3	h	K ₂	Λ	\$	NSI ⁺	Su	∫b
Ref	1.	١.	1.	1.	1.	١.	1.	1.	5	2.43	- 2.03
	1.	1.	1.	1.	1.	١.	1.	1.	20	074	- 3.82
Dec ¢	.1	1.	1.	1.	1.	1.	1.	1.	5	.340	-19.1
	.1	1.	1.	1.	1.	1.	1.	١.	20	.026	- 4.97
	. 4	1.	1.	١.	1.	١.	1.	1.	5	1.77	-12.0
Inc	1.	١.	1.	1.	١.	١.	1.	5.	5	3.30	2.11
	1.	1.	1.	1.	1.	1.	1.	5.	10	1.43	.777
	1.	١.	1.	1.	1.	١.	1.	5.	20	.637	112
Dec K;	1.	١.	1.	1.	1.	.2	1.	١.	8	1.09	- 6.62
	١.	1.	1.	1.	١.	.2	1.	1.	16	.119	- 5.47
Dec K ₃	1.	1.	1.	.2	1.	١.	١.	1.	10	1.39	.438
	1.	1.	1.	. 2	1.	1.	1.	1.	20	.557	421
Vary- ing h	1.	١.	1.	1.	. 1	1.	1.	1.	12	.440	- 2.68
	1.	1.	1.	1.	.2	1.	1.	1.	10	.71	- 2.4
	1.	1.	1.	1.	5.	1.	1.	1.	5	2.49	- 9.68
	1.	1.	1.	1.	5.	1.	1.	١.	15	.17	- 6.09
	١.	1.	1.	1.	5.	1.	1.	1.	25	07	- 5.6
	1.	1.	١.	1.	10.	1.	1.	1.	15	.044	- 1.24
lnc v	1.	10.	1.	1.	1.	١.	1.	1.	15	377	- 5.86

 $^{^{\}dagger}$ NSI is the number of spatial increments used in the method of lines.

Discussion

Over a narrow range of physical parameter variation, the preliminary results presented here are less than encouraging for the effort to increase yield by periodic operation. Those parameters related to mass transfer resistance, namely ϕ , ν , and h, do not seem to combine in any way to enhance time average yield. For instance, decreasing ϕ , which has the effect of rendering diffusion of A more significant in comparison to reaction of A, appears to be detrimental to both time average conversion and time average yield. An increase in Φ can be interpreted in several ways, e.g., the most direct is an increased residence time. This results in a decrease in both conversion and yield. The same effect is produced by a decrease in either K_2 or K_3 . Variation of h, the ratio of diffusion coefficients for A and B, shows no systematic pattern in its effect on periodic operation and is not beneficial to yield in any case. It should be noted that changing h should not affect the time average of A. This is closely born out for those cases with 15 or more spatial increments. Lastly, an increase in v, reflecting lesser external mass transfer resistance relative to diffusion, markedly decreases average yield, but has a slight favorable effect on average conversion.

It appears, for those cases considered, that steady state operation is superior. While no definitive instances of yield enhancement are presented in this work, this effort should not be abandoned. The results presented here reflect only a few combinations of system constants, and the possible variations of eight system constants are enormous.

Moreover, the probable error in this calculation via the method of lines is as high as 100% for the lower values of enhancement. In fact, the results in Table 1 illustrate that in some cases the enhancement changes sign as the number of spatial increments is increased.

It was not possible to achieve strict convergence because of the excessive computation time involved. Clearly a more efficient numerical technique is necessary to allow a larger range of system constants to be examined. Orthogonal collocation, as used by Bailey [8], may be appropriate.

CONCLUSION

For the heterogeneously catalysed Van de Vusse reaction occurring in slab catalyst particles in an isothermal CSTR, periodic square wave forcing of the input concentration may not be effective in enhancing yield relative to steady state. Preliminary approximate results show mainly detrimental effects on both yield of intermediate B and conversion of reactant A. Additional work, specifically on mathematical analysis of the integro-differential equation resulting from the model, is necessary.

LIST OF REFERENCES

REFERENCES--CHAPTER 1

- 1. Dorawala T. G. and Douglas J. M., A.I.Ch.E. J. 1971 17 974.
- 2. Ritter A. B. and Douglas J. M., Ind. Engng Chem. Fundls 1970 9 21.
- 3. Douglas J. M., Ind. Engng Chem. Proc. Des. Dev. 1967 6 43.
- 4. Douglas J. M. and Rippin D. W. T., Chem. Engng Sci. 1966 21 305.
- 5. Renken A., Chem. Engng Sci. 1972 27 1925.
- 6. Wandrey C. and Renken A., Chem. Engng Sci. 1977 32 448.
- 7. DeVera A. L. and Varma A., Chem. Engng Sci. 1979 34 1377.
- 8. DeVera A. L. and Varma A., Chem. Engng J. 1979 17 163.
- 9. Bailey J. E. and Horn F. J. M., Chem. Engng Sci. 1972 27 109.
- 10. Lee C. K. and Bailey J. E., Chem. Engng Sci. 1974 29 1157.
- 11. Towler B. F. and Rice R. G., Chem. Engng Sci. 1974 29 1828.
- 12. Imison B. W. and Rice R. G., Chem. Engng Sci. 1975 30 1421.
- 13. Bailey J. E., Chem. Engng Commun. 1973 1 111.
- 14. Farhadpour F. A. and Gibilaro L. G., Chem. Engng Sci. 1975 30 997.

REFERENCES--CHAPTER 2

- 1. Douglas J. M. and Rippin D. W. T., Chem. Engng Sci 1966 21 305.
- 2. Douglas J. M., Ind Engng Chem. Proc. Des. Dev. 1967 6 43.
- 3. Dorawala T. G. and Douglas J. M., A.I.Ch.E. J. 1971 17 974.
- 4. Ritter A. B. and Douglas J. M., Ind. Engng Chem. Fundls 1970 9 21.
- 5. Renken A., Chem. Engng Sci. 1972 27 1925.
- 6. Wandrey C. and Renken A., Chem. Engng Sci 1977 32 448.
- 7. Farhadpour F. A. and Gibilaro L. G., Chem. Engng Sci 1975 30 997.
- 8. Bailey J. E., Chem. Engng Commun. 1973 1 111.
- 9. Van de Vusse J. G., Chem. Engng Sci. 1964 19 994.
- 10. Beek J., A.I.Ch.E. J. 1972 18 228.
- 11. DeVera A. L. and Varma A., Chem. Engng Sci. 1979 34 1377.
- 12. DeVera A. L. and Varma A., Chem. Engng J. 1979 17 163.
- 13. Skeirik R. D. and DeVera A. L., Chem. Engng Sci. submitted (1980).

REFERENCES--CHAPTER 3

- 1. Horn, F. J. M., and Bailey, J. E., "An Application of the Theorem of Relaxed Control to the Problem of Increasing Catalyst Selectivity," J. Opt. Thry Appl. 2, 441 (1968).
- 2. Bailey, J. E., and Horn, F., "Catalyst Selectivity Under Steady-State and Dynamic Operation," Deutschen Bunsen Gesselschaft fur Physikalische Chemie Berichte (Ber. Bunseges. Phys. Chem.) 73 274 (1969).
- 3. Bailey, J. E., and Horn, F. J. M., "Catalyst Selectivity Under Steady-State and Dynamic Operation: An Investigation of Several Kinetic Mechanisms," Deutschen Bunsen Gesselschaft fur Physikalische Chemie Berichte (Ber. Bunseges. Phys. Chem.) 74, 611 (1970).
- 4. Bailey, J. E., and Horn, F. J. M., "Oscillatory Operation of Jacketed Tubular Reactors," Ind. Engng Chem. Fundls. 9, 299 (1970).
- 5. Bailey, J. E., and Horn, F. J. M., "Improvement of the Performance of a Fixed-Bed Catalytic Reactor by Relaxed Steady State Operation," AIChE J. 17, 550 (1971).
- 6. Bailey, J. E., Horn, F. J. M. and Lin, R. C., "Cyclic Operation of Reaction Systems: Effects of Heat and Mass Transfer Resistance," AIChE J. 17, 818 (1971).
- 7. Bailey, J. E., and Horn, F. J. M., "Cyclic Operation of Reaction Systems: The Influence of Diffusion on Catalyst Selectivity," Chem. Engng Sci. <u>27</u>, 109 (1972).
- 8. Lee, C. K., and Bailey, J. E., "Diffusion Waves and Selectivity Modifications in Cyclic Operation of a Porous Catalyst," Chem. Engng Sci. <u>29</u>, 1157 (1974).
- 9. Oruzheinkov, A. I., et al., ""Selectivity of Catalytic Processes Under Forced Cyclic Operation," React. Kinet. Catal. Lett. 10, 341 (1979).
- 10. Towler, B. F., and Rice, R. G., "A Note on the Response of a CSTR to a Spherical Catalyst Pellet," Chem. Engng Sci. 29, 1828 (1974).

- 11. Imison, B. W. and Rice, R. G., "The Transient Response of a CSTR to a Spherical Catalyst Pellet with Mass Transfer Resistance," Chem. Engng Sci. 30, 1421 (1975).
- 12. Lehr, C. G., Vurchak, S., and Kabel, R. L., "Response of a Tubular Heterogeneous Catalytic Reactor to a Step Increase in Flow Rate," AIChE J. 14, 627 (1968).
- 13. Denis, G. H., and Kabel, R. L., "The Effect on Conversion of Flow Rate Variations in a Heterogeneous Catalytic Reactor," AIChE J. 16, 972 (1970).
- 14. Al-Taie, A. S., and Kershenbaum, L. S., "Effect of Periodic Operation on the Selectivity of Catalytic Reactions," Chem. React. Engng-Houston (Weekman, V. W. and Luss, D., Ed.) ACS Sympos. Ser. (No. 65) p. 513 (1978).
- 15. Unni, M. P., Hudgins, R. R., and Silveston, P. L., "Influence of Cycling on the Rate of Oxidation of SO₂ over a Vanadia Catalyst," Can. J. Chem. Engng, 51, 623 (1973).
- 16. Skeirik, R. D., and DeVera, A. L., "Periodic Operation of Chemical Reactors I: Yield Optimization Analysis on the Forced Square Wave Feed Concentration to an Isothermal CSTR with Complex Kinetics," submitted to Chem. Engng Sci. (1980).
- 17. Abdul-Kareem, H. K., Hudgins, R. R., and Silveston, P. L., "Forced Cycling of the Catalytic Oxidation of CO over a V₂O₅ Catalyst-I, Concentration Cycling," Chem. Engng Sci. 35 2077 (1980).
- 18. Abdul-Kareem, H. K., Hudgins, R. R. and Silveston, P. L., "Forced Cycling of the Catalytic Oxidation of CO over a V₂O₅ Catalyst-II, Temperature Cycling," Chem. Engng. Sci. 35, 2085 (1980).
- 19. McGinnis, P. H., Jr., "Numerical Solution of Boundary Value Nonlinear ODE's," Chem. Engng Prog. Symp. Ser. 61 (No. 55) 2 (1965).
- 20. Ames, W. F., "Numerical Methods for Partial Differential Equations," p. 302, 2nd Ed. Academic Press, New York (1977).